hexagon:2611.00970v1

THE GOODSPEED FUNCTION: CLASSIFICATION, LEFT-TAIL GEOMETRY, AND ARITHMETIC NODAL WAVES

SAMUEL A. HAMBLETON

Abstract. Let

$$W(z) = \frac{\Gamma(z)+1}{z}, \qquad G(z) = \frac{\sin^2(\pi z) + \sin^2(\pi W(z))}{\pi^2},$$

so that the real zero set of G is $\{1\} \cup \mathbb{P}$. We develop three complementary aspects of the complex and arithmetic geometry of G.

First, we normalize the formal TUCKE classification data by a Gaussian lattice coordinate $\widehat{\xi}_G \in \mathbb{Z}[i]$ and a five-state residue $\lambda_5 \in \mathbb{Z}/5\mathbb{Z}$. Their pair faithfully recovers every formally admissible state, while the global realization of all such states by zeros of G remains conjectural.

Second, we prove the existence and asymptotic isolation of a canonical non-real Family $(-i)$ tail accumulating at 0. Its zeros lie on quartic cusps and admit a convergent parametrization

$$z_c^+ = c^{-1/2} Z(c^{-1/2})$$

by one holomorphic germ. The resulting triangular expansion recovers $\gamma, \zeta(2), \zeta(3), \ldots$ from the canonically labelled tail. From the exact unlabelled zero cloud in an arbitrarily small punctured neighbourhood of 0, we recover the Wilson germ up to its integer gauge, determine G as a punctured germ, and in the Gamma specialization reconstruct the prime-zeta function on $\Re s > 1$.

Finally, the d'Alembert wave

$$Q_G(x,t) = \tfrac{1}{2}\big(G(x-t) + G(x+t)\big)$$

has real nodes exactly at

$$\Big(\frac{p+q}{2}, \frac{q-p}{2}\Big), \qquad p, q \in \{1\} \cup \mathbb{P}.$$

Its characteristic jets separate the two endpoint jets, while vertical, horizontal, and rational-affine slices encode prime sums, fixed differences, and general two-prime affine relations. We also prove a positive fixed-gap detector and an unconditional macroscopic nodal density law derived from the prime number theorem.

1. Introduction and common framework

At first sight, the Goodspeed function introduced below appears somewhat ad hoc: it combines a Gamma-derived quantity with elementary trigonometric functions in a way that is not suggested by any standard special-function construction. Nevertheless, it is built entirely from Euler's Gamma function and elementary operations, and beneath this seemingly artificial definition lies a rigid arithmetic and geometric structure. Its real zero set consists exactly of 1 and the rational primes; its non-real zeros exhibit a discrete classification and a canonical asymptotic tail from which Gamma- and zeta-theoretic data can be reconstructed; and the same real zero divisor generates, through the one-dimensional wave equation, a nodal geometry encoding classical relations among primes. The purpose of this article is to develop these three aspects of a single analytic object and to distinguish carefully between the structures that are proved and those that remain conjectural.

Date: 24 November, 2026.

2020 *Mathematics Subject Classification.* Primary 11A41; Secondary 30C15, 33B15, 11M41, 11P32, 11N05, 35L05.

Key words and phrases. Goodspeed function, Gamma function, Wilson's theorem, primes, non-real zeros, Gaussian lattice, TUCKE coordinates, left-tail asymptotics, inverse rigidity, prime zeta function, arithmetic nodal geometry, wave equation, prime pairs, Goldbach representations, prime gaps.

To make this precise, define the Wilson–Gamma function

$$W(z) := \frac{\Gamma(z)+1}{z}$$

and the Goodspeed function

$$G(z) := \frac{\sin^2(\pi z)+\sin^2(\pi W(z))}{\pi^2}.$$

The earlier inspiration for G came from considering

$$f_{N,\varepsilon}(x) := \sin^2\left(\frac{N\pi}{x}\right)+\varepsilon\sin^2(\pi x), \qquad 0<\varepsilon\le 1.$$

Here N is a positive composite integer; see [7, p. 30, Eq. (1.66) and Lemma 1.2]. Since both summands are nonnegative on the positive real axis,

$$f_{N,\varepsilon}(x)=0 \quad\Longleftrightarrow\quad x\in\mathbb{Z}_{>0} \text{ and } x \mid N.$$

Thus locating a nontrivial positive zero is directly related to finding a nontrivial divisor of N.

The trigonometric appearance of G is somewhat deceptive. Euler's reflection formula

$$\Gamma(z)\Gamma(1-z)=\frac{\pi}{\sin(\pi z)}$$

(see [12]) shows that G may be expressed entirely in terms of the Gamma function and elementary operations:

$$G(z)=\Gamma^{-2}(z)\Gamma^{-2}(1-z)+\Gamma^{-2}\left(\frac{\Gamma(z)+1}{z}\right)\Gamma^{-2}\left(1-\frac{\Gamma(z)+1}{z}\right).$$

Thus the arithmetic and geometric structures studied below arise from a construction that, despite its initial appearance, is intrinsically Gamma-theoretic.

We shall also use the associated sheet function

$$S(z) := \frac{\sin(\pi W(z))}{\sin(\pi z)}.$$

Throughout,

$$\Omega_G := \mathbb{C}\setminus\{0,-1,-2,\ldots\}.$$

The functions W and G are holomorphic on Ω_G, while S is meromorphic there, with removable values filled by analytic continuation whenever appropriate.

The arithmetic starting point is Wilson's theorem. For real $x\in\Omega_G$, both terms in

$$\pi^2 G(x)=\sin^2(\pi x)+\sin^2(\pi W(x))$$

are nonnegative. Hence a real zero must be a positive integer n for which

$$W(n)=\frac{(n-1)!+1}{n}\in\mathbb{Z}.$$

Consequently

$$Z(G)\cap\mathbb{R}=\{1\}\cup\mathbb{P}=:\mathcal{P}_1,$$

where $\mathbb{P}$ denotes the rational primes. Here and below, $Z(G)$ denotes the set of zero locations, without multiplicity. Each $p\in\mathcal{P}_1$ is in fact a double zero: if $z=p+h$, then

$$G(p+h)=\big(1+W'(p)^2\big)h^2+O(h^3), \qquad h\to 0.$$

Thus the positive-real arithmetic divisor of G is completely explicit.

Remark 1.1 (Arithmetic singularities of the sheet function). The sheet function

$$S(z) = \frac{\sin(\pi W(z))}{\sin(\pi z)}$$

provides a complementary analytic encoding of primality.

At a positive prime p, Wilson's theorem gives $W(p) \in \mathbb{Z}$. The apparent singularity is removable, with

$$S(p) = (-1)^{W(p)-p} W'(p) \neq 0.$$

Indeed, $W'(2) = -\gamma/2$, while $W'(p) > 0$ for every prime $p \geq 3$.

At a positive composite integer n, however, $W(n) \notin \mathbb{Z}$, so S has a simple pole. Consequently, for every integer $n \geq 2$,

$$\mathbf{1}_{\mathbb{P}}(n) = 1 + \mathrm{Res}_{z=n} \frac{S'(z)}{S(z)}.$$

This distinction also has a contour interpretation. Let U be a bounded connected component of

$$\{z : \Re z > 0,\ |S(z)| > 1\},$$

whose closure lies in the open right half-plane and whose boundary is piecewise C^1. If h is holomorphic on a neighbourhood of $\overline{U}$, the residue theorem gives

$$\sum_{\substack{p \in U \\ p \in \mathbb{P}}} h(p) = \sum_{n \in U \cap \mathbb{Z}_{\geq 2}} h(n) + \frac{1}{2\pi i} \int_{\partial U} h(z) \frac{S'(z)}{S(z)}\, dz.$$

Indeed, S has no zeros in U, and its poles there are precisely the positive composite integers, all simple.

Thus the geometry of the sheet function provides an exact arithmetic contour formula, independently of the conjectural global classification of its non-real sheet zeros.

Related analytic encodings of primality based on Wilson's theorem, Gamma functions, and trigonometric expressions have appeared previously; see, for example, Connes [3]. For the classical number-theoretic background to Wilson's theorem and its converse, we refer to Hardy and Wright [9].

Away from the real axis, the zero geometry is much richer. The factorization

$$\pi^2 G(z) = \big(\sin(\pi z) + i \sin(\pi W(z))\big)\big(\sin(\pi z) - i \sin(\pi W(z))\big)$$

shows that every non-real zero satisfies

$$S(z) = \pm i.$$

The non-real zero set may therefore be viewed as a distinguished collection of i- and $-i$-points of the Gamma-derived meromorphic function S. The study of zeros, a-points, and value distribution of meromorphic functions is classical; see, for example, Nevanlinna [11] and Goldberg–Ostrovskii [6]. There is also an extensive computational literature on locating zeros and poles of meromorphic functions; a recent subdivision-based approach with error control is given by Chen [2]. The emphasis here is different: rather than locating isolated zeros numerically, we seek discrete organization, asymptotic structure, and arithmetic information carried by distinguished parts of the zero set. The purpose of this article is to study three complementary structures arising from this same function: a discrete classification of its zeros, a canonical analytic tail accumulating at the puncture 0, and an arithmetic wave whose nodes are generated by the real zero divisor.

The first direction is global and discrete. For zeros for which the analytic classification data are defined, one associates an extended TUCKE coordinate

$$\Psi(z) = (\tau, \mu, c, k, \varepsilon),$$

recording half-plane, family, quasi-index, location and sheet data. Rather than assuming a complete analytic classification, Section 2 isolates a formal admissible set and studies its intrinsic combinatorics. We construct a normalized Gaussian coordinate

$$\widehat{\xi}_G = \widehat{k} + i\widehat{c} \in \mathbb{Z}[i]$$

which separates the two principal Types and determines the family invariant. The remaining finite half-plane/sheet information is encoded uniformly by

$$\lambda_5 = 2\varepsilon - \tau \pmod 5.$$

The pair

$$(\lambda_5, \widehat{\xi}_G) \in (\mathbb{Z}/5\mathbb{Z}) \times \mathbb{Z}[i]$$

recovers every formally admissible TUCKE state. The corresponding fibres of the Gaussian coordinate have cardinality 1, 2, or 4, so the role of the five-state residue is uniform rather than pointwise minimal.

This part of the theory deliberately separates proved combinatorics from the unresolved analytic realization problem. The normalized formal lattice and its reconstruction theory are unconditional statements about the admissible set. What remains conjectural is the global assertion that every zero of G possesses exactly one admissible TUCKE state and that every formally admissible state is realized by exactly one zero. We formulate this as the Fundamental Classification Conjecture. A related invariant-coincidence statement, linking the quasi-index of a generated Family $(-i)$ zero to the Wilson index of its real generating minimum, is likewise retained globally as a conjecture, although it is proved in substantial subclasses.

The second direction is local and analytic. Section 3 studies a canonical sequence of non-real Family $(-i)$ zeros accumulating at the puncture 0. For every sufficiently large positive integer c, a distinguished real local minimum generates a unique simple conjugate pair

$$z_c^{\pm},$$

and the two branches approach the origin along the quartic cusps

$$\Im z = \pm\frac{1}{2}(\Re z)^4 + o\big((\Re z)^4\big)\,.$$

The upper tail is governed by a single holomorphic germ:

$$z_c^{+} = c^{-1/2} Z(c^{-1/2}).$$

Evaluating the same germ at negative values of the local parameter also produces the corresponding mirror tail approaching 0 from the negative-real side, linking the local analytic construction to the adjacent $k = 0$ and $k = -1$ Family $(-i)$ columns of the classification geometry.

The coefficients of Z satisfy a triangular recursion in the local coefficients of $\Gamma(1+z)$. For the canonically labelled tail, the real-part asymptotic jet therefore determines

$$\gamma, \zeta(2), \zeta(3), \ldots.$$

The arithmetic quantities appearing here are classical; the new point is the explicit inverse map from the non-real zero geometry to the Gamma coefficients, without using the positive-real prime zeros as input. The same tail also has an intrinsic geometric structure: its zero cloud has Hausdorff dimension 0 and box dimension 2/3, admits a genus-two reciprocal canonical product, and has a complex-moment zeta function whose leading poles record its first geometric scales.

The labelled and unlabelled inverse problems must be distinguished. Higher coefficients of the labelled asymptotic jet depend on the absolute integer origin of the quasi-index. By contrast, a fixed quartic horn intrinsically selects the canonical upper tail from the exact unlabelled zero cloud near

0. Within the normalized real-symmetric candidate class, these exact point locations determine the Wilson germ up to the integer gauge

$$W \longmapsto W + N, \qquad N \in \mathbb{Z},$$

and determine G exactly as a punctured germ. In the Gamma specialization the gauge is fixed by the Gamma normalization, after which a Newton–Laplace–Mellin–Möbius reconstruction recovers the prime-zeta function on

$$\Re s > 1.$$

These inverse results are local and do not assume the Fundamental Classification Conjecture.

The third direction uses only the real arithmetic divisor and is therefore logically independent of the global non-real classification. Define the Goodspeed wave by

$$Q_G(x,t) := \frac{1}{2}\big(G(x-t) + G(x+t)\big).$$

It satisfies the one-dimensional wave equation

$$(Q_G)_{tt} = (Q_G)_{xx}$$

wherever the characteristic arguments are regular. Since the real profile G is nonnegative, cancellation cannot create a node. Consequently

$$Q_G(x,t) = 0$$

if and only if

$$x - t,\ x + t \in \mathcal{P}_1.$$

Equivalently, the complete real nodal set is

$$\left\{ \left(\frac{p+q}{2}, \frac{q-p}{2} \right) : p, q \in \mathcal{P}_1 \right\}.$$

Thus the characteristic variables recover the two arithmetic endpoints of every node exactly.

This simple endpoint representation organizes several classical arithmetic questions in one plane. Vertical slices correspond to fixed sums,

$$p + q = N,$$

horizontal slices to fixed differences,

$$q - p = h,$$

and rational affine lines to relations

$$Ap + Bq = C.$$

Goldbach representations, twin primes, fixed prime gaps, Sophie Germain pairs and more general two-prime affine patterns therefore appear as directional intersections with one arithmetic nodal set. The complete characteristic jet at a node separates into the two real-axis jets of G at its endpoints, and the Hessian recovers the two endpoint curvature coefficients separately.

The wave equation itself is elementary and universal; it does not by itself produce new prime-distribution theorems. Its role here is to organize the Wilson-theoretic zero divisor into an exact characteristic geometry. Section 4 accordingly distinguishes structural identities from classical prime-correlation questions. We prove a positive, cancellation-free detector for finite fixed-gap counts and a two-dimensional macroscopic nodal density law obtained by transporting the prime number theorem through the characteristic map. By contrast, Goldbach existence, twin-prime infinitude, Polignac-type assertions and fixed-line Hardy–Littlewood–Dickson asymptotics retain their classical conjectural status. The geometry identifies the relevant directional counting problems; it does not replace the arithmetic estimates needed to solve them.

The three parts are therefore complementary but logically distinct. Section 2 supplies a global formal coordinate system and isolates the remaining classification conjecture. Section 3 proves a

substantial analytic realization near the singular point 0 and shows that this local zero geometry retains enough information to reconstruct the underlying Gamma germ and its arithmetic data. Section 4 begins instead from the already known real divisor $\mathcal{P}_1$ and develops the associated arithmetic nodal geometry. Together they describe the same function at three scales: discrete global organization, local complex asymptotics, and real two-endpoint arithmetic geometry.

AI Declaration

Extended conversations with OpenAI's ChatGPT (GPT-5.6 Sol), together with its Work Mode, played a substantial role in the exploratory development and organization of this work. The system assisted with symbolic and numerical experimentation, proof strategies, the formulation and testing of conjectures, the comparison and synthesis of intermediate results, and the drafting and refinement of mathematical arguments and exposition. In particular, these interactions contributed to the development of the discrete classification coordinates, the Gaussian-lattice normalization, the left-tail asymptotics and holomorphic-germ parametrization, the inverse-rigidity framework, and the arithmetic nodal geometry of the Goodspeed wave.

AI-assisted calculations, drafts, and proposed arguments were subsequently checked, revised, and incorporated only where the author was satisfied with their mathematical validity and consistency with the surrounding theory. The direction of the research, the interpretation of numerical experiments, the choice and revision of definitions and conjectures, the selection of results for inclusion, and the final form and correctness of the mathematical claims are the author's responsibility. The author has sought throughout to distinguish proved results from formal consequences, computational evidence, heuristic observations, and conjectural statements.

The author also acknowledges the extensive use of Wolfram Mathematica for symbolic and numerical experimentation, high-precision computation, and visualization throughout the development of the Goodspeed theory and in the preparation of the figures in this article.

2. Classification and Gaussian coordinates

The common functions W, G, and S, their domain Ω_G, and the real arithmetic divisor

$$Z(G) \cap \mathbb{R} = \mathcal{P}_1 = \{1\} \cup \mathbb{P}$$

were fixed in Section 1. We now turn to the discrete organization of the full zero set.

For those zeros for which the analytic classification data are defined, the Goodspeed theory assigns a TUCKE state

$$(\tau, \mu, c, k, \varepsilon),$$

recording half-plane, family, quasi-index, location, and sheet information. The purpose of this section is not to assume that every zero already possesses such a state. Instead, we isolate the formal admissible TUCKE set and prove that its apparently complicated combinatorics admits a simple normalization.

The principal construction is a Gaussian lattice coordinate

$$\widehat{\xi}_G = \widehat{k} + i\widehat{c} \in \mathbb{Z}[i].$$

It separates the two principal Types and determines the family invariant. The remaining finite half-plane/sheet information is encoded by

$$\lambda_5 = 2\varepsilon - \tau \pmod 5.$$

We prove that

$$(\tau, \mu, c, k, \varepsilon) \longmapsto (\lambda_5, \widehat{\xi}_G)$$

is injective on the formal admissible set and describe the image explicitly. The analytic assertion that this formal structure is realized uniquely by the complete zero set is kept separate as the Fundamental Classification Conjecture.

Figure 1 gives the complex zero geometry from which these discrete coordinates arise. The normalization developed below replaces this visually complicated configuration by the elementary lattice geometry of Figure 5.

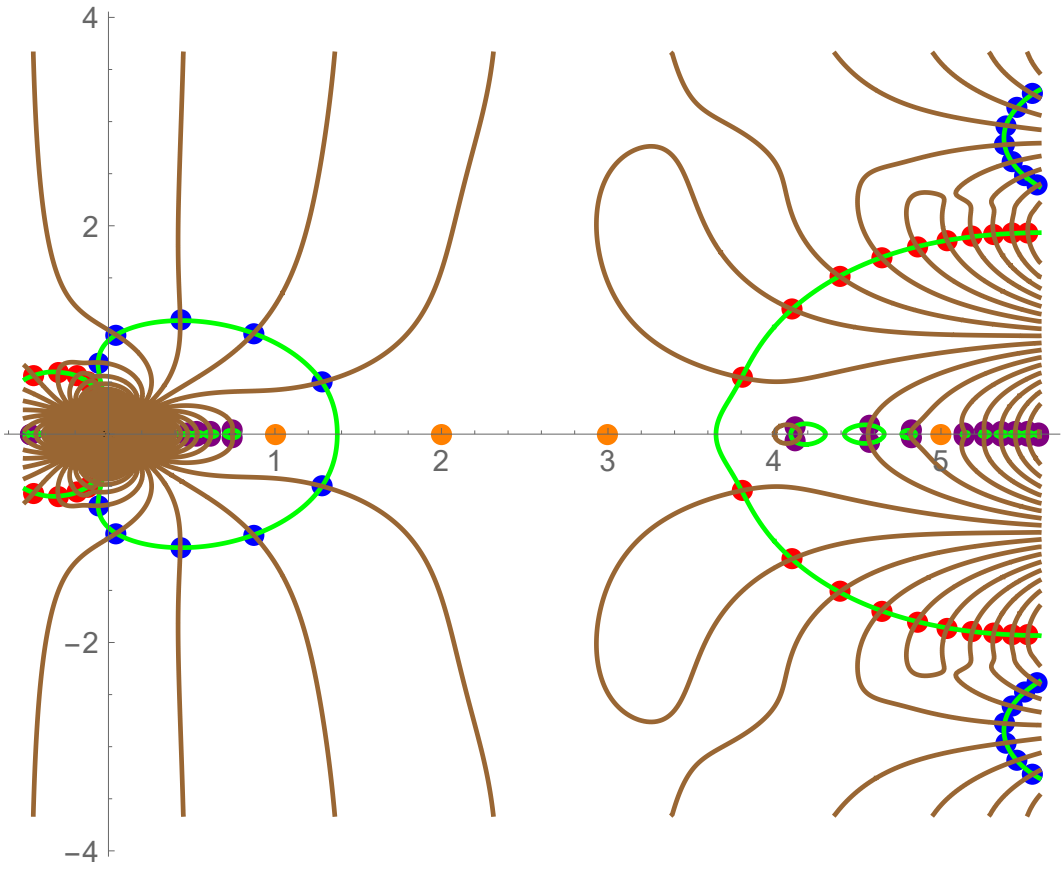


FIGURE 1. The curve $|S(z)| = 1$ in green, the curve $\Re\,(S(z)) = 0$ in brown, Family (i) zeros in orange, Family (-i) zeros in purple, Family (1) zeros in red, and Family (-1) zeros in blue.

2.1. **Analytic and discrete coordinates.** Let

$$Z(G) := \{z : G(z) = 0\}$$

on the natural domain of G, and put

$$\phi_\mu(z) := z - \mu W(z) - \frac{1}{2}.$$

For $x \in \mathbb{R}$, let

$$[x] = \left\lceil x - \frac{1}{2} \right\rceil$$

denote the nearest integer to x, with half-integer ties rounded toward $-\infty$, and $\lceil\cdot\rceil$ is the ceiling function. Thus

$$[3.6] = 4, \qquad [3.5] = 3, \qquad [3.4] = 3, \qquad [-2.5] = -3.$$

For $z = x + iy \in \mathbb{C}$, define the corresponding nearest-Gaussian- integer map coordinatewise by

$$[z]_{\mathbb{Z}[i]} := [x] + i[y].$$

Conjecture 2.1 (Invariant coincidence)**.** *Let x_C be a relevant strict real minimum satisfying*

$$G'(x_C) = 0, \qquad G''(x_C) > 0, \qquad 0 < G(x_C) < \frac{1}{2},$$

and let

$$z_C^{\pm}$$

be the associated conjugate pair on the generated Family $(-i)$ normal branch. Then

$$c(z_C^{\pm}) = [W(x_C)].$$

Remark 2.2 (Status and role of invariant coincidence)*.* The two integers in Conjecture 2.1 arise from different parts of the geometry. The quasi-index $c(z_C^{\pm})$ is defined from the complex endpoint of the generated normal branch, whereas $[W(x_C)]$ is read directly from its real generating minimum.

The conjectured identity is proved in substantial regimes, including the generated positive branches and several negative Wilson-normal and exactly certified subclasses. What is not presently available is a complete effective exhaustion of all relevant negative generating minima. We therefore retain the global identity as a conjecture.

No result on the formal Gaussian lattice in the present paper assumes Conjecture 2.1. Its role here is to motivate the real-shadow interpretation of the quasi-index c; the normalization and compression results below are statements about the formal admissible TUCKE set.

Definition 2.3 (TUCKE coordinates)**.** For a zero $z \in Z(G)$ for which the classification data are defined, the extended Goodspeed coordinate is

$$\Psi(z) = \big(\tau(z), \mu(z), c(z), k(z), \varepsilon(z)\big),$$

where

$$\tau(z) := \operatorname{sgn} \Im z$$

is the half-plane invariant,

$$\mu(z) \in \{i, -i, 1, -1\}$$

is the family invariant, and

$$\varepsilon(z) := \begin{cases} 0, & z \in \mathbb{R}, \\ -iS(z), & z \notin \mathbb{R} \end{cases}$$

is the sheet invariant.

For a non-real zero,

$$S(z) = \varepsilon(z)i, \qquad \varepsilon(z) \in \{\pm 1\}.$$

The Type 1 families are $\mu = \pm i$. Family (i) consists of the real zeros, while Family $(-i)$ consists of the non-real Type 1 zeros. For Type 1 zeros,

$$k = [\Re \phi_\mu(z)], \qquad c = [\Re(\mu \phi_\mu(z))].$$

For Type 2, let

$$\rho(z) := \frac{|W(z)|^2}{|\Im z|^2}$$

on the non-real part of $|S(z)| = 1$. We call the curve

$$\rho(z) = 1, \qquad \text{equivalently} \qquad |W(z)| = |\Im z|,$$

the *great bounding curve*. The primary Type 2 anchors m_c are the distinguished, indexed local minima of ρ on $|S(z)| = 1$ in the band

$$1 \le \rho(z) \le 4.$$

These minima provide a geometric interpretation of the quasi-index c. As the wave-like portions of $|S(z)| = 1$ develop into small, detached bounded components, or *drips*, the auxiliary curves

$$\Im\phi_\mu(z) = 0, \qquad \phi_\mu(z) = z - \mu W(z) - \frac{1}{2}, \qquad \mu \in \{1, -1\},$$

suggest a mechanism by which quasi-indices are inherited from the primary anchors. This geometric picture motivates the indexing, but does not itself give a complete pointwise assignment on disconnected components.

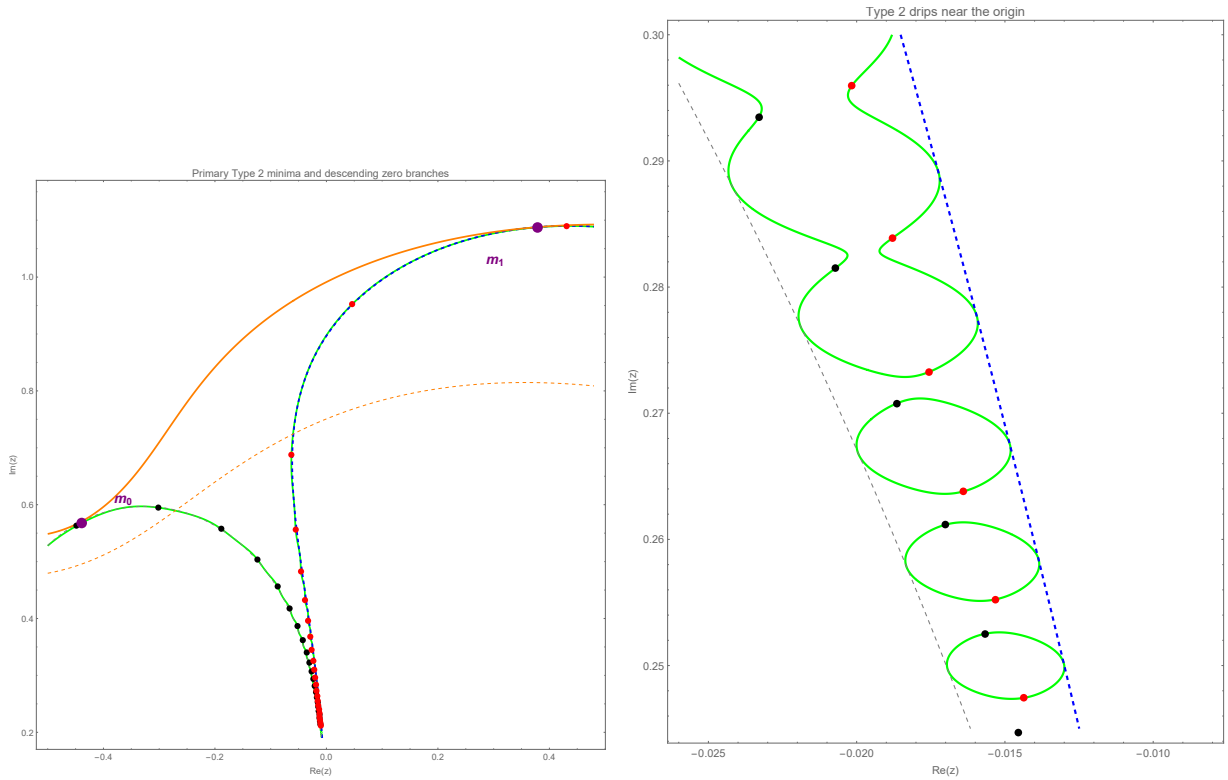


FIGURE 2. Proposed Type 2 quasi-index inheritance near the origin. Left: The green curves represent $|S(z)| = 1$, with black and red points denoting zeros numerically assigned to the Type 2 branches $(\mu, c) = (1, 0)$ and $(-1, 1)$, respectively. The purple points are the distinguished constrained minima m_0 and m_1 of $\rho(z) = |W(z)|^2/|\Im z|^2$. The solid and dotted orange curves represent the great bounding curve $|W(z)| = |\Im z|$ and $|W(z)| = 2|\Im z|$. The dashed auxiliary curves are $\Im\phi_1(z) = 0$ (grey) and $\Im\phi_{-1}(z) = 0$ (blue). Right: An enlargement showing several small bounded components of $|S(z)| = 1$ above the real axis, each containing a pair of zeros with the indicated numerical Type 2 assignments. The auxiliary curves suggest a mechanism by which quasi-indices may be inherited across distinct connected components of $|S(z)| = 1$, although this inheritance remains conjectural. The proximity of the zeros to the two auxiliary curves motivates the Nearest Auxiliary Branch Conjecture: secondary Type 2 zeros inherit their family and quasi-index from the nearest anchored connected component of $\Im\phi_\mu(z) = 0$, rather than from the connected component of $|S(z)| = 1$ on which they lie.

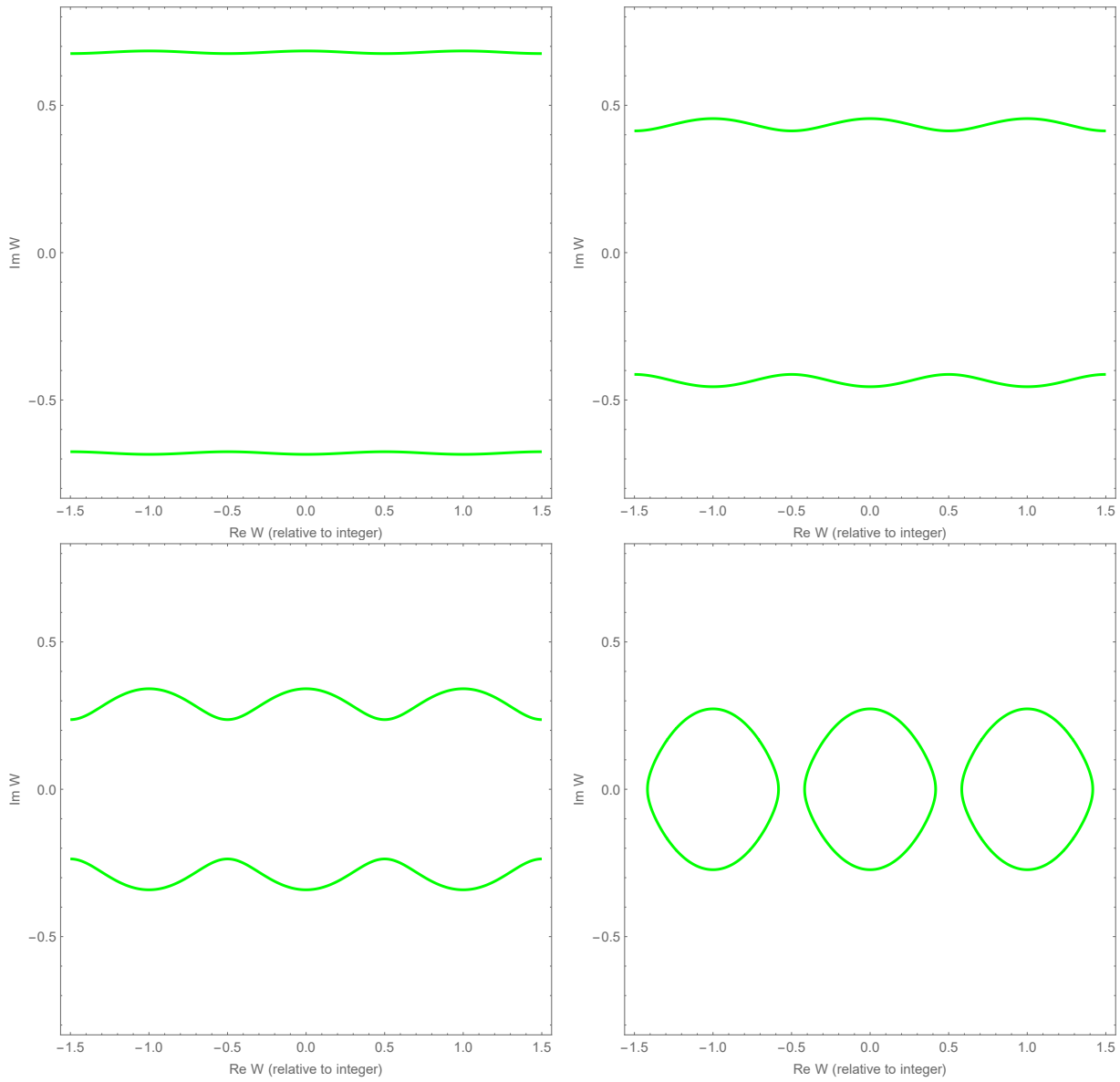


FIGURE 3. The dripping process from the connected components of $|S(z)| = 1$ with $c = 2, 3$ for $x = 10^2, 10^3, 10^4, 10^5$, $y \sim \frac{\pi^2}{\log(x)}$.

Definition 2.4 (Analytic Type classification)**.** The original analytic classification of Goodspeed zeros distinguishes two Types.

(1) Every real zero of G is Type 1, Family (i). A non-real zero is assigned Type 1, Family $(-i)$, on branches for which that assignment is established by the original local Wilson-normal classification.
(2) A non-real zero is assigned Type 2 when it belongs to a zero sequence obtained by the prescribed analytic continuation from a distinguished constrained minimum m_c of ρ on $|S| = 1$. Its original quasi-index is inherited from that minimum, and its Family is (1) or (-1).

These assignments apply on their established analytic domains. No global exhaustion or separation theorem for the complete non-real zero set is assumed.

Remark 2.5 (Coordinate formulas and Type membership). For a non-real zero with an established Type 1 assignment, the Family $(-i)$ coordinates are

$$\boxed{k = [\Re\phi_{-i}(z)], \qquad c = [\Im\phi_{-i}(z)].}$$

These formulas are not, however, a criterion for Type 1 membership: they can be evaluated at zeros of either Type.

Likewise, normal generation from a real minimum, formal Type 2 admissibility, and the existence of the phase index c_{ph} do not individually determine Type membership.

The formal admissible TUCKE set introduced below is therefore distinguished from the analytic classification of actual zeros. Whether the latter provides a unique and exhaustive classification of $Z(G)$ remains part of the global realization problem.

We therefore introduce the following explicit phase-based index.

Definition 2.6 (Phase-based quasi-index)**.** Let z be a non-real point at which $W(z^{\uparrow}) \neq 0$, and put

$$z^{\uparrow} := \Re z + i|\Im z|.$$

Let $A(z)$ be the analytic logarithm of $\Gamma(z)$ in the upper half-plane, normalized to be real on the positive real axis. Define

$$L_P(z) := A(z) - \operatorname{Log} z + \operatorname{Log}\left(1 + \frac{1}{\Gamma(z)}\right),$$

where Log denotes the principal complex logarithm.

The phase-based index is

$$c_{\mathrm{ph}}(z) := \left\lfloor 2 + \frac{\Im L_P(z^{\uparrow})}{\pi} \right\rfloor - \mathbf{1}_{\{\Re z < -11/2,\ [\Re z] \in 2\mathbb{Z}\}}.$$

For a Type 2 zero, we propose to use c_{ph} as its intrinsic quasi-index.

The upper-half-plane representative $z^{\uparrow}$ ensures

$$c_{\mathrm{ph}}(\overline{z}) = c_{\mathrm{ph}}(z).$$

The correction term accounts for the parity discrepancy of the uncorrected Wilson phase on the canonical negative-pole Type 2 branches.

Numerical calculations reproduce a large collection of Type 2 indices, including the small detached components above the origin. On the sufficiently negative canonical pole-capture family, agreement with the established index follows analytically. The proposed identification

$$c(z) = c_{\mathrm{ph}}(z)$$

for every Type 2 zero remains a global phase-index coincidence conjecture. Under this identification, the Type 2 Family is determined by

$$\mu = (-1)^{c_{\mathrm{ph}}(z)}.$$

Its location index k is the corresponding phase-continuation index, normalized to agree with

$$[\Re\phi_{\mu}(z)]$$

whenever the half-integer straightening applies.

Theorem 2.7 (Extended upper phase constancy)**.** *Put*

$$y_* := \frac{\operatorname{arsinh}(1)}{\pi}.$$

The phase-based quasi-index c_{ph} *is constant on every connected subset of either*

$$U_1 = \{z \in \mathbb{H} : |S(z)| = 1,\ \Im z \geq 1\}$$

or

$$U_* = \{z \in \mathbb{H} : |S(z)| = 1,\ \Re z \geq 4,\ \Im z > y_*\}.$$

Proof. Write $z = x + iy$. On $|S(z)| = 1$,

$$\sinh(\pi y) \leq |\sin(\pi z)| = |\sin(\pi W(z))| \leq \sinh(\pi |W(z)|),$$

so $|W(z)| \geq y$.

If $W(z)$ is real, then $\sinh(\pi y) \leq 1$, and hence $y \leq y_*$. Also, a crossing of the correction-logarithm cut in L_P requires $\Gamma(z) \in (-1, 0)$. Writing $\Gamma(z) + 1 = a \in (0, 1)$ gives

$$|W(z)| = \frac{a}{|z|} < \frac{1}{|z|}, \qquad y|z| < 1.$$

On U_*, the negative-pole correction vanishes and

$$y|z| \geq 4y > 4y_* > 1.$$

Thus neither a Wilson real-axis crossing nor a logarithmic branch-cut crossing is possible.

On U_1, Gamma recurrence and the integral bound $|\Gamma(\sigma + iy)| \leq \Gamma(\sigma)$ give $|\Gamma(z)| \leq 1$ when $x \leq -2$. Consequently,

$$|W(z)| \leq \frac{2}{|z|} \leq \frac{2}{\sqrt{5}} < 1 \leq y,$$

a contradiction. Hence $x > -2$, the negative-pole correction vanishes, and the preceding argument again excludes both kinds of phase crossing. Therefore $\Im L_P/\pi$ cannot cross an integer, and c_{ph} is locally constant on both sets. Connectedness proves the assertion. □

Theorem 2.8 (Compact-component height bound)**.** *Let C be a compact connected component of*

$$\{z \in \mathbb{H} : |S(z)| = 1\}.$$

Then C intersects $\Im W(z) = 0$. Consequently,

$$\min_{z \in C} \Im z \leq \frac{\operatorname{arsinh}(1)}{\pi} \approx 0.28055.$$

Proof. Suppose $\Im W$ has no zero on C. It then has a constant strict sign on C.

Since S is holomorphic in $\mathbb{H}$ and nonzero on its unit level, C is a compact real-analytic level graph. Every vertex has even degree, including at critical points of S. Thus C contains a Jordan cycle J.

Let D be the bounded interior of J. The harmonic maximum principle shows that $\Im W$ retains its strict sign throughout D. Therefore W takes no integer value in D, so S is holomorphic and nonvanishing there.

The harmonic function $\log|S|$ vanishes on $\partial D = J$, hence vanishes throughout D. The open mapping theorem would then force S to be constant, a contradiction.

Thus some $z = x + iy \in C$ has $\Im W(z) = 0$. At that point,

$$\sinh(\pi y) \leq |\sin(\pi z)| = |\sin(\pi W(z))| \leq 1,$$

which gives the result. □

Remark 2.9. Theorem 2.7 explains the stability of the phase index on higher Type 2 branches, whereas Theorem 2.8 shows that every detached oval lying entirely in the upper half-plane must reach the low-height region. Neither result requires global phase-index coincidence.

Theorem 2.10 (Uniform high-level regularity)**.** *At every point of $|S(z)| = 1$ satisfying $\Im z \geq 7/4$, one has*

$$\Re z > 4, \qquad |W'(z)| > \frac{3}{2}, \qquad |S'(z)| > \frac{7}{5}.$$

In particular, the unit level $|S(z)| = 1$ has no critical points in this region. The simplicity of Goodspeed zeros holds under the sharper height condition $|\Im z| \geq 61/50$, as shown below.

Proof. Write $z = x + iy$ and $W(z) = u + iv$. On $|S| = 1$,

$$\sin^2(\pi u) + \sinh^2(\pi v) = \sin^2(\pi x) + \sinh^2(\pi y).$$

For $y \geq 7/4$ this implies

$$|v| > \frac{87}{50}.$$

If $x \leq 3$, Euler's integral and Gamma recurrence give $|\Gamma(z)| \leq 2$, whereas

$$|\Gamma(z)| = |zW(z) - 1| \geq y|v| - 1 > \frac{409}{200} > 2.$$

For $3 \leq x \leq 4$, convexity gives $\Gamma(x) \leq 4x - 10$, while

$$|\Gamma(z)| \geq |z|y - 1 > xy - 1 \geq \frac{7}{4}x - 1 \geq 4x - 10.$$

Both possibilities are excluded; hence $x > 4$.

Put $F(z) = A(z) - \operatorname{Log} z$ and $\psi = \Gamma'/\Gamma$. The digamma series gives

$$\Re F'(z) = \Re\left(\psi(z) - \frac{1}{z}\right) > \frac{209}{200}.$$

Here we use

$$\Re\psi(z) \geq \psi(4) = \frac{11}{6} - \gamma, \quad \Re\frac{1}{z} \leq \frac{64}{305},$$

together with $\gamma < 0.578$. Also $|z|^{-1} < 23/100$ and $|z|^{-2} < 53/1000$.

The identity

$$W' = \left(W - \frac{1}{z}\right)F' - \frac{1}{z^2}$$

therefore yields

$$|W'| > \left(\frac{87}{50} - \frac{23}{100}\right)\frac{209}{200} - \frac{53}{1000} = \frac{30499}{20000} > \frac{3}{2}.$$

Finally, the standard complex-cotangent bounds give

$$|\cot(\pi W)| > 0.99, \qquad |\cot(\pi z)| < 1.01.$$

Since

$$\frac{S'}{S} = \pi\big(W' \cot(\pi W) - \cot(\pi z)\big),$$

we obtain

$$|S'| > \pi\left(\frac{3}{2}(0.99) - 1.01\right) > \frac{7}{5}.$$

At a non-real zero of G, where $S = \pm i$,

$$G'(z) = \frac{2}{\pi^2}\sin^2(\pi z)\, S(z)S'(z) \neq 0.$$

□

The high-level regularity estimates admit a complementary refinement for small values of G. This yields a uniform height bound for zeros obtained from real local minima, independently of their eventual Type or Family assignment.

Lemma 2.11 (Small-value derivative barrier)**.** *Let*

$$h := \frac{61}{50}, \qquad a := \frac{181}{50}.$$

If $z = x + iy$ satisfies

$$y \geq h, \qquad |G(z)| \leq \frac{2}{\pi^2},$$

then

$$x > a, \qquad |W'(z)| > \frac{21}{20}, \qquad |G'(z)| > \frac{29}{2}.$$

Proof. Write $W(z) = u + iv$ and put $s = \sinh^2(\pi y)$. Since

$$\pi^2 G(z) = \sin^2(\pi z) + \sin^2(\pi W(z)),$$

the small-value hypothesis and the identity

$$|\sin(\pi(\alpha + i\beta))|^2 = \sin^2(\pi\alpha) + \sinh^2(\pi\beta)$$

give

$$\sinh^2(\pi|v|) \geq s - 3.$$

The elementary estimates

$$\sinh^2(\pi h) > 530, \qquad \sinh^2(\pi h) - \sinh^2\big(\pi(h - 10^{-3})\big) > 3$$

therefore imply

$$s > 530, \qquad |v| > y - 10^{-3} \geq \frac{1219}{1000}. \tag{N1}$$

We first localize z in the right half-plane. For $\sigma > 0$, Euler's Gamma product gives

$$R_\sigma(y) := \frac{|\Gamma(\sigma + iy)|}{\Gamma(\sigma)} = \prod_{n=0}^{\infty} \left(1 + \frac{y^2}{(\sigma + n)^2}\right)^{-1/2}.$$

This ratio increases with σ and decreases with $y > 0$. Set $T_j(y) = |\Gamma(j + iy)|$. The standard integer and half-integer Gamma modulus identities yield, uniformly for $y \geq h$,

$$\begin{gathered} \frac{T_2(y)}{y^2} < 0.44, \quad \frac{R_{3/2}(y)}{y} < 0.46, \\ \frac{T_2(y)}{\sqrt{y^2 + 1/4}} < 0.50, \qquad T_2(y) < 0.65, \\ T_3(y) < 1.51, \qquad R_4(y) < 0.814. \end{gathered} \tag{N2}$$

These bounds follow from

$$|\Gamma(1 + iy)|^2 = \frac{\pi y}{\sinh(\pi y)}, \qquad \left|\Gamma\left(\frac{1}{2} + iy\right)\right|^2 = \frac{\pi}{\cosh(\pi y)},$$

by recurrence and finite rational Taylor bounds for the hyperbolic functions. In particular, they may be verified using $157/50 < \pi < 22/7$.

On the other hand, $\Gamma(z) = zW(z) - 1$ and (N1) imply

$$|\Gamma(z)| > \frac{1219}{1000}\sqrt{x^2 + h^2} - 1. \tag{N3}$$

For $x \leq 0$, Gamma recurrence gives $|\Gamma(z)| \leq T_2(y)/y^2$. For $0 < x \leq 1/2$, $1/2 < x \leq 1$, $1 < x \leq 2$, and $2 < x \leq 3$, the corresponding upper bounds are, respectively,

$$\frac{R_{3/2}(y)}{y}, \quad \frac{T_2(y)}{\sqrt{y^2 + 1/4}}, \quad T_2(y), \quad T_3(y).$$

Each contradicts (N3), using (N2).

For $3 \leq x \leq a$, convexity of the real Gamma function gives

$$|\Gamma(x + iy)| < 0.814(4x - 10),$$

which again contradicts (N3). Consequently $x > a$.

Put $F(z) = \mathrm{LogGamma}(z) - \mathrm{Log}\, z$ and $\psi = \Gamma'/\Gamma$. The digamma series gives

$$\Re\psi(x+iy) - \psi(x) > \frac{1}{2}\log\left(1 + \frac{y^2}{x^2}\right),$$

and

$$\Im\psi(x+iy) > \arctan(y/x).$$

Together with $\psi'(t) \le t^{-1} + t^{-2}$ for $t > 0$, these imply, for $a < x \le 4$,

$$\Re F'(z) > 0.917, \qquad \Im F'(z) > 0.365.$$

For $x \ge 4$ one has

$$\Re F'(z) > \psi(4) - \frac{4}{16+h^2} > 0.986.$$

Thus throughout the localized region,

$$|F'(z)| > \frac{493}{500}.$$

The identity

$$W'(z) = \left(W(z) - \frac{1}{z}\right) F'(z) - \frac{1}{z^2}$$

and (N1) now give

$$|W'(z)| > \left(\frac{1219}{1000} - \frac{h}{a^2+h^2}\right)\frac{493}{500} - \frac{1}{a^2+h^2} > \frac{21}{20}. \tag{N4}$$

Finally,

$$G'(z) = \frac{\sin(2\pi z) + W'(z)\sin(2\pi W(z))}{\pi}.$$

Using

$$|\sin(2\pi W)| \ge \sinh(2\pi|v|), \qquad |\sin(2\pi z)| \le \cosh(2\pi y),$$

together with (N1), (N4), and $s > 530$, we obtain

$$\begin{aligned} |G'(z)| &\ge \frac{|W'(z)|\sinh(2\pi|v|) - \cosh(2\pi y)}{\pi} \\ &> \frac{2(21/20)(s-3) - (2s+1)}{\pi} \\ &= \frac{s/10 - 73/10}{\pi} > \frac{29}{2}. \end{aligned}$$

This proves the lemma. □

Theorem 2.12 (Uniform height of real-minimum normal endpoints)**.** *Let x_C be a strict nondegenerate real local minimum of G, with*

$$g_C := G(x_C) > 0.$$

Suppose that a complete upper normal branch $z_C(t)$ exists, satisfying

$$\begin{aligned} &z_C(0) = x_C, \qquad \Im z_C(t) > 0 \quad (t > 0), \\ &G(z_C(t)) = g_C - t^2, \qquad 0 \le t \le \sqrt{g_C}, \end{aligned}$$

and remaining in the holomorphic domain of G. Let $z_C = z_C(\sqrt{g_C})$ be its terminal zero.

Then

$$\Im z_C < H_0 := \frac{61}{50} + \frac{4}{29\pi^2} = 1.2339753356748\ldots < \frac{5}{4}.$$

The conjugate endpoint satisfies the same absolute height bound.

In particular, no zero obtained through a complete real-minimum normal branch can lie in $|\Im z| \ge 5/4$.

Proof. For every real x in the domain of G,

$$0 \le G(x) \le \frac{2}{\pi^2},$$

and hence $g_C \le 2/\pi^2$.

Reverse the normal branch, parametrizing it by the value of G:

$$\zeta(s) := z_C\big(\sqrt{g_C - s}\big), \qquad 0 \le s \le g_C.$$

Thus

$$G(\zeta(s)) = s, \qquad \zeta(0) = z_C, \qquad \zeta(g_C) = x_C.$$

Put $h = 61/50$. The conclusion is immediate if $\Im z_C \le h$. Otherwise, let $s_0 \in (0, g_C)$ be the first parameter at which

$$\Im\zeta(s_0) = h.$$

On $0 \le s \le s_0$ we have

$$|G(\zeta(s))| \le g_C \le \frac{2}{\pi^2}, \qquad \Im\zeta(s) \ge h.$$

Lemma 2.11 therefore implies $|G'(\zeta(s))| > 29/2$. The inverse branch is regular on this interval, and differentiation gives

$$\zeta'(s) = \frac{1}{G'(\zeta(s))}, \qquad |\zeta'(s)| < \frac{2}{29}.$$

Consequently,

$$\begin{aligned} \Im z_C - h &\le |z_C - \zeta(s_0)| \\ &\le \int_0^{s_0} |\zeta'(s)|\, ds \\ &< \frac{2s_0}{29} < \frac{2g_C}{29} \le \frac{4}{29\pi^2}. \end{aligned}$$

This proves the asserted bound. The lower-half-plane case follows by conjugation. □

Corollary 2.13 (Simplicity of high Goodspeed zeros)**.** *Every zero z of G satisfying*

$$|\Im z| \ge \frac{61}{50}$$

is simple and obeys

$$\Re z > \frac{181}{50}, \qquad |G'(z)| > \frac{29}{2}.$$

At every such non-real zero one also has $S'(z) \ne 0$.

Proof. Apply Lemma 2.11 with $G(z) = 0$, using conjugation when $\Im z < 0$.

Since $S(z) = \pm i$ at a non-real Goodspeed zero,

$$G'(z) = \frac{2}{\pi^2}\sin^2(\pi z)\, S(z) S'(z).$$

The factor multiplying $S'(z)$ is nonzero. Hence $S'(z) \ne 0$. □

Remark 2.14 (Normal generation and Type classification). Theorem 2.12 applies to every complete real-minimum normal endpoint, independently of its Type or Family label. In particular, it applies to the generated Family $(-i)$ zeros, but also to any Type 2 zeros obtained by the same normal-generation mechanism.

The conclusion does not establish that all zeros with $|\Im z| \ge 5/4$ are Type 2. That stronger assertion would require, in addition, an exhaustion result excluding ungenerated Type 1 zeros and assigning the remaining high zeros to the original Type 2 continuation sequences.

Thus the height bound is unconditional for the generated subclass, whereas global high-altitude Type 2 classification remains a separate problem.

Theorem 2.15 (Compact high phase components)**.** *For $q \in \mathbb{Z}$ and $Y \geq 1$, let*

$$E_{q,Y} := \{z \in \mathbb{H} : |S(z)| = 1,\ \Im z \geq Y,\ c_{\mathrm{ph}}(z) = q\}.$$

Every $E_{q,Y}$ is a compact finite real-analytic graph without cycles. Each of its nontrivial connected components meets $\Im z = Y$.

If $Y \geq 7/4$, every nontrivial component is a regular embedded arc with both endpoints on $\Im z = Y$. Isolated boundary tangencies may also occur.

Proof. On the upper unit level with $y \geq 1$, Theorem 2.7 gives $x > -2$ and constancy of c_{ph} on connected subsets.

Put $q_+ = \max(q, 0)$ and $\kappa = 7/6 - \gamma > 0$. For $x > 3$, integrating the logarithmic derivative of $\Gamma(z)/z$ vertically gives

$$\Im F(x + iy) = \int_0^y \Re\left(\psi(x + it) - \frac{1}{x + it}\right) dt > \kappa y$$

and

$$\Im F(x + iy) > y(\log x - 2/3).$$

Since $c_{\mathrm{ph}} = q$, the phase-sector inequality and the principal correction logarithm imply $\Im F < q\pi$.

If $x \leq 3$, Theorem 2.10 excludes $y \geq 7/4$ on the unit level. Consequently every $z = x + iy \in E_{q,Y}$ satisfies

$$-2 < x \leq \max\left\{3, \exp\left(\frac{q_+\pi}{Y} + \frac{2}{3}\right)\right\},$$

and

$$Y \leq y \leq \max\left\{\frac{7}{4}, \frac{q_+\pi}{\kappa}\right\}.$$

The set is closed by phase constancy and is therefore compact.

The local analytic structure of a unit level gives a finite graph on this compact set. A Jordan cycle in it would lie entirely above y_*, contradicting the maximum-principle argument of Theorem 2.8. Thus the graph is a forest.

Interior vertices have even degree, so every nontrivial tree has boundary leaves on $y = Y$. When $Y \geq 7/4$, Theorem 2.10 excludes interior critical vertices. Each nontrivial tree is therefore a regular arc. □

Theorem 2.16 (Canonical logarithmic location coordinate)**.** *Let $\mu \in \{1, -1\}$ and define*

$$\mathcal{H}_\mu = \{z \in \mathbb{H} : \mu \Im W(z) > 0\}.$$

On this domain put

$$D_\mu(z) := \frac{\mathrm{Log}(1 - e^{2\pi i \mu W(z)}) - \mathrm{Log}(1 - e^{2\pi i z})}{i\pi}$$

and

$$B_\mu(z) := \phi_\mu(z) + D_\mu(z).$$

Then B_μ is holomorphic on $\mathcal{H}_\mu$, and

$$S(z) = \mu i\, e^{i\pi B_\mu(z)}.$$

Consequently, B_μ is real on $|S(z)| = 1 \cap \mathcal{H}_\mu$, and every Goodspeed zero there has an exact integer location coordinate

$$k_{\mathrm{an}}(z) := B_\mu(z) \in \mathbb{Z},$$

satisfying

$$\varepsilon(z) = \mu(-1)^{k_{\mathrm{an}}(z)}.$$

If $\Im z \geq 7/4$, choose $\mu = \operatorname{sgn} \Im W(z)$. Then

$$k_{\mathrm{an}}(z) = [\Re \phi_\mu(z)], \qquad \mu = (-1)^{c_{\mathrm{ph}}(z)}.$$

In particular, no half-integer rounding tie occurs.

Proof. On $\mathcal{H}_\mu$, both $e^{2\pi i\mu W(z)}$ and $e^{2\pi iz}$ have modulus less than one. Thus the principal logarithms in D_μ are analytic.

For $\Im a > 0$,

$$\sin(\pi a) = \frac{i}{2}e^{-i\pi a}(1 - e^{2\pi i a}).$$

Applying this to $\mu W(z)$ and z, and using $\sin(\pi W) = \mu \sin(\pi \mu W)$, gives

$$S(z) = \mu i\, e^{i\pi B_\mu(z)}.$$

Therefore

$$|S(z)| = e^{-\pi \Im B_\mu(z)}.$$

On the unit level B_μ is real, and at a Goodspeed zero $S = \varepsilon i$, forcing $B_\mu \in \mathbb{Z}$ and $\varepsilon = \mu(-1)^{B_\mu}$.

For $\Im z \geq 7/4$, the preceding regularity theorem gives $|\Im W| > 87/50$. Hence

$$|D_\mu(z)| \leq \frac{-\log(1 - e^{-2\pi \Im z}) - \log(1 - e^{-2\pi |\Im W(z)|})}{\pi} < \frac{1}{1000}.$$

Since B_μ is an integer at a zero, its real part is strictly within $1/1000$ of $\Re \phi_\mu$. This proves the rounding identity.

Finally, the negative-pole correction in c_{ph} vanishes in this region. Its logarithmic phase parity gives

$$(-1)^{c_{\mathrm{ph}}(z)} = \operatorname{sgn} \Im W(z) = \mu.$$

□

Theorem 2.17 (Intrinsic coordinates above height 61/50)**.** *Let z be a non-real zero of G with*

$$|\Im z| \geq \frac{61}{50}.$$

Put

$$z^{\uparrow} = \Re z + i|\Im z|, \qquad q = c_{\mathrm{ph}}(z), \qquad \mu = (-1)^q.$$

Then

$$q \geq 2, \qquad \mu = \operatorname{sgn} \Im W(z^{\uparrow}),$$

and

$$k_{\mathrm{an}} := B_\mu(z^{\uparrow}) \in \mathbb{Z}.$$

Moreover,

$$\left|\phi_\mu(z^{\uparrow}) - k_{\mathrm{an}}\right| < \frac{1}{3000}, \qquad k_{\mathrm{an}} = [\Re \phi_\mu(z^{\uparrow})].$$

There are no rounding ties, and

$$\varepsilon(z) = \tau(z)\mu(-1)^{k_{\mathrm{an}}}.$$

Every such zero is simple. If $q \geq 3$, its intrinsic coordinates also satisfy the formal Type 2 location and sheet admissibility rules.

No assertion about membership in the original Type 2 class is required or implied.

Proof. By conjugation it suffices first to consider $z = x + iy$ with $y \geq 61/50$.

Lemma 2.11, applied with $G(z) = 0$, gives

$$x > \frac{181}{50}, \qquad |\Im W(z)| > y - \frac{1}{1000} \geq \frac{1219}{1000}, \qquad |G'(z)| > \frac{29}{2}.$$

The negative-pole correction in c_{ph} therefore vanishes.

On $|S| = 1$ we have $|W(z)| \geq y$, and hence

$$|\Gamma(z)| = |zW(z) - 1| \geq |z|y - 1 > 2.$$

Writing $F = \mathrm{LogGamma} - \mathrm{Log}\, z$, the digamma-series estimate gives

$$\Im F(z) > \left(\frac{7}{6} - \gamma\right) y > \frac{y}{2}.$$

Since $|1/\Gamma(z)| < 1/2$,

$$\left|\Im \,\mathrm{Log}\left(1 + \frac{1}{\Gamma(z)}\right)\right| < \frac{\pi}{6}.$$

Consequently

$$\Im L_P(z) > \frac{61}{100} - \frac{\pi}{6} > 0,$$

and therefore $q \geq 2$.

As $W(z) = \exp L_P(z)$ and $\Im W(z) \neq 0$, the phase-sector parity gives

$$(-1)^q = \operatorname{sgn} \Im W(z).$$

Thus z belongs to the domain of B_μ. Theorem 2.16 gives

$$S(z) = \mu i\, e^{i\pi B_\mu(z)}.$$

Since $S(z) = \varepsilon(z) i$, it follows that

$$B_\mu(z) = k_{\mathrm{an}} \in \mathbb{Z}, \qquad \varepsilon(z) = \mu(-1)^{k_{\mathrm{an}}}.$$

Both exponential arguments in D_μ have modulus less than

$$e^{-2\pi(1219/1000)} < \frac{1}{2000}.$$

Using $|\,\mathrm{Log}(1-w)| \leq |w|/(1-|w|)$ for $|w| < 1$, we obtain

$$|D_\mu(z)| < \frac{2}{1999\pi} < \frac{1}{3000}.$$

Since $B_\mu = \phi_\mu + D_\mu$, this proves

$$|\phi_\mu(z) - k_{\mathrm{an}}| < \frac{1}{3000}.$$

The nearest-integer identity follows, with a strict margin excluding ties.

Simplicity follows from Corollary 2.13. The lower-half-plane statements follow by complex conjugation and the definition of $z^{\uparrow}$, introducing the factor τ in the sheet law.

Finally, when $q \geq 3$, the formal Type 2 location set is $K_q = \mathbb{Z}$, so the stated intrinsic coordinates satisfy its location and sheet conditions. □

Corollary 2.18 (High phase ordering and sheet alternation)**.** *On every nontrivial component of $E_{q,Y}$ with $Y \geq 7/4$, the appropriate function B_μ is a strictly monotone real coordinate. The Goodspeed zeros on the component occur exactly at its integer values, are simple, and have alternating sheet signs.*

If $q \geq 3$, the resulting intrinsic data satisfy the formal Type 2 location and sheet admissibility rules.

Proof. Theorem 2.10 gives $S' \neq 0$, and

$$\frac{S'}{S} = i\pi B'_\mu.$$

Thus B_μ has nonvanishing derivative along a regular unit-level arc, and is strictly monotone there. The remaining assertions follow from

$$S = \mu i\, e^{i\pi B_\mu}$$

and the simplicity theorem.

For $q \geq 3$, the formal location set is $K_q = \mathbb{Z}$, and $\mu = (-1)^q$, so the resulting integers obey the formal Type 2 rules. □

Remark 2.19 (Scope of the analytic phase coordinates). The preceding results give an intrinsic analytic phase index and an exact integer location coordinate on the higher unit-level geometry. They establish uniform regularity, finite high-component topology, and the sheet alternation law independently of the global classification conjecture.

The exceptional low-height components may connect different phase sectors, while compact upper components necessarily descend below y_*.

The analytic coordinates do not, by themselves, prove that every high Goodspeed zero belongs to the originally designated Type 2 family, nor do they establish global coincidence between c_{ph} and the distinguished-minimum index c. Those identification and realization questions remain separate.

The phase index also admits a geometric interpretation on the canonical negative-pole Type 2 family. Importantly, the associated components can be selected without using the distinguished minima to define their indices.

Definition 2.20 (GBC-seeded components)**.** Let

$$\mathcal{U} = \{z : |S(z)| = 1\},$$

with removable values of S filled in and its genuine poles excluded. For $R > 1$, put

$$E_R = \{z \in \mathcal{U} : \Im z > 0, \quad 1 < \rho(z) \le R\}.$$

A full connected component of $\mathcal{U}$ meeting E_R is called an R-GBC-seeded component.

For a positive integer n, put

$$\Sigma_n^+ = \left\{ z = x + iy : |x + n| \le \frac{1}{2}, \quad y > 0 \right\}.$$

For negative quasi-indices, we use the following stripwise normalization. Whenever the constrained minimum exists uniquely, define

$$m_{-n} := \operatorname*{arg\,min}_{\substack{z \in \Sigma_n^+ \\ |S(z)|=1}} \rho(z).$$

Its quasi-index is $c = -n$, equivalently $c = [\Re m_{-n}]$ in the eventual pole regime. Zeros obtained by analytic continuation from m_{-n} along its regular unit-level branch are assigned Type 2, as in Definition 2.4.

Existence and uniqueness of these anchors will be established below for all sufficiently large n.

This terminology describes a geometric class; it does not define Type 2 membership globally.

Theorem 2.21 (Eventual GBC selection of canonical Type 2 pole components)**.** *Fix $R > 1$. For every sufficiently large integer n, exactly one full connected component of $\mathcal{U}$ meets*

$$E_R \cap \Sigma_n^+.$$

It is the canonical regular Jordan component C_n enclosing the pole $-n$.

The component has a real-analytic parametrization

$$z = -n + \frac{r_n(\theta) e^{i\theta}}{n}, \qquad r_n(\theta) = 1 + O(n^{-2}),$$

uniformly with every fixed number of derivatives.

The winding degree of S on C_n is -1. The component contains exactly two Goodspeed zeros, one in each open half-plane, which are complex conjugates. The upper zero satisfies

$$S(z) = (-1)^n i.$$

The upper half of C_n has exactly one nondegenerate constrained minimum of ρ, and its minimum value tends to 1.

Its upper minimum is the unique global constrained minimum of ρ on $\Sigma_n^+ \cap \mathcal{U}$.

Consequently, this component is the canonical negative-pole Type 2 component under the stripwise normalization of Definition 2.20. Its two Goodspeed zeros are Type 2, with quasi-index $c = -n$.

In particular, for every fixed $R > 1$, the eventual selected components are independent of R.

Proof. Write

$$z = -n + \frac{w}{n}.$$

On every fixed annulus $0 < a \le |w| \le b$, Gamma recurrence gives

$$\Gamma\left(-n + \frac{w}{n}\right) = O((n-1)!^{-1})$$

and, uniformly with fixed-order derivatives,

$$W\left(-n + \frac{w}{n}\right) = -\frac{1}{n} + O(n^{-3}).$$

Consequently,

$$S\left(-n + \frac{w}{n}\right) = \frac{(-1)^{n+1}}{w} + O(n^{-2}) + O((n-1)!^{-1}). \tag{G1}$$

The radial derivative of the limiting level equation

$$|w|^{-2} - 1 = 0$$

is strictly negative near $|w| = 1$. The implicit-function theorem therefore gives a unique regular radial unit graph

$$w = r_n(\theta)e^{i\theta}, \qquad r_n = 1 + O(n^{-2}).$$

Local radial uniqueness and compactness show that its image is a full component C_n of $\mathcal{U}$.

By (G1), uniformly with the first angular derivative along C_n,

$$\frac{d}{d\theta} \arg S\left(-n + \frac{r_n(\theta)e^{i\theta}}{n}\right) = -1 + O(n^{-2}) < 0.$$

Thus S maps C_n bijectively onto the unit circle, with winding degree -1. In particular, each of the values i and $-i$ is attained exactly once. Complex conjugation identifies the two sheet zeros, and evaluation near the upper point $w = i$ gives the stated sheet.

On the upper arc, write

$$\rho(\theta) = A_n(\theta)\csc^2\theta, \qquad A_n(\theta) = 1 + O(n^{-2})$$

in $C^2[0,\pi]$. Hence

$$\frac{d^2}{d\theta^2}\log\rho(\theta) = 2\csc^2\theta + O(n^{-2}) > 0.$$

The first derivative tends to opposite infinities at the two endpoints. There is therefore one non-degenerate minimum, and its value tends to 1.

It remains to show that no other component in the same pole strip can meet the bounded-ρ seed band.

Suppose that

$$z = -n + u \in \Sigma_n^+, \qquad |S(z)| = 1, \qquad \rho(z) \le R.$$

If $|u| \ge 1/(2n)$, Gamma recurrence, Euler's integral estimate, and $|u - j| \ge j - 1/2$ for $j \ge 1$ give

$$|\Gamma(-n+u)| \le \frac{2nC}{\prod_{j=1}^{n}(j-1/2)} = o(n^{-A})$$

for every fixed $A > 0$.

Thus

$$W(z) = \frac{1}{z} + o(n^{-A}).$$

The unit-level bound $|W(z)| \geq \Im z$ implies $\Im z = O(n^{-1})$. The equality

$$|\sin(\pi z)| = |\sin(\pi W(z))|$$

then implies

$$|\Re u| = O(n^{-1}), \qquad |nu| = 1 + O(n^{-1}).$$

Such points lie on the unique annular unit component already constructed.

Now suppose $|u| < 1/(2n)$. If nu stays away from zero along a subsequence, (G1) implies

$$|S(z)| > 1$$

for all sufficiently large n. It remains to exclude $nu \longrightarrow 0$.

The seed-band inequality gives

$$|W(z)| \leq \sqrt{R}\,\Im z \leq \sqrt{R}\,|u|,$$

so that

$$\Gamma(z) = zW(z) - 1 = -1 + o(1).$$

The simple-pole expansion

$$\Gamma(-n + u) = \frac{(-1)^n}{n!\,u}(1 + o(1))$$

forces

$$u = \frac{(-1)^{n+1}}{n!}(1 + o(1)).$$

On this smaller scale, W has a unique nearby simple real zero ξ_n, with

$$|W'(\xi_n)| = \frac{n!}{n}(1 + o(1)).$$

The same local expansion, uniformly on the segment joining ξ_n to z, gives

$$|W(z)| \geq (1 + o(1))\frac{n!}{n}|z - \xi_n| \geq (1 + o(1))\frac{n!}{n}\Im z.$$

This contradicts $|W(z)| \leq \sqrt{R}\,\Im z$.

Thus every seeded unit-level point in Σ_n^+ belongs to C_n. Since

$$\Re W(z) = -\frac{1}{n} + O(n^{-3}) \neq 0 \qquad (z \in C_n),$$

we have

$$|\sin(\pi W(z))| < \sinh(\pi |W(z)|).$$

On $|S(z)| = 1$, this implies

$$\sinh(\pi \Im z) \leq |\sin(\pi z)| = |\sin(\pi W(z))| < \sinh(\pi |W(z)|),$$

and hence $\rho(z) > 1$ on C_n^+. Since the minimum of ρ on C_n^+ tends to 1, the component meets E_R for every fixed $R > 1$ and all sufficiently large n.

We now identify the distinguished minimizer without appealing to any prior Type 2 classification.

Let m_n be the unique minimum of ρ on $C_n^+ = C_n \cap \{\Im z > 0\}$, whose existence and nondegeneracy were proved above. Since

$$\rho(m_n) \longrightarrow 1,$$

we have $\rho(m_n) < 2$ for all sufficiently large n.

The stripwise exclusion just established, applied with $R = 2$, shows that every

$$z \in \Sigma_n^+ \cap \mathcal{U}, \qquad \rho(z) \leq 2,$$

belongs to C_n.

If $\rho(z) > 2$, then $\rho(z) > \rho(m_n)$. Otherwise z belongs to C_n^+, where m_n is the unique minimum. Consequently,

$$\boxed{m_n = \arg\min_{\substack{z\in\Sigma_n^+ \\ |S(z)|=1}} \rho(z)}$$

and this global constrained minimum is unique.

Moreover, the parametrization of C_n gives

$$[\Re m_n] = -n.$$

Thus $m_n = m_{-n}$ under the negative-strip normalization of Definition 2.20.

Finally, C_n is a regular Jordan curve, and the restriction

$$S|_{C_n} : C_n \longrightarrow \mathbb{S}^1$$

has strictly monotone lifted argument and degree -1, as proved above. Continuation from m_{-n} along this regular unit-level curve therefore reaches each of the sheet values i and $-i$ exactly once.

These are precisely the two Goodspeed zeros on C_n. By the analytic Type 2 assignment of Definition 2.4, they belong to the distinguished Type 2 continuation from m_{-n} and inherit the quasi-index $c = -n$. □

Theorem 2.22 (Independent pole orientation and phase-index coincidence)**.** *Let C_n be the canonical components of Theorem 2.21. For all sufficiently large n, define*

$$\mu_n = (-1)^n, \qquad a_n = \frac{1}{\sqrt{n\,n!}},$$

and

$$\mathcal{A}_\mu = \{z = x + iy : y > 0, \quad \Im\phi_\mu(z) = 0\}, \qquad \mu = \pm 1.$$

Within

$$0 < |z + n| \le \frac{1}{2n}, \qquad \Im z > 0,$$

the set $\mathcal{A}_{-\mu_n}$ is empty, whereas $\mathcal{A}_{\mu_n}$ is a unique regular upper radial arc of the form

$$z = -n + a_n r_n^{\mathrm{A}}(\theta) e^{i\theta}, \qquad 0 < \theta < \pi, \qquad r_n^{\mathrm{A}} = 1 + O(n^{-2}).$$

Thus the enclosed pole determines the independent geometric orientation

$$\mu_{\mathrm{geo}}(C_n) := -\operatorname{sgn}\operatorname{Res}_{z=-n} W(z) = (-1)^n.$$

Moreover, on the entire open upper arc $C_n^+ = C_n \cap \{\Im z > 0\}$,

$$c_{\mathrm{ph}}(z) = -n.$$

Consequently,

$$\mu_{\mathrm{geo}}(C_n) = (-1)^{c_{\mathrm{ph}}(z)} \qquad (z \in C_n^+).$$

The conjugate zero has the same phase index by the upper-representative convention.

Proof. Gamma recurrence gives

$$\operatorname{Res}_{z=-n} W(z) = \frac{(-1)^{n+1}}{n\,n!} = -\mu_n a_n^2.$$

Writing $u = z + n$, subtract the principal part to obtain

$$W(-n + u) = -\frac{\mu_n a_n^2}{u} + V_n(u),$$

where V_n is analytic and real-symmetric, and

$$\sup_{|u|\le 1/(2n)} |V_n'(u)| = O(n^{-2}).$$

For $u = re^{i\theta}$ in the upper half-plane, real symmetry yields

$$\frac{\Im W(-n+u)}{\Im u} = \frac{\mu_n a_n^2}{r^2} + O(n^{-2}).$$

The equation $\Im\phi_\mu = 0$ is

$$\frac{\Im W}{\Im u} = \mu.$$

The opposite orientation is therefore impossible. For $\mu = \mu_n$, the radial equation has exactly one regular solution, with $r = a_n(1+O(n^{-2}))$. This proves the auxiliary-arc assertion and independently determines μ_{geo}.

We next calculate the normalized phase. For every fixed $0 < a < b$, put

$$u = z + n, \qquad \frac{a}{n} \le |u| \le \frac{b}{n}, \quad \Im u > 0.$$

The Gamma recurrence and the prescribed upper-half-plane logarithm imply, for all sufficiently large n,

$$L_P(z) = \operatorname{Log}(1+\Gamma(z)) - \operatorname{Log} z - 2\pi i \left\lceil \frac{n}{2} \right\rceil.$$

In particular,

$$\Im L_P(z) = -\left(2\left\lceil \frac{n}{2} \right\rceil + 1\right)\pi + \delta_n(z),$$

where

$$\delta_n(z) = \frac{\Im z}{n}\left(1 + O_{a,b}(n^{-2}) + O_{a,b}(n^3/n!)\right) > 0$$

and $\delta_n(z) < \pi$ eventually.

Hence

$$\left\lfloor 2 + \frac{\Im L_P(z)}{\pi} \right\rfloor = 1 - 2\left\lceil \frac{n}{2} \right\rceil.$$

As $[\Re z] = -n$ eventually, the negative-pole correction in Definition 2.6 is 1 for even n and 0 for odd n. In either case,

$$c_{\mathrm{ph}}(z) = -n.$$

The canonical upper arc C_n^+ lies in such a fixed pole annulus by Theorem 2.21. This proves the phase assertion.

Finally,

$$\mu_{\mathrm{geo}}(C_n) = (-1)^n = (-1)^{-n} = (-1)^{c_{\mathrm{ph}}(z)},$$

as required. □

Remark 2.23 (Different scales of the two geometries). The canonical unit oval has scale $|z+n| \asymp n^{-1}$, whereas its independently oriented auxiliary arc has scale

$$|z+n| \asymp (n\,n!)^{-1/2}.$$

These are not the same curve, and the inner auxiliary arc is not contained in $|S| = 1$.

Their association is supplied by the uniquely enclosed pole and its residue, rather than by a literal continuation within the unit level.

The theorem is eventual and does not establish a global Type 2 selector.

Theorem 2.24 (Detached unit ovals beyond every fixed GBC seed band)**.** *For every sufficiently large positive integer N, there exists a full compact regular Jordan component C_N^+ of*

$$\{z : \Im z > 0,\ |S(z)| = 1\},$$

lying near the upper local inverse of $W = -N$.

Uniformly for $z \in C_N^+$,

$$\Im z = N^{-1/2}(1 + O(N^{-1})), \qquad \rho(z) = N^3(1 + O(N^{-1})).$$

The component contains exactly two Goodspeed zeros, both in the upper half-plane, with opposite sheet signs.

Consequently, for every fixed $R > 1$, all sufficiently large C_N^+ are disjoint from the GBC seed band E_R.

In particular, full-component selection using a fixed band $1 < \rho \le R$ cannot reach all compact upper unit-level components.

Proof. The function

$$H(z) := z^2 W(z) = \Gamma(1+z) + z$$

extends holomorphically across $z = 0$ and satisfies $H(0) = 1$.

Choose the holomorphic square root of H that equals 1 at the origin. Then

$$Q(z) := \frac{z}{\sqrt{H(z)}}$$

has $Q(0) = 0$ and $Q'(0) = 1$, so it has a local holomorphic inverse χ.

By construction,

$$W(\chi(q)) = q^{-2}.$$

For t in a fixed disc, define

$$z_N(t) = \chi\left(iN^{-1/2}\left(1 - \frac{t}{N^{3/2}}\right)^{-1/2}\right).$$

For large N this is a univalent holomorphic coordinate, and

$$W(z_N(t)) = -N + \frac{t}{\sqrt{N}}$$

holds exactly.

Expansion of the inverse germ gives

$$z_N(0) = iN^{-1/2} + O(N^{-1})$$

with real part $O(N^{-1})$, and

$$z_N(t) - z_N(0) = \frac{it}{2N^2} + O(N^{-5/2})$$

uniformly for bounded t.

Consequently,

$$S(z_N(t)) = (-1)^{N+1} it + O(N^{-1/2}), \tag{G2}$$

uniformly and holomorphically on every fixed t-disc.

On $|t| = 2$, equation (G2) gives $|S(z_N(t))| > 1$ for sufficiently large N. Furthermore, for every $|s| \le 1$, Rouché's theorem, applied to $S(z_N(t)) - s$, gives exactly one simple root in $|t| < 2$.

The inverse images of the unit circle under the resulting analytic inverse therefore form a regular Jordan curve. Its image under z_N is a full compact component C_N^+ of $|S| = 1$.

Since

$$\Im z_N(t) = N^{-1/2}(1 + O(N^{-1}))$$

uniformly on this curve, it lies entirely in the upper half-plane.

The inverse map takes each value s with $|s| = 1$ exactly once. In particular, $S = i$ and $S = -i$ each occur once on C_N^+, giving exactly two Goodspeed zeros of opposite sheets.

Finally,

$$|W(z_N(t))|^2 = N^2(1 + O(N^{-3/2}))$$

and

$$(\Im z_N(t))^2 = N^{-1}(1 + O(N^{-1})).$$

Hence

$$\rho(z_N(t)) = N^3(1 + O(N^{-1}))$$

uniformly on C_N^+.

The minimum of ρ on these components tends to infinity. Therefore no fixed band E_R can meet all of them. □

Remark 2.25 (Scope of the seed obstruction). The preceding theorem proves the existence and separation of the compact unit-level components. It does not independently assign their zeros to the original Type 2 class.

Thus the obstruction is to a global *fixed-band component selection rule*. A broader classification might still use varying-level continuation, a canonical ancestry construction, or another intrinsically specified geometric mechanism.

Such a mechanism would require separate proofs of uniqueness, exclusivity, and Type compatibility.

Let $D_\Psi \subseteq Z(G)$ denote the set of zeros for which the analytic family and continuation labels are uniquely assigned and yield a state in the formal admissible set $\mathcal{A}$ of Definition 2.26. For $z \in D_\Psi$, write

$$\Psi(z) = \big(\tau(z), \mu(z), c(z), k(z), \varepsilon(z)\big).$$

No assertion that

$$D_\Psi = Z(G)$$

is made at this stage.

For Type 1 zeros, the rounding formulas above are defined whenever the family label is assigned.

For Type 2, the original quasi-index c is determined by the distinguished minimizer and its continuation sequence wherever that assignment has been established. Definition 2.6 provides a pointwise phase-based candidate c_{ph}, conjectured to coincide with c globally. The location index k remains the corresponding continuation index with its prescribed half-integer normalization. The relation

$$\mu = (-1)^c$$

does not by itself define the Type 2 labels, and no globally valid nearest-integer formula for the Type 2 location index k is assumed.

The four-tuple

$$(\tau, \mu, c, k)$$

is the TUCK coordinate and the five-tuple

$$(\tau, \mu, c, k, \varepsilon)$$

is the TUCKE coordinate.

The terminology is mnemonic: TUCK denotes the ordered four-tuple (τ, μ, c, k), while TUCKE denotes the same coordinate with the sheet entry ε appended.

The following sheet-sign identities are used only on the analytic branches for which the corresponding continuation results have been proved. For a generated Family $(-i)$ branch with real shadow x_C, the corresponding branchwise sheet law is

$$\varepsilon(z) = \tau(z)(-1)^{c(z)+k(z)} \operatorname{sgn} W'(x_C),$$

under the crossing-exclusion hypotheses of the corresponding real-shadow result.

For Type 2, along a regular continuation sequence on which the sheet law has been anchored,

$$\varepsilon = \tau\mu(-1)^k.$$

Since $\mu = (-1)^c$, these formulas may be written, whenever the relevant analytic hypotheses have been established, as

$$\varepsilon(z) = \tau(z)(-1)^{c(z)+k(z)}\mathfrak{o}_R(z),$$

where

$$\mathfrak{o}_R = \begin{cases} 0, & \mu = i, \\ \operatorname{sgn} W'(x_C), & \mu = -i, \\ 1, & \mu = \pm 1. \end{cases}$$

These analytic identities are not asserted here as global theorems for all zeros. In Definition 2.26 below, the corresponding sheet rules are instead part of the definition of the formal admissible TUCKE set.

The intrinsic definition of the sheet invariant remains

$$\varepsilon(z) = -iS(z)$$

for every non-real zero.

2.2. **The formal admissible TUCKE set.** We now isolate the combinatorial object on which the normalization is proved.

The admissibility conditions below are formal. In particular, the Family $(-i)$ ranges encode the Wilson real-shadow geometry suggested by Conjecture 2.1 and by the branchwise results presently available, but we do not assume that every analytic Family $(-i)$ zero satisfies these ranges. The question whether the analytic zero set realizes the formal admissible set is isolated later in the Fundamental Classification Conjecture.

The two kinds of admissibility conditions encode different pieces of the previously developed analytic geometry. The sets K_c record the allowed phase-continuation indices on the Type 2 sequences, whereas the Family $(-i)$ inequalities compare the integer quasi-index c with the Wilson critical values β_k; the nonnegative-k rules additionally record the branchwise sheet normalization. These analytic origins motivate Definition 2.26, but they are not reproved here. From this point onward, the normalization results use only the explicitly stated formal set $\mathcal{A}$. Thus the combinatorial conclusions of Sections 2.3–2.7 are unconditional statements about Definition 2.26, independently of the still-conjectural realization of every formal state by a zero of G.

For $n \in \mathbb{P}_1$, write

$$w_n := W(n).$$

For each negative integer k, let x_k be the unique zero of W' in $(k, k+1)$, and put

$$\beta_k := W(x_k).$$

Thus x_k is the distinguished critical point of W on $(k, k+1)$; it is not a local minimum of G.

For Type 2 define the admissible location set $K_c \subset \mathbb{Z}$ by

$$K_c = \begin{cases} \left\{ c + \dfrac{-1+(-1)^c}{2} \right\}, & c \le -4, \\ \{-4, -3\}, & c = -3, \\ \{-3, -2, -1, 0\}, & c = -2, \\ \{-4, -3, -2, -1, 0, 1, 2, 3\}, & c = -1, \\ \{k \in \mathbb{Z} : k \ge -5\}, & c = 0, \\ \{k \in \mathbb{Z} : k \le 2\}, & c = 1, \\ \{k \in \mathbb{Z} : k \ge 2\}, & c = 2, \\ \mathbb{Z}, & c \ge 3. \end{cases}$$

Definition 2.26 (Formal admissible TUCKE set)**.** Let $\mathscr{A}$ be the union of the following formal states.

Family (i)**.** For $n \in \mathbb{P}_1$,

$$(\tau, \mu, c, k, \varepsilon) = (0, i, W(n), n-1, 0).$$

Family $(-i)$**.** Here

$$\tau \in \{\pm 1\}, \qquad \mu = -i, \qquad c \in \mathbb{Z}.$$

For $k < 0$, admissibility is

$$\begin{cases} c > \beta_k,\ c \neq 0, & k = -3, \\ c > \beta_k, & k \text{ odd},\ k \neq -3, \\ c < \beta_k, & k \text{ even}, \end{cases}$$

and both values

$$\varepsilon = \pm 1$$

are retained formally.

For $k = 0$,

$$c \geq 3, \qquad \varepsilon = \tau(-1)^{c+1}.$$

For $k > 0$,

$$\min\{W(k), W(k+1)\} < c < \max\{W(k), W(k+1)\},$$

and

$$\varepsilon = \tau(-1)^{c+k}.$$

Type 2. Here

$$\tau \in \{\pm 1\}, \qquad c \in \mathbb{Z}, \qquad k \in K_c,$$

with

$$\mu = (-1)^c$$

and

$$\varepsilon = \tau\mu(-1)^k.$$

The set $\mathscr{A}$ is a formal admissibility set. The assertion that every element of $\mathscr{A}$ is realized by exactly one zero of G will remain conjectural.

2.3. **Normalized Gaussian lattice coordinates.** The raw (k, c)-geometry is not well adapted to the global classification. We now introduce a normalization which separates the two Types.

Definition 2.27 (Normalized Goodspeed lattice coordinate)**.** Let

$$a = (\tau, \mu, c, k, \varepsilon) \in \mathscr{A}.$$

For a Type 1 state put

$$u := k, \qquad v := \begin{cases} -c, & k \geq 0, \\ (-1)^k c, & k < 0. \end{cases}$$

Define

$$D_1(u, v) := \begin{cases} (2v - 2, 0), & u \geq 4, \\ (u, v), & u < 4. \end{cases}$$

For a Type 2 state put

$$u := k - c + \frac{1 - \mu}{2}, \qquad v := c.$$

Since $\mu = (-1)^c$,

$$u = k - 2\left\lfloor \frac{c}{2} \right\rfloor.$$

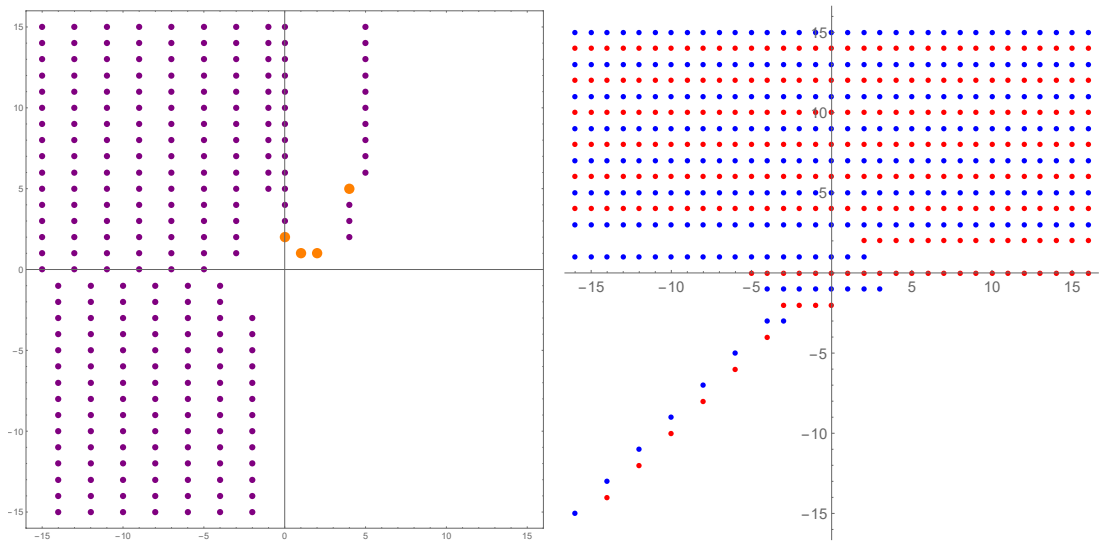


FIGURE 4. Left: The Type 1 admissible $k + ic$ with $|k|, |c| \leq 15$ before normalization. Points corresponding to $\mathbb{P}_1$ appear in orange. Points corresponding to Family (-i) zeros of G appear in purple. Right: The Type 2 admissible $k+ic$ with $|k|, |c| \leq 15$ before normalization. Points obtained from Family (1) zeros are shown in red while Points obtained from Family (-1) zeros are shown in blue.

Define

$$D_2 : \mathbb{Z}^2 \longrightarrow \mathbb{Z}^2$$

on the formal Type 2 lattice by

$$D_2(u,v) := \begin{cases} (-1,2), & (u,v) = (-5,0), \\ (v+1,2), & u = 0, \quad v \leq -3, \\ (v,-u-2), & (u,v) \in \{(0,-2),(1,-1),(2,-1)\}, \\ (u,v), & \text{otherwise.} \end{cases}$$

The final normalized lattice coordinates are

$$(\widehat{k}(a), \widehat{c}(a)) := \begin{cases} D_1(u,v), & a \text{ is Type 1}, \\ D_2(u,v), & a \text{ is Type 2}. \end{cases}$$

Define

$$\widehat{\xi}_G(a) := \widehat{k}(a) + i\widehat{c}(a) \in \mathbb{Z}[i].$$

For $z \in D_\Psi$, write

$$\widehat{\xi}_G(z) := \widehat{\xi}_G(\Psi(z)).$$

The Type 1 map folds the Wilson columns into the lower half-plane and compresses the positive Wilson geometry onto the negative even real axis. The Type 2 map first straightens the parity staircase and then moves the residual intersections into previously vacant lattice sites.

The finite exceptional relocations in D_2 are a normalization convention chosen to make the two Types disjoint and to simplify the planar image. No intrinsic analytic canonicity is claimed for these particular relocations; their role is to provide an explicit injective straightening with the geometric properties proved below.

2.4. **Geometry of the normalized formal lattice.** Let

$$\widehat{\mathcal{A}}_1^{\mathrm{form}}, \widehat{\mathcal{A}}_2^{\mathrm{form}} \subset \mathbb{Z}^2$$

denote the final normalized Type 1 and Type 2 formal admissible lattices.

Lemma 2.28 (Negative Wilson thresholds)**.** *For the critical values defined above,*

$$4 < \beta_{-1} < 5, \qquad -3 < \beta_{-2} < -2, \qquad -1 < \beta_k < 0 \quad (k \le -3).$$

Consequently, for negative k, the Family $(-i)$ admissibility conditions of Definition 2.26 reduce to

k	*admissible integers* c
-1	$c \ge 5$
-2	$c \le -3$
-3	$c \ge 1$
$k \le -5$ *odd*	$c \ge 0$
$k \le -4$ *even*	$c \le -1$.

Proof. Set

$$F(x) := x\Gamma'(x) - \Gamma(x).$$

Then

$$W'(x) = \frac{F(x) - 1}{x^2}, \qquad F'(x) = x\Gamma''(x).$$

Writing

$$\Gamma''(x) = \Gamma(x)\big(\psi(x)^2 + \psi_1(x)\big),$$

where $\psi = \Gamma'/\Gamma$ and $\psi_1 = \psi'$, and using $\psi_1(x) > 0$ away from the real poles, we see that $\Gamma''(x)$ has the same sign as $\Gamma(x)$. Since $x < 0$, it follows that F is strictly increasing on $(k, k+1)$ when k is odd and strictly decreasing there when k is even. Hence W' has at most one zero in each negative unit interval.

Moreover, $W(x)$ tends to $+\infty$ at both endpoints when k is odd and to $-\infty$ at both endpoints when k is even. Thus an interior critical point exists, and the preceding monotonicity shows that it is unique.

Now write $k = -n$, with $n \ge 3$. At the midpoint,

$$\left|\Gamma\left(-n + \frac{1}{2}\right)\right| = \frac{4^n n!\sqrt{\pi}}{(2n)!} < 1.$$

For odd k, W assumes a negative value at the midpoint, so its unique minimum satisfies $\beta_k < 0$. Whenever $W(x) < 0$ on this interval one has

$$-\frac{1}{n-1} < W(x) < 0,$$

and therefore

$$-1 < \beta_k < 0.$$

For even $k \le -4$, one has $W(x) < 0$ throughout the interval, while at the midpoint

$$W\left(-n + \frac{1}{2}\right) > -\frac{2}{n - \frac{1}{2}} > -1.$$

Since β_k is the unique maximum, again

$$-1 < \beta_k < 0.$$

It remains to treat $k = -1, -2$. Rigorous outward interval evaluation of the equations $W'(x) = 0$ brackets the two critical points by

$$-\frac{626988879}{10^9} < x_{-1} < -\frac{626986878}{10^9},$$

and

$$-\frac{1652727074}{10^9} < x_{-2} < -\frac{1652725073}{10^9}.$$

The corresponding directed interval evaluations give

$$4.4680805 < \beta_{-1} < 4.4682615$$

and

$$-2.0448204 < \beta_{-2} < -2.0447760.$$

In particular,

$$4 < \beta_{-1} < 5, \qquad -3 < \beta_{-2} < -2.$$

The stated integer ranges now follow immediately from Definition 2.26, including its separate exclusion $c \neq 0$ when $k = -3$. □

Proposition 2.29 (Disjointness)**.** *One has*

$$\widehat{\mathcal{A}}_1^{\mathrm{form}} \cap \widehat{\mathcal{A}}_2^{\mathrm{form}} = \varnothing.$$

Moreover,

$$\widehat{\mathcal{A}}_1^{\mathrm{form}} \cap (\mathbb{Z} \times \{0\}) = \{(m, 0) : m \leq -5\},$$

whereas

$$\widehat{\mathcal{A}}_2^{\mathrm{form}} \cap (\mathbb{Z} \times \{0\}) = \{(m, 0) : m \geq -4\}.$$

Hence

$$\mathbb{Z} \times \{0\} = \big(\widehat{\mathcal{A}}_1^{\mathrm{form}} \cap (\mathbb{Z} \times \{0\})\big) \dot{\cup} \big(\widehat{\mathcal{A}}_2^{\mathrm{form}} \cap (\mathbb{Z} \times \{0\})\big).$$

In particular, the normalized Gaussian coordinate determines the Type of a formally admissible state.

Proof. The normalized Type 1 lattice lies in

$$\widehat{c} \leq 0,$$

while the normalized Type 2 lattice has no points with

$$\widehat{c} \leq -5.$$

It therefore suffices to compare the five rows

$$\widehat{c} = 0, -1, -2, -3, -4.$$

By Lemma 2.28, the Type 1 and Type 2 rows are respectively

Type 1

$\widehat{c}$	$\widehat{k}$
0	$\widehat{k} \leq -5$,
-1	$\widehat{k} \leq -3$ or $\widehat{k} \in \{1, 2\}$,
-2	$\widehat{k} \leq -3$ or $\widehat{k} = 0$,
-3	$\widehat{k} \leq -2$ or $\widehat{k} = 0$,
-4	$\widehat{k} \leq -2$ or $\widehat{k} = 0$

Type 2

$\widehat{c}$	$\widehat{k}$
0	$\widehat{k} \geq -4$,
-1	$\widehat{k} \in \{-2, -1, 0, 3, 4, 5\}$,
-2	$\widehat{k} \in \{-2, -1, 1, 2\}$,
-3	$\widehat{k} \in \{-1, 1\}$,
-4	$\widehat{k} = -1$

The rows are pairwise disjoint.

On the real axis, the negative odd sites

$$-5, -7, -9, \ldots$$

come from the $c = 0$ negative Type 1 Wilson columns, whereas the Wilson-ray compression supplies

$$-6, -8, -10, \ldots.$$

This proves the claimed real-axis partition. □

Corollary 2.30 (Quadrant description)**.** *Let*

$$\widehat{\mathcal{A}}^{\mathrm{form}} := \widehat{\mathcal{A}}_1^{\mathrm{form}} \dot\cup \widehat{\mathcal{A}}_2^{\mathrm{form}}.$$

Then:

(i) every lattice point in the second and third quadrants belongs to $\widehat{\mathcal{A}}^{\mathrm{form}}$*;*
(ii) the first quadrant is completely filled except for the half-ray

$$\{(\widehat{k}, 1) : \widehat{k} \geq 3\};$$

(iii) the fourth quadrant contains exactly the eight points

$$\mathcal{E}_4 = \{(1,-1),(2,-1),(3,-1),(4,-1),(5,-1),\\ (1,-2),(2,-2),(1,-3)\};$$

(iv) both coordinate axes are completely filled.

Proof. For $\widehat{c} \geq 3$, every Type 2 horizontal row is filled. The row $\widehat{c} = 2$ acquires its negative half through D_2, and hence is also completely filled. At height $\widehat{c} = 1$, admissibility is exactly

$$\widehat{k} \leq 2,$$

giving the missing first-quadrant half-ray.

For negative imaginary coordinate, the low-row description in the proof of Proposition 2.29 fills the entire negative $\widehat{k}$-side and yields precisely the eight listed fourth-quadrant exceptions. For $\widehat{c} \leq -5$, Type 1 fills the half-plane $\widehat{k} \leq 0$. The assertions about the axes follow from the same row description and the real-axis partition. □

2.5. **Recovery of the family invariant.** The normalized position contains more information than the Type alone.

Proposition 2.31 (Positional family recovery)**.** *Let*

$$\xi = \widehat{\xi}_G(a) = \widehat{k} + i\widehat{c} \in \widehat{\mathcal{A}}^{\mathrm{form}}$$

for a formal state $a \in \mathscr{A}$*. Then the family invariant* μ *is uniquely determined by* ξ*.*

Define the normalized real Family (i) *seam by*

$$\widehat{\mathcal{S}}_i := \{(0,-2),(1,-1),(2,-1)\} \cup \left\{\big(-2(W(p)+1), 0\big) : p \in \mathbb{P},\ p \geq 5\right\}.$$

Then

$$\mu = i \iff (\widehat{k}, \widehat{c}) \in \widehat{\mathcal{S}}_i.$$

If

$$(\widehat{k}, \widehat{c}) \in \widehat{\mathcal{A}}_1^{\mathrm{form}} \setminus \widehat{\mathcal{S}}_i,$$

then

$$\mu = -i.$$

Finally, if

$$(\widehat{k}, \widehat{c}) \in \widehat{\mathcal{A}}_2^{\mathrm{form}}$$

and

$$(u, v) = D_2^{-1}(\widehat{k}, \widehat{c}),$$

then

$$c = v, \qquad \mu = (-1)^v.$$

Proof. Proposition 2.29 first determines the Type.

For Type 1, Family (i) is precisely the arithmetic Wilson seam. The zeros $1, 2, 3$ give

$$(0, -2), \qquad (1, -1), \qquad (2, -1).$$

For $p \geq 5$ prime, the Wilson-ray compression sends

$$(p-1, -W(p)) \longmapsto \big(-2(W(p)+1), 0\big).$$

All remaining Type 1 lattice points belong to Family $(-i)$.

For Type 2, the non-trivial images of D_2 are pairwise distinct and land in vacancies of the unchanged Type 2 lattice. Thus D_2 is injective on the formal Type 2 set, so the normalized point determines its unique preimage (u, v). Since $v = c$,

$$\mu = (-1)^c = (-1)^v.$$

□

Corollary 2.32 (Residual half-plane ambiguity)**.** *For a non-real formal state*

$$a = (\tau, \mu, c, k, \varepsilon) \in \mathscr{A},$$

define its formal conjugate by

$$a^* := (-\tau, \mu, c, k, -\varepsilon).$$

Then $a^* \in \mathscr{A}$ and

$$\widehat{\xi}_G(a^*) = \widehat{\xi}_G(a), \qquad \tau(a^*) = -\tau(a).$$

Thus the normalized Gaussian coordinate does not determine the half-plane invariant for a non-real formal state.

Whenever an actual conjugate pair $z, \bar{z}$ is known to carry formal states related by this involution, one likewise has

$$\widehat{\xi}_G(\bar{z}) = \widehat{\xi}_G(z).$$

No global conjugation-compatibility theorem for the analytic classification data is assumed here.

2.6. **The five-state residual coordinate.**

Definition 2.33 (Conjugation-invariant sheet product)**.** For

$$a = (\tau, \mu, c, k, \varepsilon) \in \mathscr{A},$$

define

$$\delta(a) := \begin{cases} 0, & \mu = i, \\ \tau\varepsilon, & \mu \neq i. \end{cases}$$

For a non-real zero,

$$\delta(z) \in \{\pm 1\}.$$

Conjugation reverses both τ and ε, and therefore

$$\delta(\overline{z}) = \delta(z).$$

Whenever the real-shadow orientation is defined,

$$\delta = (-1)^{c+k} \mathfrak{o}_R.$$

Proposition 2.34 (Type 2 positional recovery of δ)**.** *Let*

$$\xi = \widehat{\xi}_G(a) \in \widehat{\mathcal{A}}_2^{\mathrm{form}}, \qquad (u, v) = D_2^{-1}(\xi).$$

Then

$$c = v, \qquad k = u + v - \frac{1-\mu}{2},$$

and

$$\delta(\xi) = (-1)^{u+v}.$$

Thus $\widehat{\xi}_G$ determines δ for every Type 2 state.

Proof. For Type 2, $\mathfrak{o}_R = 1$, so $\delta = (-1)^{c+k}$.

Before D_2,

$$v = c, \qquad u = k - c + \frac{1-\mu}{2}.$$

Since $\mu = (-1)^c$,

$$k \equiv u \pmod 2,$$

and hence

$$c + k \equiv v + u \pmod 2.$$

Therefore

$$\delta = (-1)^{u+v}.$$

□

Proposition 2.35 (Residual Family $(-i)$ sheet ambiguity)**.** *The normalized Gaussian coordinate does not determine the sheet invariant in Family $(-i)$.*

Indeed, there exist formally admissible Family $(-i)$ states with identical TUCK coordinates

$$(\tau, \mu, c, k)$$

and opposite sheet signs

$$\varepsilon = \pm 1.$$

Consequently they have the same normalized Gaussian coordinate but distinct TUCKE coordinates.

Hence neither ε nor $\mathfrak{o}_R$ is determined by $\widehat{\xi}_G$ alone in Family $(-i)$.

Example 2.36 (A Type 2 compressed coordinate)**.** *Consider the lower-half-plane zero*

$$z \approx 4.641612387255721 - 1.694838128482682\, i.$$

This zero lies on the Type 2 branch generated from the distinguished minimizer m_2. Thus its Type 2 quasi-index is $c = 2$, and hence $\mu = (-1)^c = 1$. Its phase-continuation index is $k = 5$, while $\tau = \operatorname{sgn} \Im z = -1$. Numerically,

$$W(z) \approx -0.858399346652 - 1.694847637758\, i,$$

so that

$$\phi_1(z) = z - W(z) - \frac{1}{2} \approx 5.000011733907 + 0.000009509275\, i.$$

Thus the straightened coordinate is consistent with the location index $k = 5$.

The same near-integral straightening is visible at neighbouring points of the same Type 2 continuation sequence. For the upper-half-plane $c = 2$ branch, where $\mu = 1$, representative values are

k	4	5	6
z	$4.38987360 + 1.51516848i$	$4.64161239 + 1.69483813i$	$4.85644869 + 1.79909430i$
$\phi_1(z)$	$3.99997021 - 0.00003596i$	$5.00001173 - 0.00000951i$	$6.00000615 + 0.00000486i$
$\lvert\phi_1(z) - k\rvert$	4.67×10^{-5}	1.51×10^{-5}	7.85×10^{-6}

Thus the analytic Type 2 zeros lie very close, in the straightened ϕ_μ-coordinate, to the integer sites of the exact TUCK skeleton.

Moreover,

$$S(z) \approx i,$$

and therefore

$$\varepsilon = -iS(z) = 1.$$

Equivalently, the anchored Type 2 sheet law gives

$$\varepsilon = \tau\mu(-1)^k = (-1)(1)(-1)^5 = 1.$$

Hence

$$\Psi(z) = (-1, 1, 2, 5, 1).$$

For the Type 2 normalization,

$$u = k - c + \frac{1-\mu}{2} = 5 - 2 = 3, \qquad v = c = 2.$$

The point $(3, 2)$ *is not exceptional for* D_2*, so*

$$(\widehat{k}, \widehat{c}) = D_2(3, 2) = (3, 2),$$

and consequently

$$\widehat{\xi}_G(z) = 3 + 2i.$$

Finally,

$$\lambda_5(z) \equiv 2\varepsilon - \tau = 2(1) - (-1) = 3 \pmod 5.$$

Thus the compressed coordinate of this zero is

$$\widehat{C}_{G,5}(z) = (3,\, 3 + 2i).$$

Definition 2.37 (Five-state residual coordinate)**.** For $a \in \mathscr{A}$, define

$$\lambda_5(a) := \tau(a)\big(2\delta(a) - 1\big) \pmod 5.$$

Equivalently,

$$\lambda_5(a) = 2\varepsilon(a) - \tau(a) \pmod 5.$$

The five possible values are

λ_5	τ	δ
0	0	0
1	1	1
2	1	-1
3	-1	-1
4	-1	1.

Thus λ_5 encodes bijectively the five possible pairs

$$(\tau, \delta) \in \{(0,0), (1,1), (1,-1), (-1,-1), (-1,1)\}.$$

Moreover,

$$\lambda_5(\overline{z}) \equiv -\lambda_5(z) \pmod 5.$$

2.7. **Faithfulness of the compressed coordinate.**

Proposition 2.38 (Faithfulness of the five-state compression)**.** *Define*

$$\widehat{T}_5 : \mathscr{A} \longrightarrow (\mathbb{Z}/5\mathbb{Z}) \times \mathbb{Z}[i]$$

by

$$\widehat{T}_5(a) := \big(\lambda_5(a), \widehat{\xi}_G(a)\big),$$

and put

$$\widehat{K}_{G,5} := \widehat{T}_5(\mathscr{A}).$$

Then

$$\widehat{T}_5 : \mathscr{A} \longrightarrow \widehat{K}_{G,5}$$

is a bijection.

Proof. Surjectivity is immediate from the definition of $\widehat{K}_{G,5}$.

For injectivity, λ_5 determines (τ, δ), while Proposition 2.31 shows that $\widehat{\xi}_G$ determines μ.

If $\mu = i$, then $\tau = \delta = \varepsilon = 0$. If $\mu \neq i$, then $\delta = \tau\varepsilon$, so $\varepsilon = \tau\delta$. Thus $(\lambda_5, \widehat{\xi}_G)$ determines (τ, μ, ε).

It remains to recover c and k. For Type 2, the injectivity of D_2 recovers the unique preimage (u, v), and hence

$$c = v, \qquad k = u + v - \frac{1-\mu}{2}.$$

For Type 1, before D_1 the fold is invertible:

$$u = k, \qquad c = \begin{cases} -v, & u \geq 0, \\ (-1)^u v, & u < 0. \end{cases}$$

On the Wilson ray,

$$D_1(u, v) = (2v - 2, 0) = (-2(c+1), 0),$$

so the image recovers c uniquely.

If $\mu = -i$, formal admissibility places c in a unique open Wilson interval

$$W(k) < c < W(k+1), \qquad k \geq 4.$$

If $\mu = i$, then

$$c = W(p), \qquad k = p - 1$$

for a unique prime $p \geq 5$.

For $n \geq 4$,

$$W(n+1) - W(n) = \frac{(n^2 - n - 1)(n-1)! - 1}{n(n+1)} > 0,$$

so $W(n)$ is strictly increasing there and k is uniquely recovered.

Thus

$$(\lambda_5, \widehat{\xi}_G)$$

determines the complete formal TUCKE state. □

Corollary 2.39 (Fibres of the normalized Gaussian coordinate)**.** *For $a \in \mathcal{A}$, let*

$$\mathcal{F}_{\widehat{\xi}_G(a)} := \{b \in \mathcal{A} : \widehat{\xi}_G(b) = \widehat{\xi}_G(a)\}.$$

Then

$$\#\mathcal{F}_{\widehat{\xi}_G(a)} = \begin{cases} 1, & \mu(a) = i, \\ 4, & \mu(a) = -i \text{ and } k(a) < 0, \\ 2, & \mu(a) = -i \text{ and } k(a) \geq 0, \\ 2, & a \text{ is Type 2.} \end{cases}$$

In particular, every fibre has cardinality 1, 2, *or* 4.

Proof. By Proposition 2.31, the normalized Gaussian coordinate determines the Type and the family. The recovery argument in Proposition 2.38 then determines the corresponding values of c and k.

For Family (i), Definition 2.26 fixes

$$(\tau, \varepsilon) = (0, 0),$$

so the fibre has one element.

For Family $(-i)$ with $k < 0$, both values

$$\tau = \pm 1, \qquad \varepsilon = \pm 1$$

are retained independently in the formal admissible set, giving four states over the same normalized Gaussian point.

For Family $(-i)$ with $k \geq 0$, the sheet sign is determined by τ, c, k, so the two choices $\tau = \pm 1$ give exactly two states.

Finally, for Type 2 one has

$$\varepsilon = \tau\mu(-1)^k,$$

so again the two choices of τ give exactly two states. No further states can occur because the Type, family, c, and k have already been recovered from the normalized position. □

Remark 2.40 (Uniformity and the five-state residue). Corollary 2.39 shows that the residue coordinate λ_5 should not be interpreted as a pointwise minimal label for every fibre of $\widehat{\xi}_G$: the fibre cardinality varies between (1), (2), and (4).

Its role is instead uniform. Across the full formal admissible set there are exactly five possible pairs

$$(\tau, \delta) \in \{(0,0), (1,1), (1,-1), (-1,-1), (-1,1)\},$$

and Definition 2.37 identifies these five states with the five elements of $\mathbb{Z}/5\mathbb{Z}$. Moreover formal conjugation acts by

$$\lambda_5 \longmapsto -\lambda_5.$$

Consequently, among cyclic residue spaces required to distinguish all five global (τ, δ) -states by the residue coordinate alone, $\mathbb{Z}/5\mathbb{Z}$ has the smallest possible cardinality. The usefulness of λ_5 is therefore its uniformity and its simple conjugation law, rather than pointwise minimality on each Gaussian fibre.

2.8. **The Fundamental Classification Conjecture.** The preceding results are combinatorial statements about the formal admissible set. The remaining question is whether the analytic zero set realizes that formal structure exactly.

Conjecture 2.41 (Fundamental Classification Conjecture of Goodspeed theory)**.** *The analytic TUCKE assignment is total,*

$$D_\Psi = Z(G),$$

and

$$\Psi : D_\Psi \longrightarrow \mathcal{A}$$

is a bijection. Equivalently, every zero of G possesses a unique formally admissible TUCKE coordinate, and every element of $\mathcal{A}$ is realized by exactly one zero.

Remark 2.42 (Current status of injectivity). The injectivity part of Conjecture 2.41 is already known in several substantial regimes. On the real zero set it is immediate from

$$k(n) = n - 1, \qquad n \in \mathcal{P}_1.$$

For Type 2 zeros, equality of the continuation index k implies equality of the zeros whenever the two points lie on the same regular continuation sequence; the remaining global issue is therefore the possible collision of distinct continuation sequences carrying the same quasi-index c and the same pair (τ, k).

For Family $(-i)$, equality of the TUCKE data places two zeros in the same half-plane, on the same sheet $S(z) = \varepsilon i$, and in the same Gaussian cell for the straightened coordinate ϕ_{-i}. Thus the remaining problem is a signed one-root assertion in each such cell. This uniqueness is known on the certified Wilson–Rouché domains and in several asymptotic regimes, but is not yet proved globally.

Accordingly, the unresolved injectivity problem is considerably more specific than arbitrary non-uniqueness of the TUCKE data: it is reduced to inter-sequence Type 2 collisions and signed Family

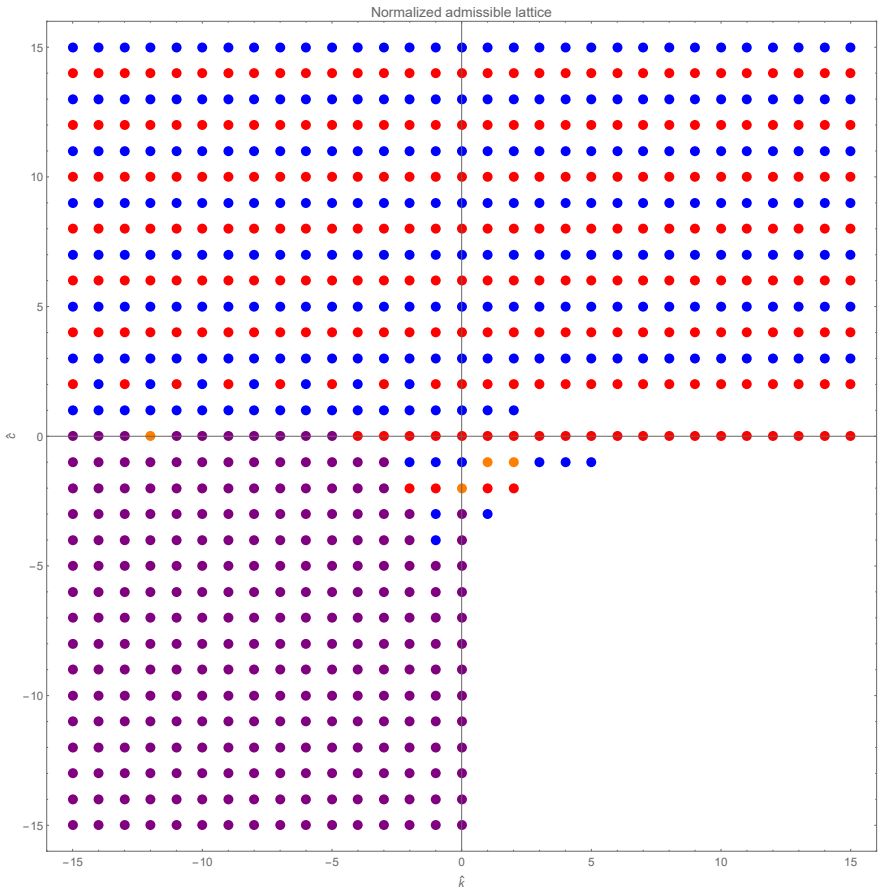


FIGURE 5. The final normalized formal admissible lattice $\widehat{\mathcal{A}}^{\mathrm{form}}$. The second and third quadrants are completely filled; the first quadrant is filled except for the half-ray $\{(\widehat{k}, 1) : \widehat{k} \geq 3\}$; the fourth quadrant contains exactly eight exceptional points; and both coordinate axes are completely filled.

$(-i)$ cell multiplicity. We leave these two analytic uniqueness problems as part of the Fundamental Classification Conjecture.

For $z \in D_\Psi$, define

$$\widehat{C}_{G,5}(z) := \big(\lambda_5(z), \widehat{\xi}_G(z)\big).$$

Since Proposition 2.38 gives a bijection

$$\widehat{T}_5 : \mathcal{A} \longrightarrow \widehat{K}_{G,5},$$

the Fundamental Classification Conjecture is equivalently the assertion that

$$D_\Psi = Z(G)$$

and

$$\widehat{C}_{G,5} : D_\Psi \longrightarrow \widehat{K}_{G,5}$$

is a bijection.

Thus every zero of G is conjecturally represented uniquely by one normalized admissible Gaussian integer and one residue class modulo 5.

Remark 2.43 (Conjugation). For the formal conjugation involution

$$a = (\tau, \mu, c, k, \varepsilon) \longmapsto a^* = (-\tau, \mu, c, k, -\varepsilon),$$

one has

$$\widehat{\xi}_G(a^*) = \widehat{\xi}_G(a), \qquad \lambda_5(a^*) \equiv -\lambda_5(a) \pmod 5.$$

Hence

$$\widehat{T}_5(a^*) = \big(-\lambda_5(a), \widehat{\xi}_G(a)\big).$$

Thus conjugation acts formally by reflection in the finite $\mathbb{Z}/5\mathbb{Z}$-coordinate while leaving the normalized Gaussian coordinate fixed. For actual zeros, the corresponding statement holds whenever the analytic TUCKE classification is known to respect conjugation.

2.9. **Discussion.** The principal outcome is a separation between two kinds of classification data. The normalized Gaussian coordinate

$$\widehat{\xi}_G = \widehat{k} + i\widehat{c}$$

contains the large-scale discrete geometry: it determines the Type and the family, and its admissible image has an elementary planar description. The residual fibre over a Gaussian lattice point is not of constant size; by Corollary 2.39, its cardinality is (1), (2), or (4), according to the family and branch. The five-state coordinate λ_5 therefore should not be viewed as pointwise minimal on every fibre. Rather, it gives a single uniform encoding of the five possible global half-plane/sheet states (τ, δ), with formal conjugation represented by

$$\lambda_5 \longmapsto -\lambda_5.$$

In this uniform sense the finite residual data are represented by the compact coordinate space

$$(\mathbb{Z}/5\mathbb{Z}) \times \mathbb{Z}[i].$$

The remaining difficulty is not combinatorial compression. It is the analytic realization problem: proving that each formal admissible state corresponds to one and only one zero of G. In this form the Fundamental Classification Conjecture is a global statement about the completeness and uniqueness of the discrete geometry of the zero set.

3. Canonical left-tail geometry and inverse arithmetic

We now pass from the global formal classification to a region in which a substantial part of the non-real geometry can be proved directly. The object of this section is the canonical Family $(-i)$ tail accumulating at the puncture 0.

For every sufficiently large positive integer c, there is a distinguished upper-half-plane zero z_c^+ with canonical state

$$\Psi(z_c^+) = \big(1, -i, c, 0, (-1)^{c+1}\big),$$

and we write

$$z_c^- := \overline{z_c^+}.$$

The construction below proves the existence, uniqueness and simplicity of these zeros independently of the global Fundamental Classification Conjecture. Their sheet values satisfy

$$S(z_c^+) = (-1)^{c+1} i.$$

The local geometry already displays two characteristic scales:

$$\Re z_c^+ \asymp c^{-1/2}, \qquad \Im z_c^+ \asymp c^{-2}.$$

Consequently the conjugate tails approach the puncture along quartic cusps,

$$\Im z \sim \pm \frac{1}{2} (\Re z)^4.$$

Figure 6 shows the surrounding sheet geometry at a visible scale, while Figure 7 resolves the canonical tail, its generating real minima, and the quartic horn used later in the unlabelled inverse problem.

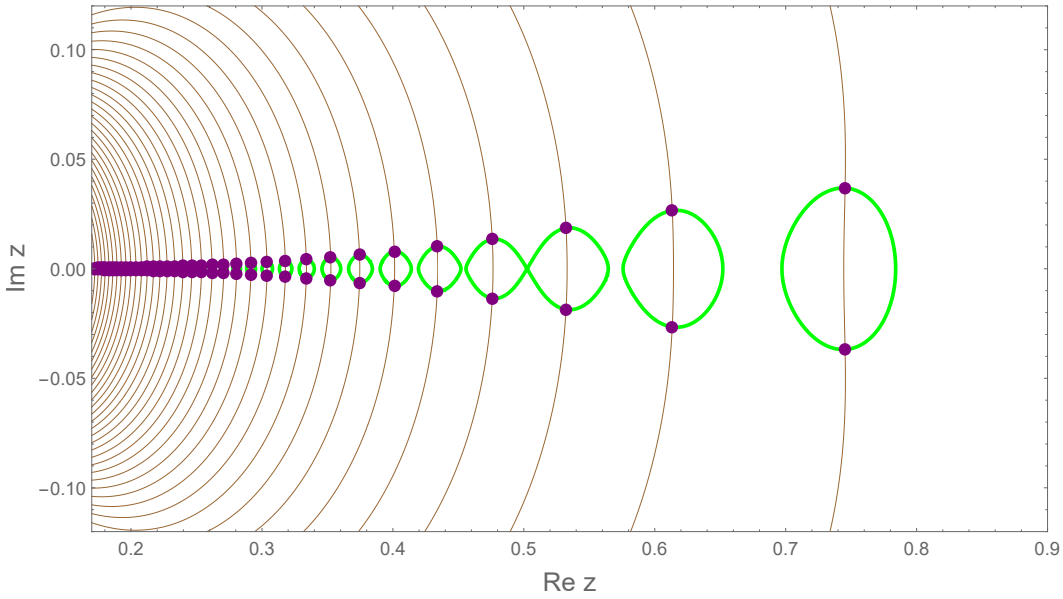


FIGURE 6. Local sheet geometry of the left tail. The unit-level set $|S(z)| = 1$ is shown in green, and the phase locus $\Re S(z) = 0$ is shown in brown. Their non-real intersections satisfy $S(z) = \pm i$ and hence are zeros of G; numerically located Family $(-i)$ zeros are marked in purple. The displayed region lies in $0 < \Re z < 1$ and shows the left-tail geometry before the finer asymptotic quartic structure near the puncture is resolved in Figure 7.

3.1. **Existence, uniqueness and local geometry.** We retain the functions W, G, S of Section 1. The identity

$$z^2 W(z) = \Gamma(1+z) + z$$

gives

$$W(z) = z^{-2} + az^{-1} + b(z), \qquad a := 1 - \gamma, \tag{1}$$

where b is holomorphic near 0 and real on the real axis. This local expansion is the only special-function input required in the proofs below. Choose $\delta \in (0, 1/4)$ sufficiently small that $W'(x) < 0$ for $0 < x < \delta$. For every sufficiently large integer c, define the *left Wilson window*

$$I_c := \left\{ x \in (0, \delta) : |W(x) - c| \le \frac{1}{2} \right\}.$$

Thus I_c is a compact interval on the decreasing positive branch of W. Write

$$D_r(x) := \{z \in \mathbb{C} : |z - x| < r\}.$$

All asymptotic estimates in this section are as $c \to \infty$, equivalently $x_c \to 0^+$, with uniform implied constants.

Theorem 3.1 (Canonical minima and their local zero pairs)**.** *For every sufficiently large integer c, the window I_c contains exactly one real local minimum x_c of G. It satisfies*

$$G'(x_c) = 0, \qquad G''(x_c) > 0, \qquad 0 < G(x_c) < \tfrac{1}{2}.$$

Define

$$\rho_c := \sqrt{\frac{2G(x_c)}{G''(x_c)}}. \tag{2}$$

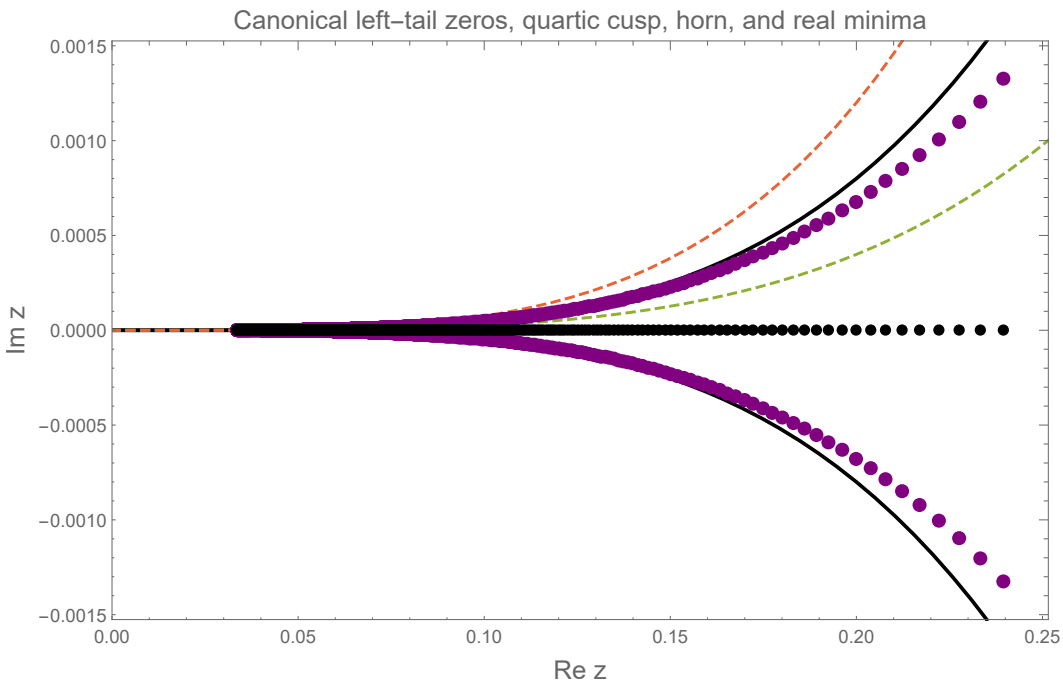


FIGURE 7. Geometry of the canonical left tail. The purple points are the canonical conjugate zero pairs $z_c^{\pm}$ for $20 \le c \le 900$, and the black points are their generating real local minima x_c. The solid black curves are the asymptotic quartic cusps $y = \pm\frac{1}{2}x^4$, along which $z_c^{\pm} \to 0$. The dashed curves $y = \frac{1}{4}x^4$ and $y = \frac{3}{4}x^4$ bound a fixed quartic horn containing the eventual canonical upper tail. This horn later provides an intrinsic way to isolate that tail from the unlabelled non-real zero cloud near the origin.

The natural Rouché neighbourhood $D_{2\rho_c}(x_c)$ contains exactly two zeros of G, counted with multiplicity: one simple upper-half-plane zero z_c^+ and one simple lower-half-plane zero z_c^-. Moreover,

$$z_c^- = \overline{z_c^+}, \qquad \rho_c = \tfrac{1}{2}x_c^4(1 + O(x_c)), \qquad z_c^{\pm} = x_c \pm i\rho_c + O(x_c^6). \tag{3}$$

Proof. For sufficiently small positive x, put

$$r(x) := -\frac{\sin(2\pi x)}{W'(x)}, \qquad d(x) := \frac{1}{2\pi}\arcsin r(x), \tag{4}$$

using the principal real arcsine. From (1),

$$\begin{aligned} W'(x) &= -2x^{-3} - ax^{-2} + O(1), \\ r(x) &= \pi x^4 - \tfrac{a\pi}{2}x^5 + O(x^6), \\ d(x) &= \tfrac{1}{2}x^4 - \tfrac{a}{4}x^5 + O(x^6), \qquad d'(x) = O(x^3). \end{aligned} \tag{5}$$

Here d extends holomorphically across 0, which justifies differentiating its expansion. In particular, $0 < r(x) < 1$ and $0 < d(x) < 1/4$ after shrinking δ.

The identity

$$G'(x) = \frac{\sin(2\pi x) + W'(x)\sin(2\pi W(x))}{\pi}$$

shows that a critical point in I_c satisfies precisely one of

$$W(x) - c = d(x), \qquad W(x) - c = \tfrac{1}{2} - d(x).$$

Both $W(x)-c-d(x)$ and $W(x)-c-\frac{1}{2}+d(x)$ are strictly decreasing on I_c and change sign between its endpoints. Each therefore has exactly one zero. At the first, denoted x_c, the identity

$$G''(x) = 2\cos(2\pi x) + \frac{W''(x)}{\pi}\sin(2\pi W(x)) + 2W'(x)^2\cos(2\pi W(x)) \tag{6}$$

gives $G''(x_c) = 8x_c^{-6}(1+O(x_c)) > 0$. At the second it gives $G''(x) = -8x^{-6}(1+O(x)) < 0$. Thus x_c is the unique local minimum in the window, and it is strict and nondegenerate. Also $x_c \to 0^+$ and

$$W(x_c) - c = d(x_c), \qquad g_c := G(x_c) = x_c^2 + O(x_c^4), \qquad A_c := \tfrac{1}{2}G''(x_c) = 4x_c^{-6}(1+O(x_c)). \tag{7}$$

These estimates give the asserted bounds on $G(x_c)$ and the formula for $\rho_c = \sqrt{g_c/A_c}$.

Write $x = x_c$, $g = g_c$, $A = A_c$ and $\rho = \rho_c$. On the closed disc $|z-x| \le 2\rho = O(x^4)$, the Laurent expansion gives

$$W(z) - c = O(x), \qquad W^{(j)}(z) = O(x^{-j-2}) \quad (1 \le j \le 5). \tag{8}$$

In particular, $\sin(2\pi W(z)) = O(x)$ there. Differentiating the defining expression for G three times therefore yields

$$\sup_{|z-x|\le 2\rho} |G'''(z)| = O(x^{-8}).$$

Taylor's formula, with $h = z - x$, now gives

$$G(x+h) = g + Ah^2 + R(h), \qquad R(h) = O(x^{-8}|h|^3). \tag{9}$$

On $|h| = 2\rho$,

$$|g + Ah^2| \ge 3g \asymp x^2, \qquad |R(h)| = O(x^4).$$

Rouché's theorem consequently gives exactly two zeros, counted with multiplicity, in $D_{2\rho}(x)$. Its intersection with the real axis lies in $(0,1)$, where G is strictly positive. Schwarz symmetry therefore makes the two zeros a nonreal conjugate pair, and the multiplicity count makes each simple.

For the upper zero, $h = z_c^+ - x$, equation (9) gives

$$|(h - i\rho)(h + i\rho)| = O(x^{10}).$$

Since $\Im h > 0$, we have $|h + i\rho| \ge \rho \asymp x^4$, so $h = i\rho + O(x^6)$. Conjugation gives the lower estimate. □

Theorem 3.2 (Integer-indexed asymptotics)**.** *Write*

$$z_c^{\pm} = x_c + \varepsilon_c \pm iY_c, \qquad Y_c > 0.$$

Then

$$x_c = c^{-1/2} + \frac{1-\gamma}{2c} + O(c^{-3/2}), \tag{10}$$

$$Y_c = \frac{1}{2c^2} + \frac{3(1-\gamma)}{4c^{5/2}} + O(c^{-3}), \tag{11}$$

$$\varepsilon_c = -\frac{3}{8c^{7/2}} + O(c^{-4}). \tag{12}$$

More intrinsically,

$$Y_c = \tfrac{1}{2}x_c^4 - \tfrac{1-\gamma}{4}x_c^5 + O(x_c^6), \qquad \varepsilon_c = -\tfrac{3}{8}x_c^7 + O(x_c^8). \tag{13}$$

Proof. Set $x = x_c$ and $a = 1-\gamma$. Equations (1) and (7) give

$$c = x^{-2} + ax^{-1} + O(1).$$

Thus $x^{-1} = \sqrt{c} - a/2 + O(c^{-1/2})$, proving (10). A more precise use of (6) gives

$$A := \tfrac{1}{2}G''(x) = 4x^{-6}(1 + ax + O(x^2)).$$

Since $G(x) = x^2(1 + O(x^2))$, it follows that

$$\rho_c = \tfrac{1}{2}x^4 - \tfrac{a}{4}x^5 + O(x^6).$$

Theorem 3.1 gives $Y_c = \rho_c + O(x^6)$, proving the first estimate in (13).

To recover the smaller horizontal displacement, put

$$B := \tfrac{1}{6}G'''(x) = -12x^{-7}(1 + O(x)), \qquad C := \tfrac{1}{24}G^{(4)}(x) = O(x^{-12}).$$

The formula for B follows from the leading term $G'''(x) = 6W'(x)W''(x)\cos(2\pi W(x)) + O(x^{-5})$. On the disc of Theorem 3.1, (8) also gives

$$\sup|G^{(5)}| = O(x^{-14}).$$

Indeed, the most singular term is a constant multiple of $(W')^5\sin(2\pi W)$, and the extra factor $\sin(2\pi W) = O(x)$ supplies this bound; all other terms are smaller. Consequently, at $h = \varepsilon_c + iY_c = O(x^4)$,

$$0 = G(x + h) = G(x) + Ah^2 + Bh^3 + Ch^4 + O(x^6).$$

The preliminary bounds $\varepsilon_c = O(x^6)$ and $Y_c \sim x^4/2$ show that $C\Im(h^4) = O(x^6)$ and $B\varepsilon_c^2 Y_c = O(x^9)$. Taking imaginary parts therefore yields

$$0 = 2A\varepsilon_c Y_c - BY_c^3 + O(x^6).$$

Since $2AY_c \asymp x^{-2}$,

$$\varepsilon_c = \frac{BY_c^2}{2A} + O(x^8) = -\tfrac{3}{8}x^7 + O(x^8).$$

Finally, (10) gives

$$x_c^4 = c^{-2} + 2ac^{-5/2} + O(c^{-3}), \quad x_c^5 = c^{-5/2} + O(c^{-3}), \quad x_c^7 = c^{-7/2} + O(c^{-4}).$$

Substitution proves (11) and (12). □

Corollary 3.3 (Asymptotic isolation)**.** *Put $\Delta_c := x_c - x_{c+1}$. Then*

$$\Delta_c \sim \frac{1}{2c^{3/2}}, \qquad \frac{Y_c}{\Delta_c} \sim c^{-1/2}, \qquad \frac{\rho_c}{\Delta_c} \sim c^{-1/2}, \qquad \frac{|\varepsilon_c|}{\Delta_c} \sim \frac{3}{4c^2}. \tag{14}$$

In particular,

$$\frac{2\rho_c + 2\rho_{c+1}}{\Delta_c} \sim 4c^{-1/2} \longrightarrow 0, \tag{15}$$

so the natural Rouché discs are pairwise disjoint for all sufficiently large indices. The real parts of successive pairs have spacing $\Re z_c^+ - \Re z_{c+1}^+ \sim \Delta_c$.

Proof. Let $F(x) := W(x) - d(x)$, so that $F(x_c) = c$ and $F'(x) = -2x^{-3}(1 + O(x)) < 0$. The mean value theorem gives

$$\Delta_c = \frac{1}{-F'(\xi_c)}, \qquad \xi_c \in (x_{c+1}, x_c).$$

Since $x_c \sim c^{-1/2}$, also $\xi_c \sim c^{-1/2}$, proving the spacing formula. All the ratios follow from Theorems 3.1 and 3.2. Equation (15) separates successive disc projections on the real axis, and therefore separates all the discs in the eventual tail. Finally, $|\varepsilon_c| + |\varepsilon_{c+1}| = o(\Delta_c)$. □

Proposition 3.4 (Alternating sheets)**.** *For every sufficiently large integer c,*

$$S(z_c^+) = (-1)^{c+1}i, \qquad S(z_c^-) = (-1)^c i. \tag{16}$$

Proof. Write $x = x_c$ and $h = z_c^+ - x$. The foundational estimates give

$$\begin{aligned} W(z_c^+) - c &= d(x) + W'(x)h + O(x^{-4}|h|^2) \\ &= -ix + O(x^2). \end{aligned}$$

As $z_c^+ = x + O(x^4)$,

$$S(z_c^+) = (-1)^c \frac{\sin(\pi(W(z_c^+) - c))}{\sin(\pi z_c^+)} = (-1)^{c+1} i + O(x).$$

But $G(z_c^+) = 0$ implies $S(z_c^+) \in \{i, -i\}$ exactly. The estimate therefore fixes its sign for sufficiently large c. Schwarz symmetry gives the lower sign. □

Corollary 3.5 (Quartic cusp and transversality)**.** *Write $z_c^\pm = X_c \pm iY_c$, where $Y_c > 0$. Then*

$$Y_c \sim \tfrac{1}{2} X_c^4, \qquad x_c - X_c \sim \tfrac{3}{8} X_c^7. \tag{17}$$

In particular, $X_c < x_c$ eventually. Moreover,

$$G'(z_c^\pm) = \pm 4ic\big(1 + O(c^{-1/2})\big), \qquad |G'(z_c^\pm)| \sim 4c, \tag{18}$$

$$S'(z_c^\pm) = 2(-1)^{c+1} c^2 \big(1 + O(c^{-1/2})\big). \tag{19}$$

The real curves $\Re S = 0$ and $|S| = 1$ are regular and meet orthogonally at these zeros. Their tangents are respectively asymptotically vertical and asymptotically horizontal.

Proof. Since $X_c = x_c + O(x_c^7)$, equation (17) follows from (13). For $x = x_c$ and $h = z_c^\pm - x$, the third-derivative bound used in (9) gives

$$G'(x + h) = G''(x)h + O(x^{-8}|h|^2) = \pm 4ix^{-2}(1 + O(x)).$$

As $x_c^{-2} = c(1 + O(c^{-1/2}))$, this proves (18). At a nonreal zero, differentiation of

$$G(z) = \frac{\sin^2(\pi z)}{\pi^2}\big(1 + S(z)^2\big)$$

gives the exact identity

$$G'(z) = \frac{2}{\pi^2} \sin^2(\pi z) S(z) S'(z).$$

Using $\sin^2(\pi z_c^\pm) = \pi^2 x_c^2 (1 + O(x_c^2))$ and Proposition 3.4, we obtain

$$S'(z_c^\pm) = 2(-1)^{c+1} x_c^{-4}(1 + O(x_c)),$$

which is (19). The error terms in these complex derivative estimates are understood in modulus. In particular, $S'(z_c^\pm) \neq 0$. Thus S is conformal locally; the imaginary axis and unit circle meet orthogonally at $\pm i$, so their inverse images do as well. Finally,

$$S'(z_c^\pm)/|S'(z_c^\pm)| = (-1)^{c+1} + O(c^{-1/2}).$$

The tangent directions of the two inverse images consequently tend to the vertical and horizontal directions, respectively. □

The zeros constructed above form the eventual canonical Family $(-i)$ left tail described by the classification framework of Section 2. The TUCKE coordinate conventions are those of Section 2.1. In that notation, the corresponding generating minima are denoted x_C; on the canonical left tail, the local construction and integer indexing developed here identify the relevant label with the canonical quasi-index c, and we therefore write x_c. This identification supplies the family terminology and the interpretation of c as the canonical quasi-index. The existence, asymptotic, and local-geometric assertions above, however, were proved directly from the local expansion of W at the origin and do not depend on the global classification theory.

c	X_c	Y_c	$2Y_c/X_c^4$	$(x_c - X_c)/X_c^7$
20	0.23958909	$1.32684343 \times 10^{-3}$	0.80534424	0.20455646
50	0.14704124	$2.11833965 \times 10^{-4}$	0.90629380	0.28143923
100	0.10261157	$5.24454773 \times 10^{-5}$	0.94613411	0.31937005
200	0.07194523	$1.29743762 \times 10^{-5}$	0.96851971	0.34241402
500	0.04518950	$2.05152260 \times 10^{-6}$	0.98391204	0.35869400
900	0.03358708	$6.29467852 \times 10^{-7}$	0.98926953	0.36433388
Limit	0	0	1	3/8

TABLE 1. Numerical illustration of the canonical Family $(-i)$ left tail. Here $z_c^+ = X_c + iY_c$, and x_c is its generating real minimum. The normalized ratios approach the limits predicted by Corollary 3.5. Ratios are computed from unrounded coordinates.

3.2. **The exact sheet equation and convergent parametrization.** Section 3.1 constructs and isolates the canonical conjugate pairs. We now use their exact sheet signs to describe the entire eventual tail by a single holomorphic germ.

Retain

$$H(z) := z^2 W(z) = \Gamma(1+z) + z, \qquad H(0) = 1, \tag{20}$$

and define, in a neighbourhood of 0,

$$A(z) := \frac{1}{\pi} \operatorname{arsinh}(\sin \pi z). \tag{21}$$

Here arsinh is the holomorphic inverse of sinh at 0, normalized by $\operatorname{arsinh}(0) = 0$ and $\operatorname{arsinh}'(0) = 1$. Thus A is an odd holomorphic germ, $A(z) = z + O(z^3)$, with real Taylor coefficients.

Proposition 3.6 (Exact canonical branch identity)**.** *For every sufficiently large integer c,*

$$W(z_c^+) - c = -iA(z_c^+) = -\frac{i}{\pi} \operatorname{arsinh}(\sin \pi z_c^+). \tag{22}$$

The conjugate lower tail satisfies

$$W(z_c^-) - c = +iA(z_c^-). \tag{23}$$

Proof. Put $w_c := W(z_c^+) - c$. The localisation (8) from the proof of Theorem 3.1 gives

$$w_c = O(x_c) \longrightarrow 0. \tag{24}$$

Proposition 3.4 and the integrality of c imply

$$\sin(\pi w_c) = (-1)^c \sin(\pi W(z_c^+)) = -i \sin(\pi z_c^+).$$

On the other hand, the defining inverse identity for arsinh gives

$$\sin(-i\pi A(z)) = -i \sinh(\pi A(z)) = -i \sin(\pi z).$$

Both w_c and $-iA(z_c^+)$ tend to 0. Since the derivative of $w \mapsto \sin(\pi w)$ at 0 is $\pi \neq 0$, this map is injective on a fixed neighbourhood of 0. Hence (22) holds exactly. This also explains the branch choice: the normalisation (24) selects the inverse sine at 0 and excludes its other branches. Finally, Schwarz symmetry of W and A gives (23). □

Put $t = c^{-1/2}$ and write $z = tZ$. For $t \neq 0$ and Z near 1, the identity $W(z) = H(z)/z^2$ rewrites $W(z) - t^{-2} = -iA(z)$ as

$$Z^2 = H(tZ) + it^2 Z^2 A(tZ). \tag{25}$$

Accordingly, define

$$F(t,Z) := Z^2 - H(tZ) - it^2 Z^2 A(tZ). \tag{26}$$

This function is holomorphic near $(0,1)$, including at $t=0$. In particular,

$$F(0,1) = 1 - H(0) = 0, \qquad \partial_Z F(0,1) = 2 \neq 0, \tag{27}$$

because

$$\partial_Z F(t,Z) = 2Z - tH'(tZ) - it^2\big(2ZA(tZ) + tZ^2 A'(tZ)\big).$$

Theorem 3.7 (Canonical holomorphic parametrization)**.** *There is a unique holomorphic germ Z at 0, with $Z(0)=1$, satisfying (25). It has a representative holomorphic on $|t|<\delta$ for some $\delta>0$, and for every sufficiently large positive integer c,*

$$z_c^+ = c^{-1/2} Z(c^{-1/2}). \tag{28}$$

These are precisely the canonical upper zeros constructed in Theorem 3.1; in particular,

$$\begin{aligned} G(z_c^+) = 0, \qquad S(z_c^+) = (-1)^{c+1} i, \\ W(z_c^+) - c = -iA(z_c^+). \end{aligned} \tag{29}$$

The Taylor expansion

$$Z(t) = 1 + \sum_{m\geq 1} q_m t^m \tag{30}$$

converges absolutely on $|t|<\delta$ and locally uniformly there. Consequently the exact identity

$$z_c^+ = c^{-1/2}\left(1 + \sum_{m\geq 1} q_m c^{-m/2}\right) \tag{31}$$

holds for all sufficiently large integers c.

Proof. By (27), the analytic implicit-function theorem gives $\delta,\epsilon>0$ and a holomorphic function $Z(t)$, $Z(0)=1$, such that, for every $|t|<\delta$, the equation $F(t,\cdot)=0$ has exactly one solution in $|Z-1|<\epsilon$, namely $Z(t)$. This proves existence and uniqueness of the normalised holomorphic germ.

To identify it with the already constructed zeros, set $t_c := c^{-1/2}$ and $\widehat{Z}_c := z_c^+/t_c$. Section 3.1 gives $\widehat{Z}_c \to 1$; indeed, $W(x_c) - c = O(x_c^4)$ and the Laurent expansion imply $cx_c^2 \to 1$, while $z_c^+ = x_c + O(x_c^4)$. Proposition 3.6 gives $F(t_c, \widehat{Z}_c) = 0$. For sufficiently large c, the point $(t_c, \widehat{Z}_c)$ belongs to the fixed implicit-function neighbourhood. The pointwise uniqueness just established therefore implies $\widehat{Z}_c = Z(t_c)$, proving (28) and (29).

Finally, holomorphy on a disc gives the stated convergence of the Taylor series. Substitution of $t = t_c$ proves (31). Thus the parametrization is convergent near 0, not merely a formal asymptotic expansion. □

The identification uses uniqueness of the solution of $F(t,\cdot)=0$ near 1 for each small t. The Rouché uniqueness in Theorem 3.1 has already specified the geometric sequence; no additional disc-containment argument is needed for $tZ(t)$. After discarding a finite initial segment, we may therefore use (28) directly, with simplicity supplied by Theorem 3.1.

For the transition to Section 3.3, write $H(z) = 1 + h_1 z + h_2 z^2 + O(z^3)$, where $h_1 = 1-\gamma$. Since $it^2 Z^2 A(tZ) = O(t^3)$, comparison through degree two gives

$$Z(t) = 1 + \frac{h_1}{2} t + \left(\frac{h_1^2}{8} + \frac{h_2}{2}\right) t^2 + O(t^3). \tag{32}$$

The general coefficient recursion and its arithmetic consequences are developed in Section 3.3.

Remark 3.8. For the fixed sheet germ A, the implicit-function argument uses only the holomorphy of H near 0 together with $H(0) = 1$; this is precisely the local mechanism underlying Theorem 3.7. In particular, the construction is not specific to the higher Gamma coefficients.

Remark 3.9 (The mirror tail on the negative-real side). The holomorphic germ Z of Theorem 3.7 is defined for both positive and negative sufficiently small values of t. Hence, for every sufficiently large positive integer c, put

$$\widetilde{z}_c^{+} := -c^{-1/2} Z(-c^{-1/2}).$$

Since $t = -c^{-1/2}$ still satisfies $t^{-2} = c$, equation (25) gives

$$W(\widetilde{z}_c^{+}) - c = -iA(\widetilde{z}_c^{+}),$$

and consequently

$$G(\widetilde{z}_c^{+}) = 0, \qquad S(\widetilde{z}_c^{+}) = (-1)^{c+1} i.$$

Expansion of equation (25) to the first non-real order gives

$$\Im\big(tZ(t)\big) = \frac{1}{2} t^4 + O(t^5).$$

Thus

$$\Re \widetilde{z}_c^{+} \sim -c^{-1/2}, \qquad \Im \widetilde{z}_c^{+} \sim \frac{1}{2} c^{-2} > 0.$$

The same holomorphic germ therefore produces an upper-half-plane tail approaching 0 from the negative-real side; its conjugate gives the corresponding lower tail.

This also identifies its eventual Gaussian location index. Since

$$\phi_{-i}(z) = z + iW(z) - \frac{1}{2}$$

and $W(\widetilde{z}_c^{+}) = c - iA(\widetilde{z}_c^{+})$,

$$\Re \phi_{-i}(\widetilde{z}_c^{+}) = \Re\big(\widetilde{z}_c^{+} + A(\widetilde{z}_c^{+})\big) - \frac{1}{2} = -\frac{1}{2} - 2c^{-1/2} + O(c^{-1}).$$

Hence

$$[\Re \phi_{-i}(\widetilde{z}_c^{+})] = -1$$

for all sufficiently large c. In the Gaussian-classification terminology, this mirror tail therefore supplies the eventual $k = -1$ Family $(-i)$ states corresponding to the $k = 0$ positive-real-side canonical tail.

3.3. **All-orders geometry and arithmetic coefficients.** Retain the convergent germs of Section 3.2, and write

$$H(z) = 1 + \sum_{m \geq 1} h_m z^m, \qquad Z(t) = 1 + \sum_{m \geq 1} q_m t^m, \qquad q_m = R_m + iI_m.$$

We now pass from their holomorphic relation to the coefficient identities that encode the arithmetic information in the real-part jet. Throughout this section, put $z_c^{+} = r_c + iy_c$, with $y_c > 0$.

Proposition 3.10 (All-orders asymptotic expansions)**.** *For every fixed integer $N \geq 1$,*

$$z_c^{+} = c^{-1/2} + \sum_{m=1}^{N} q_m c^{-(m+1)/2} + O_N\Big(c^{-(N+2)/2}\Big), \tag{33}$$

$$r_c = c^{-1/2} + \sum_{m=1}^{N} R_m c^{-(m+1)/2} + O_N\Big(c^{-(N+2)/2}\Big), \tag{34}$$

$$y_c = \sum_{m=1}^{N} I_m c^{-(m+1)/2} + O_N\Big(c^{-(N+2)/2}\Big). \tag{35}$$

Moreover, $I_1 = I_2 = 0$, so for $N \geq 3$ the last sum starts at $m = 3$.

Proof. Theorem 3.7 gives a Taylor series convergent on a fixed disc about 0. For each fixed N, its remainder after degree N is $O_N(t^{N+1})$. Multiplying by $t = c^{-1/2}$ and taking real and imaginary parts proves the three expansions. The coefficients q_1, q_2 are real by (32). Thus these finite-order asymptotic expansions are truncations of the convergent parametrization, with constants allowed to depend on N. □

Proposition 3.11 (Triangularity of the Gamma coefficients)**.** *We have $h_1 = 1 - \gamma$. For every $m \geq 2$,*

$$h_m = \frac{(-1)^m}{m}\zeta(m) + A_m\big(\gamma, \zeta(2), \ldots, \zeta(m-1)\big), \tag{36}$$

where A_m is a polynomial with rational coefficients, determined universally by exponentiation of the log-Gamma series.

Proof. The classical convergent expansion, with the logarithm vanishing at 0, is

$$\log\Gamma(1+z) = -\gamma z + \sum_{j\geq 2} \frac{(-1)^j \zeta(j)}{j} z^j, \qquad |z| < 1; \tag{37}$$

see [12, §5.7(i)]. Write its coefficients as $\ell_1 = -\gamma$ and $\ell_j = (-1)^j\zeta(j)/j$ for $j \geq 2$. In the coefficient of z^m in $\exp(\sum_{j\geq 1} \ell_j z^j)$, the only contribution involving ℓ_m is the linear term $\ell_m z^m$. Every product of at least two positive-degree terms contributing to degree m uses only $\ell_1, \ldots, \ell_{m-1}$, with rational coefficients from the exponential series. Since $H(z) = \Gamma(1+z) + z$, this proves $h_1 = 1 - \gamma$ and (36). In particular, $\zeta(m)$ enters this coefficient construction for the first time in h_m, linearly with coefficient $(-1)^m/m$. □

Theorem 3.12 (Triangular recursion for the zero germ)**.** *For every $m \geq 1$,*

$$\begin{gathered} q_m = \frac{1}{2}h_m + Q_m(h_1, \ldots, h_{m-1}; \pi^2), \\ Q_m \in \mathbb{Q}[i, \pi^2][h_1, \ldots, h_{m-1}]. \end{gathered} \tag{38}$$

The polynomials Q_m are universal for the fixed germ A. More explicitly, if

$$Z_{<m}(t) := 1 + \sum_{j=1}^{m-1} q_j t^j,$$

then, with $[t^m]$ denoting Taylor coefficient extraction,

$$2q_m = [t^m]\left\{H(tZ_{<m}) + it^2 Z_{<m}^2 A(tZ_{<m}) - Z_{<m}^2\right\}. \tag{39}$$

Proof. The odd series $\operatorname{arsinh}(\sin u)$ has rational coefficients, since both constituent Taylor series do. Therefore

$$A(z) = \sum_{j\geq 0} \alpha_j \pi^{2j} z^{2j+1}, \qquad \alpha_j \in \mathbb{Q}, \qquad A(z) = z - \frac{\pi^2}{3}z^3 + O(z^5). \tag{40}$$

Thus every coefficient of A belongs to $\mathbb{Q}[\pi^2]$.

Compare coefficients of t^m in (25). The new coefficient q_m enters Z^2 as $2q_m$. In $H(tZ)$, changing Z by $q_m t^m$ can affect only degrees $m+1$ and higher. Similarly, since the phase term starts as it^3Z^3, that change affects its coefficients only from degree $m+3$ onward. We may consequently replace Z by $Z_{<m}$ on the right and in all earlier contributions on the left, giving (39).

The term $h_m(tZ_{<m})^m$ contributes exactly h_m at degree m, because $Z_{<m}(0) = 1$. Every other term uses only $h_1, \ldots, h_{m-1}$, $q_1, \ldots, q_{m-1}$ and coefficients of A. Starting with $q_1 = h_1/2$, induction eliminates the earlier q_j and proves (38) in the stated coefficient ring. The nonzero diagonal factor $1/2$ is therefore a consequence of the coefficient equation itself. □

The first coefficients make this mechanism explicit:

$$q_1 = \frac{h_1}{2}, \qquad q_2 = \frac{h_1^2}{8} + \frac{h_2}{2}, \qquad q_3 = \frac{h_1 h_2 + h_3}{2} + \frac{i}{2}. \tag{41}$$

These follow by comparing degrees one, two and three in the recursion; in particular, $I_3 = 1/2$. For the next two height coefficients, use

$$it^2 Z^2 A(tZ) = it^3 Z^3 - \frac{i\pi^2}{3} t^5 Z^5 + O(t^7).$$

Taking imaginary parts through degrees four and five, with h_j real and $I_1 = I_2 = 0$, gives

$$2I_4 = \frac{3}{2} h_1, \qquad 2I_5 + q_2 = h_2 + 3q_2 + \frac{3}{4} h_1^2 - \frac{\pi^2}{3}.$$

Hence

$$I_3 = \frac{1}{2}, \qquad I_4 = \frac{3h_1}{4}, \qquad I_5 = \frac{h_1^2}{2} + h_2 - \frac{\pi^2}{6}. \tag{42}$$

Exponentiating (37) through degree three also gives

$$h_2 = \frac{\gamma^2 + \zeta(2)}{2}, \qquad h_3 = -\frac{\gamma^3}{6} - \frac{\gamma\zeta(2)}{2} - \frac{\zeta(3)}{3}.$$

Substitution into (41) and (42), using $\pi^2 = 6\zeta(2)$ [12, Eq. 25.6.1], yields

$$r_c = c^{-1/2} + \frac{1-\gamma}{2} c^{-1} + \left(\frac{(1-\gamma)^2}{8} + \frac{\gamma^2}{4} + \frac{\zeta(2)}{4} \right) c^{-3/2} + O(c^{-2}), \tag{43}$$

$$y_c = \frac{1}{2} c^{-2} + \frac{3(1-\gamma)}{4} c^{-5/2} + \frac{(1-\gamma)^2 + \gamma^2 - \zeta(2)}{2} c^{-3} + O(c^{-7/2}). \tag{44}$$

Thus the initial geometry already exhibits γ and $\zeta(2)$.

Theorem 3.13 (Arithmetic triangularity of the real-part jet)**.** *We have*

$$R_1 = \frac{1-\gamma}{2}, \tag{45}$$

and, for every $m \geq 2$,

$$R_m = \frac{(-1)^m}{2m} \zeta(m) + B_m\big(\gamma, \zeta(2), \ldots, \zeta(m-1)\big), \tag{46}$$

where B_m is a universal polynomial with rational coefficients. In this triangular coefficient construction, the first occurrence of $\zeta(m)$ in the real-part jet has the nonzero diagonal coefficient $(-1)^m/(2m)$.

Proof. Since all h_j are real, taking real parts in (38) leaves $h_m/2$ as its new term. By (36), this contributes $(-1)^m \zeta(m)/(2m)$, while the remaining h_j involve only earlier arithmetic data. For $m \geq 3$, every power of π^2 in the real part of Q_m may be replaced by the corresponding power of $6\zeta(2)$, which is already among those earlier data. The resulting remainder polynomial has rational coefficients.

At $m = 2$, the phase term has not yet entered, and (41) gives explicitly

$$R_2 = \frac{1}{4}\zeta(2) + \frac{\gamma^2}{4} + \frac{(1-\gamma)^2}{8}.$$

This establishes the claimed diagonal also in that case, with B_2 depending only on γ. Finally, (45) follows from $q_1 = h_1/2$. □

Corollary 3.14 (Recursive recovery from real parts)**.** *The real-part asymptotic jet of the canonical non-real left tail recursively determines*

$$\gamma, \zeta(2), \zeta(3), \zeta(4), \dots.$$

More explicitly, the sequence r_c, with its canonical integer labels c, determines its real coefficients successively by

$$R_m = \lim_{c\to\infty} c^{(m+1)/2} \left(r_c - c^{-1/2} - \sum_{j=1}^{m-1} R_j c^{-(j+1)/2} \right), \qquad m \ge 1, \tag{47}$$

where the sum is empty for $m = 1$. Then

$$\begin{aligned} \gamma &= 1 - 2R_1, \\ \zeta(m) &= (-1)^m 2m \left[R_m - B_m\big(\gamma, \zeta(2), \dots, \zeta(m-1)\big) \right], \qquad m \ge 2. \end{aligned} \tag{48}$$

Proof. For each fixed m, apply (34) with $N = m$. After subtracting the preceding terms and multiplying by $c^{(m+1)/2}$, the remainder is $O(c^{-1/2})$. This proves (47). Equation (45) determines γ; the nonzero diagonal in (46) then determines each $\zeta(m)$ once the earlier values are known, giving (48). □

Numerical illustration (recovery of arithmetic constants). The inverse reconstruction of Corollary 3.14 can be illustrated using only the real parts $X_c = \Re z_c^+$ of the canonical non-real zeros.

Put

$$u_c := c(X_c - c^{-1/2}).$$

By Proposition 3.10 and Theorem 3.13,

$$u_c = R_1 + R_2 c^{-1/2} + R_3 c^{-1} + R_4 c^{-3/2} + O(c^{-2}),$$

where

$$R_1 = \frac{1-\gamma}{2}, \qquad R_2 = \frac{(1-\gamma)^2}{8} + \frac{\gamma^2}{4} + \frac{\zeta(2)}{4}.$$

To accelerate convergence, define

$$\widehat{R}_1(c) := \frac{-u_c + 14u_{4c} - 56u_{16c} + 64u_{64c}}{21}$$

and

$$\widehat{R}_2(c) := \frac{\sqrt{c}}{3}\left(2u_c - 26u_{4c} + 88u_{16c} - 64u_{64c}\right).$$

Cancellation of the intermediate powers of $c^{-1/2}$ gives

$$\widehat{R}_1(c) = R_1 + O(c^{-2}), \qquad \widehat{R}_2(c) = R_2 + O(c^{-3/2}).$$

Consequently, the approximations

$$\widehat{\gamma}_c := 1 - 2\widehat{R}_1(c),$$

$$\widehat{\zeta}_c(2) := 4\widehat{R}_2(c) - \widehat{\gamma}_c^2 - \frac{(1-\widehat{\gamma}_c)^2}{2}$$

converge to γ and $\zeta(2)$, respectively.

The numerical agreement illustrates the triangular arithmetic recovery of Theorem 3.13 and Corollary 3.14. In particular, neither constant is supplied as an input to the extrapolation formulas.

c	$\widehat{\gamma}_c$	$\widehat{\zeta}_c(2)$
20	0.57716483	1.63809009
50	0.57720676	1.64304195
100	0.57721335	1.64423867
200	0.57721507	1.64468059
500	0.57721557	1.64486786
900	0.57721563	1.64490621
1000	0.57721564	1.64491022
5000	0.57721566	1.64493187
Limit	0.57721566	1.64493407

TABLE 2. Numerical recovery of Euler's constant γ and $\zeta(2)$ from the real parts of canonical Family $(-i)$ zeros. The four-scale extrapolation uses the zeros indexed by $c, 4c, 16c, 64c$. All calculations use high-precision unrounded zero coordinates.

Remark 3.15 (Dependence on the absolute integer labels). Corollary 3.14 is a statement about the canonically labelled tail. The absolute integer origin of the labels is essential for the higher arithmetic coefficients.

Indeed, suppose the same geometric sequence is relabelled by

$$c' = c + N, \qquad N \in \mathbb{Z}.$$

Writing the original real-part expansion as

$$r_c = c^{-1/2} + R_1 c^{-1} + R_2 c^{-3/2} + O(c^{-2}),$$

one obtains, in terms of c',

$$r_{c'-N} = (c')^{-1/2} + R_1 (c')^{-1} + \left(R_2 + \frac{N}{2}\right)(c')^{-3/2} + O((c')^{-2}).$$

Thus R_1, and hence $\gamma = 1 - 2R_1$, is unchanged, whereas

$$R_2 \longmapsto R_2 + \frac{N}{2}.$$

Since the $m = 2$ instance of the triangular recovery has diagonal coefficient $1/4$, the value inferred for $\zeta(2)$ would change by $2N$.

Accordingly, the reconstruction of $\zeta(2), \zeta(3), \ldots$ in Corollary 3.14 presupposes the canonical integer labels. The unlabelled problem, including recovery of the integer gauge, is treated separately in Section 3.6. Under the corresponding Wilson gauge $W_N = W + N$, one also has

$$S_N = (-1)^N S,$$

so the sheet-character reconstruction of Section 3.5 likewise uses the canonical label origin.

3.4. **Zero-cloud geometry.** We now regard the canonical tail as a geometric divisor accumulating at 0. Retain $z_c^+ = r_c + iy_c$, with $y_c > 0$. Choose c_0 sufficiently large that all the preceding results hold, the points $z_c^\pm$ are distinct, and their real parts are positive and strictly decreasing. Put

$$\mathcal{E}_0 := \{z_c^+, z_c^- : c \geq c_0\}, \qquad \ell_c := \Re z_c^+ - \Re z_{c+1}^+.$$

The statements below concern this canonical cloud. Adding its limit point 0 does not change either of its dimensions.

Theorem 3.16 (Fractal geometry of the canonical zero cloud)**.** *The horizontal gaps satisfy*

$$\ell_c \sim \frac{1}{2} c^{-3/2}. \tag{49}$$

The cloud has Hausdorff dimension 0*, whereas its lower and upper box dimensions coincide:*

$$\dim_H \mathcal{E}_0 = 0, \qquad \underline{\dim}_B \mathcal{E}_0 = \overline{\dim}_B \mathcal{E}_0 = \frac{2}{3}. \tag{50}$$

The gap zeta function

$$\zeta_{\mathrm{gap}}(s) := \sum_{c \geq c_0} \ell_c^s, \qquad \ell_c^s := \exp(s \log \ell_c), \tag{51}$$

has abscissa of absolute convergence 2/3*. Moreover, the reciprocal counting function, including both conjugates,*

$$N_{\mathrm{rec}}(R) := \#\{z \in \mathcal{E}_0 : |z|^{-1} \leq R\}, \tag{52}$$

satisfies

$$N_{\mathrm{rec}}(R) = 2R^2 + 2(1-\gamma)R + O(1) \sim 2R^2 \qquad (R \to \infty). \tag{53}$$

Proof. The gap estimate is the real-part spacing proved in Corollary 3.3. Theorem 3.2 also gives $r_c \asymp c^{-1/2}$ and $y_c = O(c^{-2})$. Countability immediately implies the Hausdorff-dimension assertion.

Let $N_\varepsilon(\mathcal{E}_0)$ be the least number of squares of side ε, with sides parallel to the coordinate axes, covering the cloud. For the lower bound, choose $N = \lfloor \kappa \varepsilon^{-2/3} \rfloor$, with a sufficiently small fixed $\kappa > 0$. From (49), there is $b > 0$ such that $\ell_c \geq b c^{-3/2}$ for $c \geq c_0$; hence the upper points with $c_0 \leq c \leq N$ have successive horizontal separations greater than 2ε. Each covering square contains at most one of these points, so $N_\varepsilon(\mathcal{E}_0) \gg \varepsilon^{-2/3}$.

For the upper bound, put $M = \lceil \varepsilon^{-2/3} \rceil$. The points with $c \leq M$ require $O(M)$ squares. The remaining conjugate tail lies in a rectangle of horizontal size $O(M^{-1/2})$ and vertical size $O(M^{-2})$. Since these sizes are respectively $O(\varepsilon^{1/3})$ and $O(\varepsilon^{4/3})$, that rectangle requires $O(\varepsilon^{-2/3})$ squares. Thus

$$N_\varepsilon(\mathcal{E}_0) \asymp \varepsilon^{-2/3}, \tag{54}$$

which proves both box-dimension assertions. Adding 0 changes the covering number by at most one.

For $\sigma = \Re s$, the absolute values in (51) satisfy

$$|\ell_c^s| = \ell_c^\sigma \sim 2^{-\sigma} c^{-3\sigma/2}.$$

The series therefore converges absolutely exactly when $\sigma > 2/3$. The same horizontal gap scale accounts for this abscissa and for the box dimension.

Finally, let $a := 1 - \gamma$. The first two location terms in (43), together with $y_c = O(c^{-2})$, give

$$|z_c^+| = c^{-1/2} + \frac{a}{2} c^{-1} + O(c^{-3/2}), \qquad u_c := |z_c^+|^{-1} = \sqrt{c} - \frac{a}{2} + O(c^{-1/2}).$$

For $f(u) := u^2 + au$, it follows that $f(u_c) = c + O(1)$ uniformly. As f is strictly increasing for large positive u, the indices with $u_c \leq R$ are bracketed between the cutoffs $c \leq f(R) - K$ and $c \leq f(R) + K$ for some fixed K. Their number is consequently $R^2 + aR + O(1)$. Each index contributes both conjugates at the same reciprocal radius, proving (53). □

Remark 3.17 (Canonical products for the real and non-real zero divisors). The real prime divisor of G admits an ordinary Weierstrass product. Recall that every point of $\mathcal{P}_1 = \{1\} \cup \mathbb{P}$ is a zero of multiplicity two. With the genus-one primary factor

$$E_1(u) := (1-u)e^u,$$

define

$$P_{\mathbb{P}}(z) := (1-z)^2 \prod_{p \in \mathbb{P}} E_1\left(\frac{z}{p}\right)^2 = (1-z)^2 \prod_{p \in \mathbb{P}} \left(1 - \frac{z}{p}\right)^2 e^{2z/p}.$$

Since

$$\log E_1(u) = -\frac{u^2}{2} + O(u^3) \qquad (u \to 0)$$

and

$$\sum_{p\in\mathbb{P}} \frac{1}{p^2} < \infty,$$

the product converges locally uniformly on $\mathbb{C}$. It defines an entire function whose zeros are precisely the points of $\mathcal{P}_1$, each with multiplicity two.

Thus $P_{\mathbb{P}}$ reproduces the complete real zero divisor of G, although it does not reproduce its non-real zeros. The quotient

$$R_{\mathbb{P}}(z) := \frac{G(z)}{P_{\mathbb{P}}(z)}$$

extends holomorphically across every point of $\mathcal{P}_1$ on the natural domain Ω_G, and has no real zeros there.

The contrast with the canonical non-real left tail is instructive. The prime zeros escape to infinity and admit a genus-one product in z, whereas the canonical non-real zeros accumulate at 0 with modulus asymptotic to $c^{-1/2}$. Their corresponding product must therefore be constructed in the reciprocal coordinate $1/z$, as established by the reciprocal canonical-product theorem below.

The accumulation at 0 precludes a nonzero entire function of z with this divisor. For a canonical product we therefore pass to the reciprocal coordinate $w = 1/z$, in which the zeros $1/z_c^{\pm}$ tend to infinity. Write $\alpha_c := z_c^+$, so that $z_c^- = \overline{\alpha_c}$, and define the primary factor

$$E_2(u) := (1-u)\exp\left(u + \frac{u^2}{2}\right). \tag{55}$$

Theorem 3.18 (Reciprocal canonical product)**.** *The canonical scale gives*

$$\sum_{c\geq c_0} |\alpha_c|^2 = \infty, \qquad \sum_{c\geq c_0} |\alpha_c|^3 < \infty. \tag{56}$$

Thus genus two is the least standard primary-factor genus with absolutely summable logarithmic remainders. The reciprocal product

$$P_0(z) := \prod_{c\geq c_0} E_2\Big(\frac{\alpha_c}{z}\Big)\, E_2\Big(\frac{\overline{\alpha_c}}{z}\Big) \tag{57}$$

converges locally uniformly on $\mathbb{C}\setminus\{0\}$. Its zeros are exactly $\mathcal{E}_0$, each simple, and 0 is an essential singularity of P_0.

Proof. Both assertions in (56) follow from $|\alpha_c| \asymp c^{-1/2}$. Near $u = 0$ the logarithm normalized to vanish there satisfies

$$\log E_2(u) = -\sum_{m\geq 3} \frac{u^m}{m}, \qquad |\log E_2(u)| \leq C|u|^3 \quad (|u| \leq \tfrac{1}{2}). \tag{58}$$

On a compact set $K \subset \mathbb{C}\setminus\{0\}$, put $d := \min_{z\in K} |z| > 0$. For all sufficiently large c, the two factor arguments have modulus at most $1/2$ uniformly on K, and

$$\sum_c \sup_{z\in K} \left(|\log E_2(\alpha_c/z)| + |\log E_2(\overline{\alpha_c}/z)|\right) \leq 2Cd^{-3} \sum_c |\alpha_c|^3 < \infty,$$

where the sum on the left is over that tail. Its logarithm therefore converges locally uniformly, and its exponential is holomorphic and nonvanishing. Multiplication by the finite initial product proves the claimed convergence.

Each factor in (57) has one simple zero, at its displayed α_c or $\overline{\alpha_c}$. The nonvanishing tail proves that there are no other zeros and that their multiplicities remain one, as in Theorem 3.1. The

limit is not identically zero, since at any point outside the displayed divisor its finite head and exponential tail are nonzero.

For completeness, conjugate pairing does not permit a lower genus: $\Re(\alpha_c^2) = r_c^2 - y_c^2 \sim c^{-1}$. For $E_1(u) := (1-u)e^u$, the paired logarithmic modulus at $z = i$ is

$$\log |E_1(\alpha_c/i)E_1(\overline{\alpha_c}/i)| = \Re(\alpha_c^2) + O(|\alpha_c|^3).$$

Its sum diverges to $+\infty$. For genus zero, the paired factor at $z = -1$ is $|1+\alpha_c|^2$, whose logarithm is $2r_c + O(|\alpha_c|^2) \sim 2c^{-1/2}$, again with divergent sum.

Finally, infinitely many zeros approach 0. If its singularity were removable, the identity theorem would force the extension to vanish identically. A pole would make the function nonzero in a sufficiently small punctured neighbourhood. Both are impossible, so 0 is essential. □

The product is canonical in the reciprocal variable: explicitly, $P_0(z) = Q(1/z)$, where the same logarithmic estimate shows that $Q(w) = \prod_{c \geq c_0} E_2(\alpha_c w)E_2(\overline{\alpha_c} w)$ is entire and $Q(0) = 1$.

Theorem 3.19 (Complex-moment zeta function)**.** *For $\Re s > 2$, define*

$$\begin{aligned} \Xi_0(s) &:= \sum_{c \geq c_0} \big((z_c^+)^s + (z_c^-)^s\big), \\ (z_c^\pm)^s &:= \exp\big(s \operatorname{Log} z_c^\pm\big). \end{aligned} \tag{59}$$

using the principal logarithm on the right half-plane. The series converges absolutely and locally uniformly there and admits the meromorphic continuation

$$\Xi_0(s) = 2\zeta\left(\frac{s}{2}\right) + (1-\gamma)s\zeta\left(\frac{s+1}{2}\right) + H_0(s), \tag{60}$$

where H_0 is holomorphic on $\Re s > 0$. The only poles in this half-plane are the simple poles at 2 and 1, with residues

$$\operatorname*{Res}_{s=2} \Xi_0(s) = 4, \qquad \operatorname*{Res}_{s=1} \Xi_0(s) = 2(1-\gamma). \tag{61}$$

Proof. Put $a := 1 - \gamma$. The first two terms of the location expansion give

$$z_c^\pm = c^{-1/2}\left(1 + \frac{a}{2}c^{-1/2} + O(c^{-1})\right),$$

so the defining series converges absolutely and locally uniformly for $\Re s > 2$. On every compact set K of s-values, expansion of the principal logarithm and exponential gives uniformly

$$\begin{aligned} (z_c^+)^s + (z_c^-)^s &= 2c^{-s/2} + as\, c^{-(s+1)/2} + e_c(s), \\ |e_c(s)| &\leq C_K c^{-(\Re s + 2)/2}. \end{aligned} \tag{62}$$

Each e_c is entire in s. Its sum converges locally uniformly on $\Re s > 0$, because on every compact subset the exponent in the bound is uniformly greater than one. Hence

$$\begin{aligned} H_0(s) := \sum_{c \geq c_0} e_c(s) \\ - 2\sum_{c=1}^{c_0-1} c^{-s/2} - as \sum_{c=1}^{c_0-1} c^{-(s+1)/2} \end{aligned}$$

is holomorphic there; the two finite corrections are entire. Summing (62) first on $\Re s > 2$ proves (60), and the classical continuation of ζ extends it meromorphically to $\Re s > 0$.

The Riemann zeta function has its unique simple pole at 1, with residue 1; see [12, §25.2(i)]. The affine arguments $s/2$ and $(s+1)/2$ each supply a factor of 2 to the corresponding residue. This yields (61). Both residues are nonzero, since $0 < \gamma < 1$. □

The two poles record the leading $c^{-1/2}$ scale and its first correction involving Euler's constant. The product and moment constructions are also related directly: if $r_0 := \sup_{c\geq c_0} |\alpha_c|$, then for $|z| > r_0$,

$$\log P_0(z) = -\sum_{m\geq 3} \frac{\Xi_0(m)}{m z^m}, \tag{63}$$

with the logarithm tending to 0 at infinity. This follows from (58) by absolute interchange of the two sums.

Remark 3.20. The gap zeta function measures successive horizontal separations, whereas Ξ_0 takes complex moments of the positions themselves. The radial convention based on $|z_c^{\pm}|^{2s}$ has leading poles at 1 and 1/2; it is a different normalization and is not used here.

3.5. **Arithmetic carried by the tail.** The arithmetic functions appearing in this section are classical consequences of the Gamma coefficients; no new identities for η, ζ, or the prime-zeta function are claimed here. The point is instead inverse-geometric. Once the canonical integer labels are fixed, the non-real zero geometry determines these classical arithmetic quantities through explicit reconstruction maps, without using the positive-real zeros of G as input.

There are two distinct channels. The sheet signs together with the canonical labels c encode an alternating Dirichlet series, while the canonically labelled real-part asymptotic jet determines the integer zeta values and, through them, the ordered rational primes. We use Proposition 3.4 and Corollary 3.14 as established inputs.

Theorem 3.21 (Sheet-character Dirichlet series)**.** *For $\Re s > 0$, the series*

$$E_G(s) := \sum_{c\geq c_0} \frac{-iS(z_c^+)}{c^s} \tag{64}$$

converges locally uniformly and satisfies

$$E_G(s) = \eta(s) - \sum_{1\leq c<c_0} \frac{(-1)^{c+1}}{c^s}, \tag{65}$$

where

$$\eta(s) = \sum_{c\geq 1} \frac{(-1)^{c+1}}{c^s} = (1-2^{1-s})\zeta(s). \tag{66}$$

The expression $(1-2^{1-s})\zeta(s)$ has the removable value $\eta(1) = \log 2$ at $s = 1$.

This encoding uses the non-real sheet signs and canonical labels alone.

Proof. Proposition 3.4 gives $-iS(z_c^+) = (-1)^{c+1}$ for $c \geq c_0$. To justify convergence, put $A_M(u) := \sum_{M\leq c\leq u}(-1)^{c+1}$, so that $|A_M(u)| \leq 1$. For integers $N \geq M \geq 1$, Abel summation gives

$$\sum_{c=M}^{N} (-1)^{c+1} c^{-s} = A_M(N)N^{-s} + s\int_M^N A_M(u)u^{-s-1}\,du.$$

Consequently, if $K \subset \{\Re s > 0\}$ is compact, $\sigma_K := \min_K \Re s > 0$ and $B_K := \max_K |s|$, then

$$\sup_{s\in K}\left|\sum_{c=M}^{N}(-1)^{c+1}c^{-s}\right| \leq \left(1+\frac{B_K}{\sigma_K}\right)M^{-\sigma_K}.$$

This proves the uniform Cauchy property on K, hence local uniform convergence and holomorphy. Removing the finite initial sum gives (65) directly.

For $\Re s > 1$, absolute convergence permits separation into odd and even terms:

$$\eta(s) = \sum_{c\geq 1} c^{-s} - 2\sum_{c\geq 1}(2c)^{-s} = \big(1 - 2^{1-s}\big)\zeta(s).$$

Both sides are holomorphic on $\Re s > 0$ after filling the removable value at $s = 1$, so the identity extends throughout that half-plane by analytic continuation. At $s = 1$,

$$\eta(1) = \log 2.$$

□

Let $\mathbb{P}$ denote the rational primes and, for $\Re s > 1$, define

$$P_{\mathrm{pr}}(s) := \sum_{p\in\mathbb{P}} p^{-s}. \tag{67}$$

We write $\log\zeta(s)$ for the holomorphic logarithm supplied by the Euler product, normalized to be real for real $s > 1$. In this subsection, μ denotes the classical Möbius function, rather than the Family invariant of Section 2. Its coefficients can be computed by the divisor recurrence

$$\mu(1) = 1, \qquad \mu(k) = -\sum_{\substack{d\mid k\\ d<k}} \mu(d) \quad (k > 1),$$

so forming them requires only integer divisibility, without a supplied enumeration of the primes.

For background on the prime zeta function and its relation to the Riemann zeta function, see [5].

Proposition 3.22 (Prime-zeta moments from the left-tail jet)**.** *For $\Re s > 1$,*

$$\begin{aligned} \log\zeta(s) &= \sum_{r\geq 1} \frac{1}{r} P_{\mathrm{pr}}(rs), \\ P_{\mathrm{pr}}(s) &= \sum_{k\geq 1} \frac{\mu(k)}{k} \log\zeta(ks). \end{aligned} \tag{68}$$

Both series converge absolutely and locally uniformly on that half-plane. In particular, for every integer $m \geq 2$,

$$P_{\mathrm{pr}}(m) = \sum_{k\geq 1} \frac{\mu(k)}{k} \log\zeta(km). \tag{69}$$

Thus the canonically labelled real-part jet determines all the integer moments $P_{\mathrm{pr}}(2), P_{\mathrm{pr}}(3), \ldots$.

Proof. The Euler product [12, Eq. 25.2.11] gives

$$\log\zeta(s) = \sum_{p\in\mathbb{P}} \sum_{r\geq 1} \frac{p^{-rs}}{r} = \sum_{r\geq 1} \frac{P_{\mathrm{pr}}(rs)}{r}.$$

These sums converge absolutely and locally uniformly: if $\Re s \geq \sigma_0 > 1$, their absolute sum is at most $\sum_p p^{-\sigma_0}/(1 - p^{-\sigma_0}) < \infty$.

For real $u \geq \sigma_0 > 1$, integral comparison yields

$$0 < \log\zeta(u) \leq \zeta(u) - 1 \leq 2^{-u}\left(1 + \frac{2}{u-1}\right) \leq C_{\sigma_0} 2^{-u},$$

where $C_{\sigma_0} := 1 + 2/(\sigma_0 - 1)$. The Euler logarithm therefore satisfies, uniformly for $\Re s \geq \sigma_0$,

$$|\log\zeta(ks)| \leq \log\zeta(k\Re s) \leq C_{\sigma_0} 2^{-k\sigma_0}.$$

Since $|\mu(k)| \le 1$, this proves the required convergence of the Möbius series. It also justifies the double-sum rearrangement, because

$$\sum_{k,r\ge 1} \frac{|\mu(k)|}{kr} |P_{\mathrm{pr}}(krs)| \le \sum_{k\ge 1} \frac{|\mu(k)|}{k} \log \zeta(k\sigma_0) < \infty.$$

Grouping by $d = kr$ now gives

$$\begin{aligned} \sum_{k\ge 1} \frac{\mu(k)}{k} \log \zeta(ks) &= \sum_{d\ge 1} \frac{P_{\mathrm{pr}}(ds)}{d} \sum_{k\mid d} \mu(k) \\ &= P_{\mathrm{pr}}(s), \end{aligned}$$

using $\sum_{k\mid d} \mu(k) = 1$ for $d = 1$ and 0 otherwise. For integer $m \ge 2$, the same bound gives $\log \zeta(km) \le 3\, 2^{-km}$. Corollary 3.14 supplies every value $\zeta(km)$ appearing in (69), which proves the integer-moment recovery assertion. □

Theorem 3.23 (Recursive recovery of the prime divisor)**.** *Let $2 = p_1 < p_2 < p_3 < \cdots$ be the ordered rational primes. Their integer moments determine the first prime by*

$$p_1 = \lim_{m\to\infty} P_{\mathrm{pr}}(m)^{-1/m}. \tag{70}$$

More generally, once $p_1, \dots, p_{r-1}$ have been recovered, put

$$T_r(m) := P_{\mathrm{pr}}(m) - \sum_{j<r} p_j^{-m}. \tag{71}$$

Then

$$p_r = \lim_{m\to\infty} T_r(m)^{-1/m}. \tag{72}$$

The limits are taken through integers $m \ge 2$ and use positive real roots.

Proof. For fixed r, the exact moment identity gives

$$\begin{aligned} T_r(m) &= \sum_{j\ge r} p_j^{-m} = p_r^{-m}(1 + \varepsilon_{r,m}), \\ \varepsilon_{r,m} &:= \sum_{j>r} \left(\frac{p_r}{p_j}\right)^m. \end{aligned}$$

Every integer p_j in the last sum is at least $p_r + 1$. Consequently, for $m \ge 2$,

$$\begin{aligned} 0 \le \varepsilon_{r,m} &\le p_r^m \sum_{n=p_r+1}^{\infty} n^{-m} \\ &\le \left(\frac{p_r}{p_r+1}\right)^m \left(1 + \frac{p_r+1}{m-1}\right) \longrightarrow 0. \end{aligned}$$

It follows that $T_r(m)^{-1/m} = p_r(1+\varepsilon_{r,m})^{-1/m} \to p_r$. For $r = 1$ the subtracted sum is empty, giving (70). □

Corollary 3.24 (Prime recovery from non-real geometry)**.** *The canonically labelled real-part asymptotic jet of the upper non-real left tail determines the locally finite prime counting measure*

$$\nu_{\mathrm{pr}} := \sum_{p\in\mathbb{P}} \delta_p, \tag{73}$$

where δ_p is the unit point mass at p. Equivalently, it determines the ordered prime set $2, 3, 5, 7, \dots$. Only the non-real zero locations and their canonical integer labels are used; positive-real zeros of G are not input to the reconstruction.

Proof. Corollary 3.14 recovers the values $\zeta(m)$ for all integers $m \geq 2$. Proposition 3.22 then recovers $P_{\mathrm{pr}}(m)$ at those integers, and Theorem 3.23 recovers each p_r in order. The resulting measure is locally finite since its support is a subset of the positive integers. None of these steps uses a positive-real zero of G. □

After this reconstruction, the independent statement from Section 1,

$$Z(G) \cap \mathbb{R}_{>0} = \{1\} \cup \mathbb{P},$$

identifies the recovered primes with the prime part of that real zero set. This identification is a consequence of comparing the two results, not a premise of the recovery.

The two arithmetic channels are thus separate. With the canonical labels understood, they are

$$\{-iS(z_c^+)\}_{c \geq c_0} \longrightarrow \eta(s),$$

and

$$\begin{aligned} \{\Re z_c^+\}_{c \geq c_0} &\xrightarrow{\text{complete asymptotic jet}} \{\zeta(m)\}_{m \geq 2} \\ &\longrightarrow \{P_{\mathrm{pr}}(m)\}_{m \geq 2} \longrightarrow \mathbb{P}. \end{aligned}$$

The first uses sheet signs; the second uses positions through their real-part jet and the resulting integer moments.

3.6. **Inverse rigidity.** Exact locations give a direct sampled-value reconstruction of the analytic germ. We first retain the canonical labels, then discard their absolute origin, and finally retain only the embedded non-real zero set near 0. Throughout, A is the principal holomorphic germ defined in (21). A determination of a germ means uniqueness on some neighbourhood of 0; a global conclusion will always specify the continuation class.

Theorem 3.25 (Labelled sampled-value rigidity)**.** *The exact labelled canonical upper tail (c, z_c^+) determines the holomorphic germ H at 0. Its sampled values are*

$$\begin{aligned} H(z_c^+) &= (z_c^+)^2 \left(c - iA(z_c^+)\right) \\ &= (z_c^+)^2 \left(c - \frac{i}{\pi} \operatorname{arsinh}(\sin(\pi z_c^+))\right). \end{aligned} \tag{74}$$

Proof. Multiply the exact branch identity of Proposition 3.6 by $(z_c^+)^2$. The sampling points are distinct and tend to 0. Any two holomorphic germs with these sampled values therefore agree by the identity theorem: their accumulation point is interior to the domain of H, even though it is a puncture for W and G. □

Corollary 3.26 (Recovery of the Wilson–Gamma system)**.** *The labelled samples determine*

$$W(z) = \frac{H(z)}{z^2}, \qquad \Gamma(z) = zW(z) - 1, \tag{75}$$

as meromorphic germs, and hence determine S and G on their local analytic loci. If two candidate Wilson germs compatible with the same labelled samples have meromorphic continuations to one connected domain D containing a punctured neighbourhood of 0, those continuations coincide on D.

Proof. The displayed identities and the definitions of S, G give local recovery. The meromorphic identity theorem gives uniqueness on D. For the actual Gamma system such continuation exists independently; local rigidity alone does not assert continuation of an arbitrary germ. □

The integer gauge. For every $N \in \mathbb{Z}$, put $W_N = W + N$ and $H_N = H + Nz^2$. Directly,

$$H_N(0) = 1, \qquad S_N = (-1)^N S, \qquad G_N = G, \tag{76}$$

and

$$W_N(z_c^+) - (c + N) = W(z_c^+) - c.$$

Thus an integer translation of all labels preserves the point locations and G exactly. Absolute labels fix a representative of W; unlabelled locations cannot distinguish these representatives. The apparent reflection $W \mapsto -W + N$ is excluded by the normalization $H(0) = 1$, since it would give $H(0) = -1$.

Second-order gauge fixing in the Gamma specialization. The integer gauge can already be fixed locally at second order if the known Gamma normalization is imposed. Write

$$H(z) = 1 + h_1 z + h_2 z^2 + O(z^3).$$

Under

$$H_N(z) = H(z) + Nz^2$$

the coefficients transform by

$$h_1^{(N)} = h_1, \qquad h_2^{(N)} = h_2 + N.$$

For the Gamma specialization,

$$h_1 = 1 - \gamma$$

and

$$h_2 = \frac{\gamma^2 + \zeta(2)}{2} = \frac{\gamma^2}{2} + \frac{\pi^2}{12}.$$

Thus h_1 first determines γ, independently of the integer gauge, and among the integer translates there is exactly one value of h_2 satisfying the displayed Gamma identity. Hence the Gamma-specialized integer gauge may already be selected from the second-order germ.

This provides a local alternative to the recurrence criterion used in Theorem 3.31 when one is willing to use the known second Gamma coefficient as structural input. It does not remove the integer ambiguity for a general normalized candidate.

For the comparison arguments below, a *normalized candidate* means a real-symmetric holomorphic germ H_* with $H_*(0) = 1$; put $W_* = H_*/z^2$ and define S_*, G_* as in Section 1. Its canonical upper branch is

$$z^+_{*,c} = tZ_*(t), \qquad t = c^{-1/2},$$
$$Z_*^2 = H_*(tZ_*) + it^2 Z_*^2 A(tZ_*), \qquad Z_*(0) = 1.$$

The implicit-function argument of Section 3.2 applies unchanged. At integer levels its equation gives

$$W_*(z^+_{*,c}) - c = -iA(z^+_{*,c}), \qquad G_*(z^+_{*,c}) = 0, \qquad S_*(z^+_{*,c}) = (-1)^{c+1} i.$$

The coefficient comparison in (41), with real coefficients of H_*, gives $\Im(tZ_*(t)) = t^4/2 + O(t^5)$ for positive t. This small amount of generality is needed to compare possible reconstructions; it invokes no global classification.

Proposition 3.27 (Puncture-local quantization)**.** *For every sufficiently small non-real zero z of G, there are unique $c \in \mathbb{Z}$ and $\eta \in \{\pm 1\}$ such that*

$$W(z) - c = -\eta i A(z), \qquad S(z) = \eta(-1)^{c+1} i. \tag{77}$$

Along any sequence of such zeros tending to 0*,*

$$|c| \longrightarrow \infty, \qquad cz^2 \longrightarrow 1. \tag{78}$$

Consequently the possible asymptotic rays, after passage to a subsequence, are $z \sim \pm c^{-1/2}$ for $c > 0$ and $z \sim \pm i|c|^{-1/2}$ for $c < 0$. The same assertions hold for every normalized candidate.

Proof. Factorization at a non-real zero gives $\sin(\pi W(z)) = \sigma i \sin(\pi z)$, where $\sigma = \pm 1$. Writing $W(z) = u + iv$, use

$$|\sin(\pi(u + iv))|^2 = \sin^2(\pi u) + \sinh^2(\pi v)$$

to obtain $|v| + \operatorname{dist}(u, \mathbb{Z}) = O(|z|)$. There is therefore a unique nearby integer c, with $W(z) - c = O(|z|)$. Put $\eta = -\sigma(-1)^c$. The inverse sine at 0, exactly as in Proposition 3.6, gives $W(z) - c =$

$-\eta i A(z)$. This also proves uniqueness of η, since $A(z) \neq 0$ for small nonzero z. Multiplication by z^2 yields

$$cz^2 = H(z) + \eta i z^2 A(z) \longrightarrow 1.$$

It implies both $|c| \to \infty$ and the stated ray alternatives. Only holomorphy and $H(0) = 1$ were used, so the proof also applies to the candidates. □

Theorem 3.28 (Intrinsic quartic-horn recognition)**.** *For every fixed $0 < a < 1/2 < b$, there are $\delta > 0$ and an integer C such that*

$$Z(G) \cap \{x + iy : 0 < x < \delta,\ ax^4 < y < bx^4\} = \{z_c^+ : c \geq C\}. \tag{79}$$

In particular, $a = 1/4$ and $b = 3/4$ give the selector in Figure 7. The equality is one of unlabelled embedded point sets. The same recognition holds for the canonical upper tail of each normalized candidate.

Proof. Write $W(z) = z^{-2} + h_1 z^{-1} + B(z)$, where $h_1 = 1 - \gamma$ and B is real-symmetric and holomorphic. Uniformly for $z = x + iy$ with $0 < y \leq bx^4$, $\Im B(x + iy) = O(y)$, as follows by integrating B' vertically from the real axis. Hence

$$\begin{aligned} \Im W(x + iy) &= -\frac{2xy}{(x^2 + y^2)^2} - \frac{h_1 y}{x^2 + y^2} + O(y) \\ &= -2yx^{-3}(1 + O(x)) < 0 \end{aligned} \tag{80}$$

for sufficiently small x. The factor y in every error makes this uniform even arbitrarily close to the real axis. Also $\Re A(x + iy) = x + O(x^3) > 0$. For a zero in this low horn, (77) gives $\Im W = -\eta \Re A$, forcing $\eta = +1$. Since $z/x \to 1$, (78) then forces $c > 0$ and $z\sqrt{c} \to 1$. The point $(c^{-1/2}, z\sqrt{c})$ lies in the fixed implicit-function neighbourhood of Section 3.2; its pointwise uniqueness identifies z with z_c^+. Thus every sufficiently small zero in the low horn is canonical.

Conversely, Corollary 3.5 gives $\Im z_c^+/(\Re z_c^+)^4 \to 1/2$, so every sufficiently late canonical point satisfies both vertical horn inequalities. The real parts are eventually strictly decreasing by Corollary 3.3. Choose C sufficiently large and then choose δ between $\Re z_C^+$ and $\Re z_{C-1}^+$, below the preceding exclusion threshold. This gives the literal suffix equality (79). For a normalized candidate the same proof uses real h_1, the upper quartic scale established above, and $\frac{d}{dt}\Re(tZ_*(t)) = 1 + O(t) > 0$. □

Intrinsic order. For any canonical germ Z_*, the real-analytic function $t|Z_*(t)|$ on the positive real axis has derivative $1 + O(t) > 0$ near 0. Thus $|z_{*,c}^+|$ strictly decreases, and $|1/z_{*,c}^+|$ strictly increases, for all sufficiently large c. The unlabelled tail consequently has an intrinsic eventual order. Two such tails agree as *set germs at* 0 if their intersections with some sufficiently small punctured disc agree; equivalently, they agree after deletion of finite heads.

Theorem 3.29 (Unlabelled canonical-tail rigidity)**.** *Let H_1, H_2 be normalized candidates. Their canonical upper tails agree as unlabelled set germs at 0 if and only if, for some $N \in \mathbb{Z}$,*

$$H_2 = H_1 + Nz^2, \qquad W_2 = W_1 + N. \tag{81}$$

In that case $G_2 = G_1$ as punctured germs. Integer translation is therefore the complete ambiguity.

Proof. By the intrinsic order, equal tail set germs have suffixes satisfying

$$z_k := z_{C_1+k}^{(1),+} = z_{C_2+k}^{(2),+}, \qquad k = 0, 1, \ldots.$$

Put $N = C_2 - C_1$. Their exact branch identities imply $W_2(z_k) - W_1(z_k) = N$. Thus $H_2 - H_1 - Nz^2$ is holomorphic at 0 and vanishes on the distinct points $z_k \to 0$. The identity theorem proves (81), and (76) gives $G_2 = G_1$.

Conversely, suppose $W_2 = W_1 + N$. At $z = z_c^{(1),+}$,

$$W_2(z) - (c + N) = -iA(z), \qquad z\sqrt{c + N} \longrightarrow 1.$$

The fixed implicit-function uniqueness for H_2 gives $z = z_{c+N}^{(2),+}$ for all sufficiently large c. Their unlabelled tail germs therefore agree. □

Continuation. If W_1, W_2 continue meromorphically to one connected domain D containing a punctured neighbourhood of 0, the meromorphic identity theorem gives $W_2 = W_1 + N$ throughout D. Consequently $G_2 = G_1$ on their common analytic locus. This clause concerns continuation of W; G can have essential singularities at poles of W.

Corollary 3.30 (The unlabelled non-real divisor determines the prime divisor)**.** *Let $\mathscr{D}$ be the embedded non-real zero set of the actual Gamma-specialized G in an arbitrarily small punctured neighbourhood of 0, with no additional markings. Among normalized real-symmetric candidates with the same non-real zero-set germ, these locations determine the canonical upper tail intrinsically, determine W modulo $\mathbb{Z}$, and determine G exactly as a punctured germ. Within the natural meromorphic continuation class for W on $\mathbb{C}$, they determine G on Ω_G and hence its positive-real zero set $\{1\} \cup \mathbb{P}$.*

Proof. Apply the fixed horn $x^4/4 < y < 3x^4/4$ to the point set. Theorem 3.28, for each candidate, selects its canonical upper tail. Theorem 3.29 then gives W modulo integers and G exactly; the continuation clause gives the global conclusion in the stated class. Only after G has been recovered do we apply Section 1's independent real-zero theorem to identify $\{1\} \cup \mathbb{P}$. No positive-real zero is input to this reconstruction. □

The raw input in this corollary consists solely of point locations in the given complex coordinate near the marked puncture 0. No labels, sheet values, multiplicities, conjugate-pair markings, generating minima, or unit-level curves are supplied. We next specify a reconstruction of the full prime-zeta function from the same data, rather than only the integer moments obtained in Section 3.5.

Once the Gamma representative has been selected, the subsequent Laplace, Mellin, and Möbius steps use classical transform identities; the inverse-geometric content is that the exact unlabelled zero cloud supplies the Gamma germ from which those transforms begin.

Theorem 3.31 (Direct zero-cloud transform to the prime-zeta function)**.** *Under the Gamma-specialized hypothesis of Corollary 3.30, the exact embedded point locations of the unlabelled non-real zero cloud determine $P_{\mathrm{pr}}(s)$ for every $\Re s > 1$ by the following composite analytic construction.*

Here "determine" is meant in the exact-data sense: the point locations are assumed known exactly. No numerical-stability assertion for finite, truncated, or noisy zero data is made. The Gamma recurrence used below is structural prior information specifying the Gamma specialization and is used to select the correct representative of the integer-gauge family.

Select the fixed horn and order its eventual points by increasing reciprocal modulus. After deleting a finite head, write

$$|\alpha_0| > |\alpha_1| > \cdots, \qquad \alpha_k \longrightarrow 0.$$

For each $M \in \mathbb{Z}$, form the data and Newton series

$$Y_k^{(M)} := \alpha_k^2\big(M + k - iA(\alpha_k)\big), \tag{82}$$

$$\mathcal{N}_M(z) := \sum_{k=0}^{\infty} Y^{(M)}[\alpha_0, \ldots, \alpha_k] \prod_{j=0}^{k-1} (z - \alpha_j), \tag{83}$$

where brackets denote divided differences of the specified data and the empty product is 1. Choose $0 < R < 1$ and retain the tail inside the domain of A, with $|\alpha_k| \le d < R/2$. Then the series converges uniformly on every $|z| \le r < R - 2d$.

Continue $F_M := \mathcal{N}_M - z$ to $\Omega := \{\Re z > -1\}$ in the Gamma continuation class. There is exactly one integer M_* in this reconstructed gauge family for which

$$F_{M_*}(z+1) = (z+1)F_{M_*}(z) \quad (z \in \Omega). \tag{84}$$

The selected function is $F_{\mathscr{G}}(z) = \Gamma(1+z)$. Define

$$\Phi_{\mathscr{G}}(z) := \frac{F''_{\mathscr{G}}(z)}{F_{\mathscr{G}}(z)} - \left(\frac{F'_{\mathscr{G}}(z)}{F_{\mathscr{G}}(z)}\right)^2, \tag{85}$$

and, for $t > 0$ and any $\sigma > 0$, take the symmetric inversion limit

$$K_{\mathscr{G}}(t) := \lim_{T\to\infty} \frac{1}{2\pi i} \int_{\sigma-iT}^{\sigma+iT} e^{zt}\Phi_{\mathscr{G}}(z)\, dz = \frac{t}{e^t - 1}. \tag{86}$$

Finally, for $\Re s > 1$, put

$$\mathcal{Z}_{\mathscr{G}}(s) := \frac{1}{F_{\mathscr{G}}(s-1)} \int_0^\infty t^{s-2} K_{\mathscr{G}}(t)\, dt, \tag{87}$$

$$\mathcal{P}_{\mathscr{G}}(s) := \sum_{k\geq 1} \frac{\mu(k)}{k} \log \mathcal{Z}_{\mathscr{G}}(ks). \tag{88}$$

The integral converges absolutely, the last series converges absolutely and locally uniformly, and

$$\mathcal{Z}_{\mathscr{G}}(s) = \zeta(s), \qquad \mathcal{P}_{\mathscr{G}}(s) = P_{\mathrm{pr}}(s) \quad (\Re s > 1). \tag{89}$$

The logarithm is the holomorphic branch real for real $s > 1$.

Proof. Convergent reconstruction. There is an unknown integer C such that $\alpha_k = z^+_{C+k}$. The exact branch samples give

$$Y_k^{(M)} = H(\alpha_k) + (M - C)\alpha_k^2.$$

Thus the Newton polynomials interpolate the holomorphic function $f_M(z) := H(z) + (M - C)z^2$. For their degree-$n$ partial sum $P_{M,n}$, Cauchy's interpolation remainder is

$$f_M(z) - P_{M,n}(z) = \frac{1}{2\pi i} \int_{|\zeta|=R} \frac{f_M(\zeta)}{\zeta - z} \prod_{j=0}^{n} \frac{z - \alpha_j}{\zeta - \alpha_j}\, d\zeta.$$

On $|z| \leq r < R - 2d$, its modulus is bounded by a constant times $\big((r+d)/(R-d)\big)^{n+1}$, which tends to zero. This proves genuine local uniform convergence and

$$\mathcal{N}_M = H + (M - C)z^2, \qquad F_M = \Gamma(1+z) + (M - C)z^2. \tag{90}$$

These germs possess holomorphic continuations to Ω because the data come from the actual Gamma system. Reconstruction on Ω means that unique continuation of the Newton germ; the local interpolation estimate alone makes no global existence claim.

Fixing the integer gauge. Put $k = M - C$. The recurrence defect of F_M is

$$F_M(z+1) - (z+1)F_M(z) = k\big((z+1)^2 - (z+1)z^2\big).$$

The polynomial is not identically zero, so the recurrence selects $k = 0$, or $M_* = C$. This uniqueness is within the additive gauge family (90); no unrestricted characterization of Gamma by its recurrence is being asserted. Changing the retained finite head changes the temporary origin C but leaves $F_{\mathscr{G}}$ unchanged.

Laplace and Mellin steps. The recovered function $F_{\mathscr{G}} = \Gamma(1+z)$ is zero-free on Ω, and its logarithmic second derivative satisfies

$$\Phi_{\mathscr{G}}(z) = \psi'(1+z) = \int_0^\infty e^{-zt} \frac{t}{e^t - 1}\, dt, \qquad \Re z > -1. \tag{91}$$

This follows by differentiating the classical digamma integral [12, Eq. 5.9.16]. The kernel extends smoothly to $t = 0$ with value 1 and decays exponentially at infinity. The classical pointwise Laplace inversion formula [12, Eq. 1.14.20] therefore gives (86) for $t > 0$. In particular, it is $\Phi_{\mathscr{D}}$, not $F_{\mathscr{D}}$, whose inverse Laplace transform is $t/(e^t - 1)$.

Now $K_{\mathscr{D}}(t) = 1 + O(t)$ at 0 and $K_{\mathscr{D}}(t) = O(te^{-t})$ at infinity, so (87) converges absolutely and locally uniformly on $\Re s > 1$. The classical Mellin identity [12, Eq. 25.5.1] gives

$$\int_0^\infty t^{s-2} K_{\mathscr{D}}(t)\, dt = \Gamma(s)\zeta(s).$$

Its denominator is already recovered: $F_{\mathscr{D}}(s-1) = \Gamma(s)$. Thus $\mathcal{Z}_{\mathscr{D}} = \zeta$ on the whole half-plane. Proposition 3.22, including its normal-convergence proof for complex arguments, now gives $\mathcal{P}_{\mathscr{D}} = P_{\mathrm{pr}}$ there. □

This is a composite analytic transform, rather than a single linear kernel sum over the zeros. It uses exact locations, convergent interpolation and unique analytic continuation. No numerical conditioning or stability under perturbation is claimed.

Corollary 3.32 (The inverse hierarchy)**.** *In the Gamma specialization, the embedded non-real zero set in a sufficiently small punctured neighbourhood of* 0*, without any additional markings, determines*

$$\begin{aligned} &\mathscr{D} \implies \textit{the canonical upper tail intrinsically} \\ &\implies W \bmod \mathbb{Z} \implies G \textit{ exactly as a punctured germ,} \\ &\textit{in the natural continuation class:}\quad G \textit{ on } \Omega_G \implies \{1\} \cup \mathbb{P}. \end{aligned} \tag{92}$$

With the Gamma recurrence fixing the integer representative, the same data determine the full analytic function $P_{\mathrm{pr}}(s)$ on $\Re s > 1$ by the explicit composite transform above.

Proof. Combine Theorem 3.28, Theorem 3.29, Corollary 3.30 and Theorem 3.31. The positive-real zero theorem enters only after recovery of G; it is not an input to either inverse reconstruction. □

4. Arithmetic nodal waves

The preceding sections concern the complex zero geometry of G. We now turn to a construction that uses only its already known real arithmetic divisor

$$\mathcal{P}_1 = \{1\} \cup \mathbb{P}.$$

As emphasized in Section 1, this part of the theory is logically independent of the Fundamental Classification Conjecture.

Put

$$\mathbb{R}_* := \mathbb{R} \setminus \{0, -1, -2, \ldots\}$$

and define the regular real spacetime domain

$$\mathcal{D}_{\mathbb{R}} := \{(x,t) \in \mathbb{R}^2 : x - t,\ x + t \in \mathbb{R}_*\}.$$

For $(x,t) \in \mathcal{D}_{\mathbb{R}}$, define the Goodspeed wave

$$Q_G(x,t) := \frac{1}{2}\big(G(x-t) + G(x+t)\big).$$

Since $G \geq 0$ on $\mathbb{R}_*$ and

$$Z(G) \cap \mathbb{R}_* = \mathcal{P}_1,$$

the arithmetic content of this construction comes from the real Wilson–Gamma divisor rather than from the wave equation itself.

This construction meets several classical themes without coinciding with any of them. The additive and simultaneous-primality questions arising from the nodal slices belong to the Hardy–Littlewood and Dickson programmes for prime sums and prime values of affine-linear forms; see [8,

4]. Our use of nodal geometry is also different from the theory of arithmetic random waves, where arithmetic enters through Laplace eigenfunctions on the torus and one studies probabilistic nodal statistics; see Krishnapur, Kurlberg, and Wigman [10]. Here the wave is deterministic: arithmetic enters through the real zero divisor of G, and characteristic evolution converts pairs of those zeros into an exact spacetime nodal set.

The elementary evolution law is recorded first.

Proposition 4.1 (Wave equation and Cauchy data)**.** *Wherever the defining characteristic arguments are regular, the Goodspeed wave satisfies*

$$(Q_G)_{tt} = (Q_G)_{xx}.$$

On the regular part of the initial line, its Cauchy data are

$$Q_G(x,0) = G(x), \qquad (Q_G)_t(x,0) = 0.$$

Proof. Direct differentiation gives

$$(Q_G)_{tt}(x,t) = \frac{1}{2}\big(G''(x-t) + G''(x+t)\big) = (Q_G)_{xx}(x,t).$$

At $t = 0$, substitution gives $Q_G(x,0) = G(x)$, while the two first time derivatives cancel. □

Thus the Goodspeed wave propagates with unit speed: in the standard form $u_{tt} = c^2 u_{xx}$ one has $c = 1$, and its characteristic coordinates are precisely $x - t$ and $x + t$. For the classical one-dimensional wave equation, the d'Alembert representation, and the associated characteristic and spacetime viewpoints, see, for example, Strauss [15].

The wave equation is universal for a d'Alembert expression of this form: the same calculation applies to every C^2 initial profile. Solving that equation is not, by itself, the arithmetic novelty. The arithmetic content comes from the positivity of G and its special positive-real zero divisor.

Introduce the characteristic variables

$$p = x - t, \qquad q = x + t,$$

and the positive characteristic cone

$$\mathcal{C}_+ := \{(x,t) \in \mathbb{R}^2 : x > |t|\} = \{p > 0,\ q > 0\}.$$

The characteristic map

$$L(p,q) := \left(\frac{p+q}{2}, \frac{q-p}{2}\right)$$

will identify the real nodal set with

$$L(\mathcal{P}_1 \times \mathcal{P}_1).$$

Thus every node records exactly two arithmetic endpoints, while interchanging those endpoints reflects the node across $t = 0$.

The remainder of this section develops the consequences of this endpoint description. We first identify the nodal set and its counting measure, then study the complete local characteristic jet and Hessian at a node. Vertical, horizontal, and rational-affine slices are used to organize prime sums, fixed differences, and more general two-prime affine relations. Finally, we separate exact structural identities from the classical prime-correlation questions that remain conjectural and prove two unconditional quantitative results: a positive finite fixed-gap detector and a macroscopic nodal density law obtained from the prime number theorem.

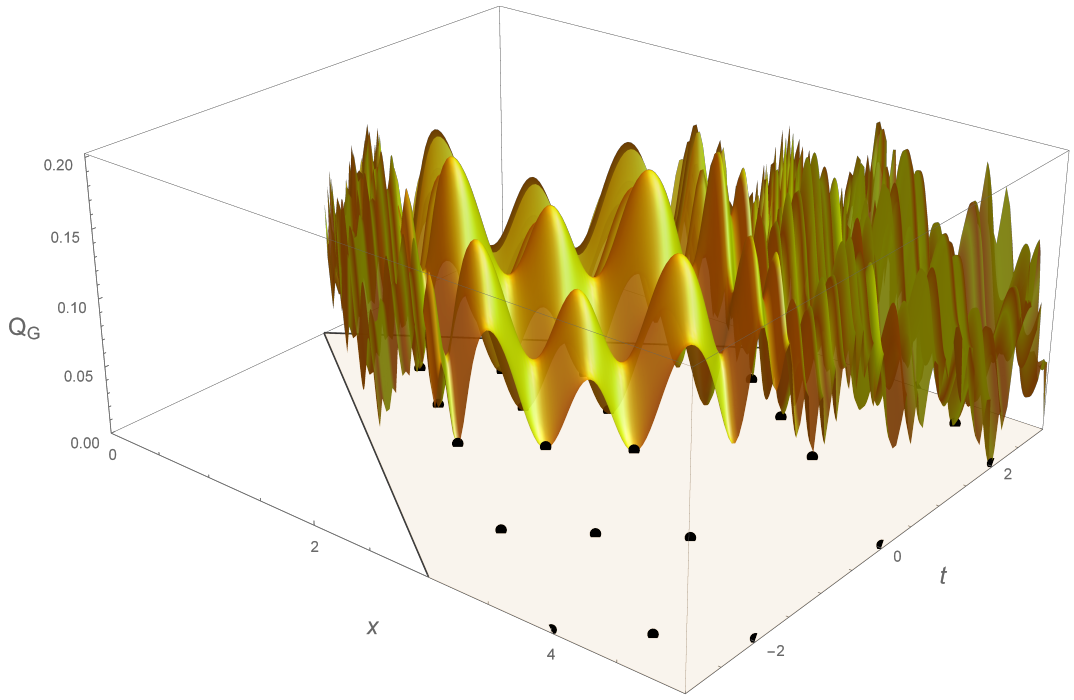


FIGURE 8. The Goodspeed wave $Q_G(x,t)$ on a bounded portion of the positive characteristic cone. The wave is nonnegative throughout this region. The marked points on the zero plane are the arithmetic nodes

$$(x,t) = \left(\frac{p+q}{2}, \frac{q-p}{2}\right), \qquad p,q \in \mathcal{P}_1, \quad p \le q,$$

with characteristic endpoints in the displayed range. Thus the isolated zero minima of the wave encode pairs of positive-real arithmetic zeros of G.

4.1. **Arithmetic nodal set.** We first identify the nodal set on the full regular real spacetime domain. The positive characteristic cone will emerge automatically from the arithmetic endpoints.

Theorem 4.2 (Arithmetic nodal set of the Goodspeed wave)**.** *For every* $(x,t) \in \mathcal{D}_{\mathbb{R}}$,

$$Q_G(x,t) \ge 0,$$

and

$$Q_G(x,t) = 0 \quad \Longleftrightarrow \quad x - t \in \mathcal{P}_1 \text{ and } x + t \in \mathcal{P}_1.$$

Consequently every real node lies in $\mathcal{C}_+$*. With*

$$L(p,q) := \left(\frac{p+q}{2}, \frac{q-p}{2}\right),$$

the full regular real nodal set is

$$\mathcal{N}_G := \{(x,t) \in \mathcal{D}_{\mathbb{R}} : Q_G(x,t) = 0\} = L(\mathcal{P}_1 \times \mathcal{P}_1) \subset \mathcal{C}_+.$$

Its restriction to nonnegative time is

$$\mathcal{N}_G \cap \{t \ge 0\} = \left\{ \left(\frac{p+q}{2}, \frac{q-p}{2}\right) : p,q \in \mathcal{P}_1,\ p \le q \right\}.$$

Proof. Let

$$p = x - t, \qquad q = x + t.$$

For $(x,t) \in \mathcal{D}_{\mathbb{R}}$, both p and q belong to $\mathbb{R}_*$. Section 1 gives

$$G(p) \geq 0, \qquad G(q) \geq 0,$$

and therefore

$$Q_G(x,t) = \frac{1}{2}\big(G(p) + G(q)\big) \geq 0.$$

No cancellation is possible. Hence

$$Q_G(x,t) = 0 \quad \Longleftrightarrow \quad G(p) = G(q) = 0 \quad \Longleftrightarrow \quad p, q \in \mathcal{P}_1.$$

Since $\mathcal{P}_1 \subset (0,\infty)$, every such node satisfies $p, q > 0$, equivalently $x > |t|$, and therefore lies in $\mathcal{C}_+$.

Solving the characteristic equations gives

$$(x,t) = L(p,q).$$

Conversely every $p, q \in \mathcal{P}_1$ produces such a node. Finally,

$$t = \frac{q-p}{2} \geq 0 \quad \Longleftrightarrow \quad p \leq q.$$

□

The map L is an invertible linear map on $\mathbb{R}^2$ and restricts to a homeomorphism from $(0,\infty)^2$ onto $\mathcal{C}_+$, with inverse

$$L^{-1}(x,t) = (x-t, x+t).$$

Thus a node records exactly the two positive-real arithmetic endpoints of its characteristics. Interchanging the endpoints reflects the node across $t = 0$; the two orderings coincide only on the diagonal $p = q$.

Geometrically, the normalized characteristic change $(x,t) \mapsto (p/\sqrt{2}, q/\sqrt{2})$ is the counterclockwise rotation through $\pi/4$. In characteristic coordinates the entire nodal set becomes simply $\mathcal{P}_1 \times \mathcal{P}_1$. Thus the arithmetic nodal set is, in characteristic coordinates, simply the Cartesian product $\mathcal{P}_1 \times \mathcal{P}_1$; the spacetime picture is its rotated and rescaled image. To retain the counting information, let δ_a denote unit point mass at a and define

$$\mu_{\mathcal{P}_1} := \sum_{p \in \mathcal{P}_1} \delta_p, \qquad \mathcal{N}_G := L_{\#}\big(\mu_{\mathcal{P}_1} \otimes \mu_{\mathcal{P}_1}\big).$$

The endpoint measure is defined on $(0,\infty)$ and is also regarded as a measure on $\mathbb{R}$ by extension by zero. Here push-forward means $f_{\#}\nu(B) = \nu(f^{-1}(B))$ for Borel sets B. For $X \geq 1$, set

$$\mu_{\mathcal{P}_1,X} := \sum_{\substack{p \in \mathcal{P}_1 \\ p \leq X}} \delta_p, \qquad \mathcal{N}_{G,X} := L_{\#}\big(\mu_{\mathcal{P}_1,X} \otimes \mu_{\mathcal{P}_1,X}\big).$$

These are finite endpoint truncations. Define the two coordinate maps

$$s(x,t) := 2x, \qquad d(x,t) := 2t,$$

and the reflected endpoint measure by

$$\widetilde{\mu}_{\mathcal{P}_1,X}(A) := \mu_{\mathcal{P}_1,X}(-A) \qquad (A \subset \mathbb{R} \text{ Borel}).$$

Convolution is taken on $\mathbb{R}$; in particular, $\delta_a * \delta_b = \delta_{a+b}$.

Theorem 4.3 (The Goodspeed nodal measure and its additive projections)**.** *The measure $\mathcal{N}_G$ is a locally finite purely atomic measure on $\mathbb{R}^2$, with*

$$\mathcal{N}_G = \sum_{p,q \in \mathcal{P}_1} \delta_{((p+q)/2,(q-p)/2)}, \qquad \operatorname{supp} \mathcal{N}_G = \mathscr{N}_G.$$

Each ordered characteristic pair (p, q) carries unit mass. For every $X \geq 1$, its finite endpoint truncation satisfies

$$s_{\#}\mathcal{N}_{G,X} = \mu_{\mathcal{P}_1,X} * \mu_{\mathcal{P}_1,X},$$
$$d_{\#}\mathcal{N}_{G,X} = \widetilde{\mu}_{\mathcal{P}_1,X} * \mu_{\mathcal{P}_1,X}.$$

The global sum projection is also locally finite and satisfies

$$s_{\#}\mathcal{N}_G = \mu_{\mathcal{P}_1} * \mu_{\mathcal{P}_1}.$$

Proof. Pushing forward the product of the endpoint counting measures gives

$$\mathcal{N}_G = \sum_{p,q\in\mathcal{P}_1} \delta_{L(p,q)},$$

which is the asserted atomic formula. Since L is injective, distinct ordered pairs give distinct atoms, each of mass one.

If $K \subset \mathbb{R}^2$ is compact, then $L^{-1}(K)$ is compact and meets $\mathcal{P}_1 \times \mathcal{P}_1 \subset \mathbb{N}^2$ in only finitely many points. Thus $\mathcal{N}_G(K) < \infty$. Moreover, $\mathcal{P}_1 \times \mathcal{P}_1$ is closed and discrete in $\mathbb{R}^2$, and so is its image under L. Every point of this image is an atom of positive mass. Theorem 4.2 therefore gives $\operatorname{supp}\mathcal{N}_G = \mathscr{N}_G$.

The projection identities follow directly from

$$s(L(p, q)) = p + q, \qquad d(L(p, q)) = q - p.$$

Indeed,

$$s_{\#}\mathcal{N}_{G,X} = \sum_{\substack{p,q\in\mathcal{P}_1\\ p,q\leq X}} \delta_{p+q} = \mu_{\mathcal{P}_1,X} * \mu_{\mathcal{P}_1,X},$$
$$d_{\#}\mathcal{N}_{G,X} = \sum_{\substack{p,q\in\mathcal{P}_1\\ p,q\leq X}} \delta_{-p+q} = \widetilde{\mu}_{\mathcal{P}_1,X} * \mu_{\mathcal{P}_1,X}.$$

For the global sum projection, take a compact set $B \subset \mathbb{R}$ and choose $M > 0$ with $B \subset [-M, M]$. If $p, q > 0$ and $p + q \in B$, then $p, q \leq M$, leaving only finitely many endpoint pairs. Hence the sum projection is locally finite, and the same atomic computation yields

$$s_{\#}\mathcal{N}_G = \sum_{p,q\in\mathcal{P}_1} \delta_{p+q} = \mu_{\mathcal{P}_1} * \mu_{\mathcal{P}_1}.$$

□

The full-cone measure retains the ordering of the endpoints. Its restriction to $t \geq 0$ imposes $p \leq q$, giving one representative of each unordered pair, with diagonal pairs still carrying unit mass. These are counting weights, independent of the analytic multiplicities of the zeros of G. Throughout, the endpoint 1 remains part of $\mathcal{P}_1$; it has not been discarded in either the nodal measure or its projections.

The truncation in the difference identity is essential. Every diagonal arithmetic node $L(p, p) = (p, 0)$ belongs to $d^{-1}(\{0\})$, so

$$(d_{\#}\mathcal{N}_G)(\{0\}) = \mathcal{N}_G\big(d^{-1}(\{0\})\big) = \sum_{p\in\mathcal{P}_1} 1 = \infty.$$

The untruncated difference push-forward is consequently not locally finite. Finite endpoint truncation gives the appropriate Radon-measure formulation of the prime-difference identity, with the exceptional endpoint 1 included.

The projection formulas show that prime sums and prime differences, together with the contributions involving 1, are the two linear coordinate projections of one arithmetic spacetime nodal measure. For example, the ordered pair $(p, q) = (3, 17)$ gives the node $(x, t) = (10, 7)$, at which

$$2x = 20 = p + q, \qquad 2t = 14 = q - p.$$

Having identified the nodal set and its counting measure, we next examine the local geometry at an individual arithmetic node.

4.2. **Local geometry and arithmetic recovery at a node.** We now fix an arithmetic node and examine the information carried by the wave near it. The two characteristic directions separate the endpoint contributions at every derivative order. At second order, this separation identifies two positive curvature coefficients and gives a direct geometric description of the node.

Lemma 4.4 (Quadratic arithmetic zeros)**.** *For every $r \in \mathcal{P}_1$,*

$$G(r) = G'(r) = 0, \qquad A_r := \frac{G''(r)}{2} = 1 + W'(r)^2 > 0.$$

In particular, every positive-real arithmetic zero of G has order exactly two.

Proof. Both r and $W(r)$ are integers, including $W(1) = 2$. Since W is analytic near r,

$$W(r + h) - W(r) = W'(r)h + O(h^2).$$

Using the integer periodicity of the squared sine in the definition of G therefore gives

$$\begin{aligned} G(r + h) &= \frac{\sin^2(\pi h) + \sin^2\big(\pi(W(r + h) - W(r))\big)}{\pi^2} \\ &= \big(1 + W'(r)^2\big)h^2 + O(h^3). \end{aligned}$$

The assertions follow by comparison with the Taylor expansion of G. The coefficient is strictly positive because $W'(r)$ is real. □

For $r \in \mathcal{P}_1$, write

$$c_{r,n} := \frac{G^{(n)}(r)}{n!} \qquad (n \geq 0).$$

Thus $c_{r,0} = c_{r,1} = 0$ and $c_{r,2} = A_r$.

Theorem 4.5 (Two-endpoint lifting and characteristic-jet splitting)**.** *Let $p, q \in \mathcal{P}_1$, and put*

$$(x_0, t_0) = \left(\frac{p + q}{2}, \frac{q - p}{2}\right).$$

For $x = x_0 + \xi$ and $t = t_0 + \tau$, set

$$u := \xi - \tau, \qquad v := \xi + \tau.$$

Then, wherever the characteristic arguments are regular,

$$Q_G(x_0 + \xi, t_0 + \tau) = \frac{1}{2}\big(G(p + u) + G(q + v)\big).$$

For every fixed integer $N \geq 2$, as $(\xi, \tau) \to (0, 0)$,

$$Q_G(x_0 + \xi, t_0 + \tau) = \frac{1}{2}\sum_{n=2}^{N}\big(c_{p,n}u^n + c_{q,n}v^n\big) + O_{p,q,N}\big((|\xi| + |\tau|)^{N+1}\big).$$

In particular,

$$Q_G(x_0 + \xi, t_0 + \tau) = \frac{1}{2}\big(A_p(\xi - \tau)^2 + A_q(\xi + \tau)^2\big) + O_{p,q}\big((|\xi| + |\tau|)^3\big).$$

Define the characteristic differential operators

$$D_- := \frac{1}{2}(\partial_x - \partial_t), \qquad D_+ := \frac{1}{2}(\partial_x + \partial_t).$$

At every regular spacetime point,

$$D_-^n Q_G(x,t) = \frac{1}{2}G^{(n)}(x-t), \qquad D_+^n Q_G(x,t) = \frac{1}{2}G^{(n)}(x+t), \qquad n \geq 1,$$

and all mixed characteristic derivatives vanish:

$$D_-^a D_+^b Q_G \equiv 0, \qquad a, b \geq 1.$$

Proof. The node coordinates satisfy $x_0 - t_0 = p$ and $x_0 + t_0 = q$. Hence

$$x - t = p + u, \qquad x + t = q + v,$$

and substitution into the definition of Q_G proves the exact decomposition. Taylor expansion of G at each endpoint, using Lemma 4.4, gives

$$G(r+h) = \sum_{n=2}^{N} c_{r,n} h^n + O_{r,N}(|h|^{N+1}).$$

Apply this with $(r,h) = (p,u)$ and (q,v). Since $|u|, |v| \leq |\xi| + |\tau|$, the stated remainder follows. Taking $N = 2$ gives the quadratic expansion.

In the characteristic coordinates $(x-t, x+t)$, the chain rule identifies D_- with differentiation in the first coordinate and D_+ with differentiation in the second. Each operator therefore differentiates only its corresponding summand of Q_G. Repeated differentiation proves the pure derivative identities, and differentiating in both coordinates annihilates each summand. □

Consequently, the complete characteristic jet at an arithmetic node splits canonically into the two real-axis endpoint jets of G. Explicitly,

$$\begin{aligned} G^{(n)}(p) &= 2(D_-^n Q_G)(x_0, t_0), \\ G^{(n)}(q) &= 2(D_+^n Q_G)(x_0, t_0), \end{aligned} \qquad n \geq 1,$$

while the zeroth-order endpoint values are both zero. Thus the local wave data recover the two endpoint jets independently, with the characteristic directions labelling the two contributions.

Corollary 4.6 (Hessian splitting and local arithmetic recovery)**.** *At the node (x_0, t_0) of Theorem 4.5,*

$$(Q_G)_{xx} = (Q_G)_{tt} = A_p + A_q, \qquad (Q_G)_{xt} = A_q - A_p.$$

In particular, the two endpoint curvature coefficients are recovered by

$$A_p = \frac{(Q_G)_{xx} - (Q_G)_{xt}}{2}, \qquad A_q = \frac{(Q_G)_{xx} + (Q_G)_{xt}}{2},$$

where all derivatives are evaluated at (x_0, t_0). The Euclidean Hessian is

$$\operatorname{Hess} Q_G(x_0, t_0) = \begin{pmatrix} A_p + A_q & A_q - A_p \\ A_q - A_p & A_p + A_q \end{pmatrix},$$

with orthonormal eigenpairs

$$\left(\frac{(1,-1)}{\sqrt{2}},\, 2A_p\right), \qquad \left(\frac{(1,1)}{\sqrt{2}},\, 2A_q\right).$$

Every arithmetic node is therefore an isolated strict local minimum of Q_G. In the orthonormal characteristic coordinates

$$\alpha := \frac{\xi - \tau}{\sqrt{2}}, \qquad \beta := \frac{\xi + \tau}{\sqrt{2}},$$

its quadratic part is $A_p\alpha^2 + A_q\beta^2$. The small positive levels near the node are asymptotic to the ellipses

$$A_p\alpha^2 + A_q\beta^2 = \varepsilon,$$

whose leading semiaxes are

$$\sqrt{\frac{\varepsilon}{A_p}}, \qquad \sqrt{\frac{\varepsilon}{A_q}}.$$

Proof. Differentiate the exact decomposition twice and use $G''(p) = 2A_p$ and $G''(q) = 2A_q$. This gives the Hessian entries, and adding and subtracting the first and mixed entries gives the recovery formulas. Multiplication by the two displayed unit vectors gives the eigenvalues $2A_p$ and $2A_q$.

The gradient vanishes by Lemma 4.4. Since $A_p, A_q > 0$, the Hessian is positive definite, so the node is a nondegenerate strict local minimum and is isolated in the zero set. The orthonormal change of variables gives

$$Q_G(x_0 + \xi, t_0 + \tau) = A_p\alpha^2 + A_q\beta^2 + O_{p,q}\big((|\alpha| + |\beta|)^3\big).$$

For precision, set $(\alpha, \beta) = \sqrt{\varepsilon}\,(a, b)$ and divide the level equation by ε. On bounded (a, b)-sets the rescaled function converges, together with its first derivatives, to $A_pa^2 + A_qb^2$. Its unit level is regular, so the implicit function theorem gives convergence of the local rescaled level curves to $A_pa^2 + A_qb^2 = 1$. This proves the ellipse asymptotics and the stated leading semiaxes. □

The two characteristic directions thus carry the two endpoint curvatures independently. When $p = q$, one has $A_p = A_q$, and the quadratic form is isotropic. In general its second-order anisotropy is measured by $A_q - A_p$.

The arithmetic recovery uses both location and curvature. The node location itself gives

$$p = x_0 - t_0, \qquad q = x_0 + t_0,$$

and its Hessian gives A_p and A_q separately. Thus the local spacetime data recover both arithmetic endpoints and their corresponding real-axis curvature coefficients. This statement includes the exceptional endpoint 1 throughout.

For prime endpoints, the curvature coefficient satisfies a useful identity involving the Wilson quotient. This should be viewed as a relation among arithmetic data attached to a known endpoint r, not as independent recovery of information unavailable from the node location. For a rational prime r, write

$$w_r := \frac{(r-1)! + 1}{r} = W(r).$$

Let $H_m := \sum_{k=1}^{m} k^{-1}$ and let γ denote Euler's constant.

Corollary 4.7 (Wilson-quotient identity from endpoint curvature)**.** *For every rational prime $r \geq 3$,*

$$W'(r) = \sqrt{A_r - 1}, \qquad w_r = (r-1)!\big(H_{r-1} - \gamma\big) - r\sqrt{A_r - 1}.$$

Consequently, for each known prime endpoint $r \geq 3$, its curvature coefficient and Wilson quotient are related explicitly by the displayed formula.

Proof. Write $\psi = \Gamma'/\Gamma$. Differentiating W gives

$$W'(z) = \frac{z\Gamma'(z) - \Gamma(z) - 1}{z^2}.$$

At a prime r, use $\Gamma(r) = (r-1)!$, $\Gamma'(r) = (r-1)!\psi(r)$, and $\Gamma(r) + 1 = rw_r$ to obtain

$$W'(r) = \frac{(r-1)!\, r\psi(r) - rw_r}{r^2}, \qquad w_r = (r-1)!\psi(r) - rW'(r).$$

The classical identity $\psi(r) = H_{r-1} - \gamma$ follows from the digamma recurrence and $\psi(1) = -\gamma$. To determine the sign, observe that for $r \geq 3$,

$$W'(r) = \frac{(r-1)!\big(r\psi(r) - 1\big) - 1}{r^2} > 0.$$

Indeed, $\gamma < 1$ gives $\psi(r) \geq H_2 - \gamma > 1/2$, while $(r-1)! \geq 2$, so the numerator is strictly positive. Lemma 4.4 now gives $W'(r) = \sqrt{A_r - 1}$. Substitution proves the formula, and Corollary 4.6 supplies the separate curvature coefficient for each endpoint. □

The Wilson-quotient formula reorganizes arithmetic information already present in the local curvature of G. The wave construction carries that information independently along the two characteristic directions; it does not create a new independent arithmetic invariant. Section 4.3 turns from the geometry at an individual node to the locations of nodes on prime-sum and prime-difference slices.

4.3. **Goldbach and prime-pair slices.** Vertical and horizontal slices read the two elementary additive relations between characteristic endpoints:

$$p + q = 2x, \qquad q - p = 2t.$$

Throughout this section, nodes belong to $\mathscr{N}_G \subset \mathcal{C}_+$. A node is called *non-exceptional* when both characteristic endpoints are rational primes; the remaining arithmetic nodes involve the endpoint 1.

Theorem 4.8 (Sum and difference slices)**.** *For $N > 0$, the vertical slice is*

$$\mathscr{N}_G \cap \{x = N/2\} = \left\{ \left(\frac{N}{2}, \frac{q-p}{2} \right) : p, q \in \mathcal{P}_1,\ p + q = N \right\}.$$

Equivalently, for $|t| < N/2$,

$$Q_G\left(\frac{N}{2}, t \right) = 0 \quad \Longleftrightarrow \quad \frac{N}{2} - t,\ \frac{N}{2} + t \in \mathcal{P}_1.$$

For $h \in \mathbb{R}$, the horizontal slice is

$$\mathscr{N}_G \cap \{t = h/2\} = \left\{ \left(p + \frac{h}{2}, \frac{h}{2} \right) : p, p + h \in \mathcal{P}_1 \right\}.$$

Equivalently, for $x > |h|/2$,

$$Q_G\left(x, \frac{h}{2} \right) = 0 \quad \Longleftrightarrow \quad x - \frac{h}{2},\ x + \frac{h}{2} \in \mathcal{P}_1.$$

Proof. By Theorem 4.2, a point of $\mathcal{C}_+$ is a node exactly when its characteristic endpoints $p = x - t$ and $q = x + t$ belong to $\mathcal{P}_1$. On $x = N/2$ their sum is N, and the node has time coordinate $(q-p)/2$. On $t = h/2$ their difference is h, so $q = p + h$ and $x = p + h/2$. Conversely, each endpoint pair in the displayed sets gives a point of $\mathcal{C}_+$ with the required coordinates and hence a node. □

These identities are exact. They identify individual intersections with individual arithmetic representations, without any limiting process or asymptotic estimate.

Corollary 4.9 (Goldbach slices)**.** *For every even integer $N \geq 4$, the nodes on $x = N/2$ with $t \geq 0$ correspond bijectively to representations*

$$N = p + q, \qquad p, q \in \mathcal{P}_1, \quad p \leq q.$$

After excluding representations involving 1, the remaining nodes correspond exactly to the unordered Goldbach representations of N. Consequently, the strong Goldbach conjecture is equivalent to the assertion that every even integer $N \geq 4$ has a node on $x = N/2$, $t \geq 0$, whose two characteristic endpoints are rational primes.

Proof. Apply the vertical identity of Theorem 4.8 and observe that $t = (q-p)/2 \geq 0$ is equivalent to $p \leq q$. The inverse characteristic map makes the correspondence bijective. Requiring both endpoints to lie in $\mathbb{P}$ gives precisely a Goldbach representation. □

The restriction to nonnegative time counts each unordered representation once. Equal prime summands are allowed: a representation $N = 2p$ gives the node $(p, 0)$. The exceptional endpoint 1 must nevertheless be excluded when asserting a genuine Goldbach representation.

Example 4.10 (The vertical slice $x = 10$)**.** *The complete list of unordered $\mathcal{P}_1$-representations of* 20 *is*

$$20 = 1 + 19 = 3 + 17 = 7 + 13.$$

Their nodal coordinates and arithmetic interpretations are

(p, q)	(x, t)	*interpretation*
$(1, 19)$	$(10, 9)$	*exceptional endpoint* 1
$(3, 17)$	$(10, 7)$	*Goldbach representation*
$(7, 13)$	$(10, 3)$	*Goldbach representation*

Thus the vertical line contains three arithmetic nodes in $t \geq 0$, of which exactly two are Goldbach nodes.

Corollary 4.11 (Fixed prime-pair slices)**.** *For every positive even integer h, the non-exceptional nodes on $t = h/2$ correspond bijectively to prime pairs $p, q \in \mathbb{P}$ with $q - p = h$, through*

$$(p, p + h) \longmapsto \left(p + \frac{h}{2}, \frac{h}{2}\right).$$

In particular, the line $t = 1$ contains the exceptional node $(2, 1)$ arising from $(1, 3)$, and all its other arithmetic nodes correspond exactly to twin-prime pairs. For $x > 1$ and $x \neq 2$,

$$Q_G(x, 1) = 0 \quad \Longleftrightarrow \quad x - 1,\ x + 1 \text{ are twin primes.}$$

Proof. Restrict the horizontal identity of Theorem 4.8 to prime endpoints. When $h = 2$, an exceptional pair must have smaller endpoint 1 and larger endpoint 3, giving $(x, t) = (2, 1)$. Every remaining pair consists of two primes differing by 2. □

For example,

$$(3, 5) \longmapsto (4, 1), \qquad (5, 7) \longmapsto (6, 1), \qquad (11, 13) \longmapsto (12, 1).$$

The twin-prime conjecture therefore has the equivalent geometric form

The horizontal line $t = 1$ contains infinitely many
non-exceptional arithmetic nodes.

This is a reformulation of the conjecture, not an infinitude result. Figure 9 places the sum and difference examples in the same two-dimensional nodal picture.

Fixed prime differences must be distinguished from gaps between successive primes. Call an arithmetic node a *consecutive-prime node* when its characteristic endpoints $p < q$ are consecutive rational primes.

Corollary 4.12 (Polignac slices)**.** *For every integer $m \geq 1$, Polignac's conjecture for the even gap $2m$ is equivalent to the assertion that the horizontal line $t = m$ contains infinitely many consecutive-prime nodes.*

Proof. At a node on $t = m$, the characteristic endpoints satisfy $q - p = 2m$. Imposing that these endpoints are consecutive primes gives exactly the prime gaps counted by Polignac's conjecture, and the characteristic map is a bijection between these pairs and their nodes. □

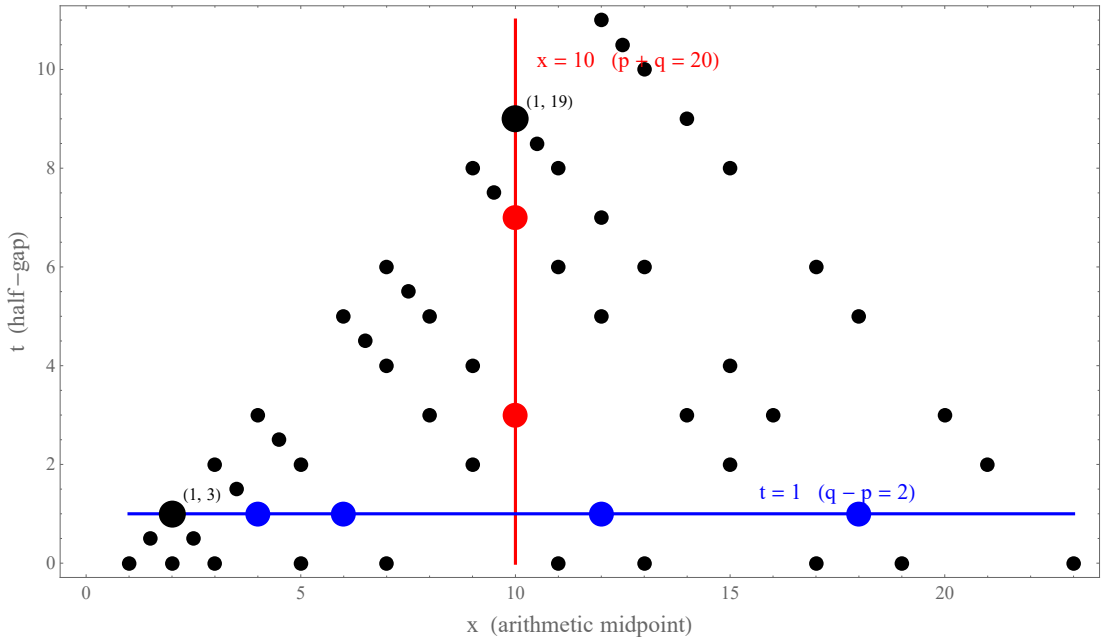


FIGURE 9. Arithmetic nodes in the (x,t)-plane for $p,q \in \mathcal{P}_1$ with $1 \le p \le q \le 23$, plotted at $((p+q)/2,(q-p)/2)$. Vertical slices encode endpoint sums, and horizontal slices encode endpoint differences. The highlighted line $x = 10$ contains the three nodes associated with $20 = 1+19 = 3+17 = 7+13$; $(10,9)$ involves the exceptional endpoint 1. The highlighted line $t = 1$ encodes gap 2: its exceptional node $(2,1)$ comes from $(1,3)$, while its remaining displayed nodes correspond to twin-prime pairs.

The consecutive-prime condition is essential. The equation $q - p = 2m$ alone allows primes strictly between the endpoints. For instance, $(3,7)$ gives a node on $t = 2$, but the intervening prime 5 makes it unsuitable for the consecutive-gap interpretation. Twin-prime pairs are automatically consecutive, so this distinction does not alter the interpretation of $t = 1$ after its exceptional node is removed.

Proposition 4.13 (An unconditional bounded nodal strip)**.** *There exists a finite constant $B > 0$ such that Q_G has infinitely many consecutive-prime arithmetic nodes in the horizontal strip*

$$0 < t \le \frac{B}{2}.$$

Proof. The modern bounded-gap theory for consecutive primes, initiated by Zhang and subsequently strengthened by Maynard and the Polymath8 project, gives a finite constant B such that infinitely many consecutive-prime pairs $p < q$ satisfy $q - p \le B$; see [16, 13, 14]. Each such pair gives the consecutive-prime node

$$(x,t) = \left(\frac{p+q}{2}, \frac{q-p}{2}\right), \qquad 0 < t \le \frac{B}{2}.$$

Distinct pairs give distinct nodes, proving the assertion. □

Corollary 4.14 (An infinite fixed horizontal nodal slice)**.** *There exists an integer*

$$j \in \{1,2,\dots,123\}$$

such that the horizontal line $t = j$ contains infinitely many non-exceptional consecutive-prime nodes of the Goodspeed wave. Equivalently,

$$\#\{x > 0 : Q_G(x, j) = 0, \quad x - j,\ x + j \text{ are consecutive primes}\} = \infty.$$

Proof. The unconditional bounded-gap theorem of Polymath8 [14] gives infinitely many pairs of consecutive primes $p < q$ satisfying

$$q - p \le 246.$$

Apart from the single pair $(2, 3)$, consecutive prime gaps are positive even integers. Thus infinitely many of these pairs have

$$q - p \in \{2, 4, \dots, 246\}.$$

By the pigeonhole principle, at least one even integer $2j$ in this finite set occurs infinitely often as a consecutive-prime gap.

Each such pair determines the distinct Goodspeed node

$$\left(\frac{p+q}{2}, \frac{q-p}{2}\right) = \left(\frac{p+q}{2}, j\right).$$

Hence the line $t = j$ contains infinitely many non-exceptional consecutive-prime nodes. □

The bounded-strip proposition and its corollary are unconditional consequences of established bounded-gap theory. Although at least one fixed horizontal line $t = j$, with $1 \le j \le 123$, contains infinitely many consecutive-prime nodes, the argument does not identify such a line. In particular, it does not establish infinitude for any prescribed even prime gap. The twin-prime conjecture, Polignac's conjecture for each specified even gap, and Goldbach existence remain open.

For fixed even $h > 0$, recall the endpoint count

$$C_h(Y) := \#\{p \in \mathbb{P} : p + h \in \mathbb{P},\ p + h \le Y\}.$$

The horizontal dictionary identifies it exactly with

$$C_h(Y) = \#\left\{\left(x, \frac{h}{2}\right) \in \mathscr{N}_G : x - \frac{h}{2},\ x + \frac{h}{2} \in \mathbb{P}, \quad x + \frac{h}{2} \le Y\right\}.$$

The cutoff is on the larger characteristic endpoint; equivalently, the midpoint satisfies $x \le Y - h/2$. These counts include all prime pairs of difference h, without requiring consecutiveness. The classical Hardy–Littlewood prime-pair conjecture predicts growth on the scale $Y/(\log Y)^2$, with an h-dependent arithmetic constant. It is therefore equivalently a conjectural counting law along the fixed horizontal slice $t = h/2$. Section 4.4 will introduce the arithmetic coefficient and its local factors.

The Goldbach, twin-prime, Polignac, and fixed-gap Hardy–Littlewood statements in this section are exact geometric reformulations of classical arithmetic problems. The Goodspeed wave supplies a common nodal geometry in which they become vertical or horizontal slice questions; it does not by itself provide the prime-correlation estimates required to prove the conjectural statements. The bounded-strip consequence has a different logical status because it follows from the unconditional bounded-gap theorem.

Vertical and horizontal slices are only two special directions in this geometry. Section 4.4 extends the dictionary to rational affine slices, placing other two-prime relations within the same nodal framework.

4.4. **Rational affine slices and larger arithmetic families.** The sum and difference slices of Section 4.3 belong to a common affine dictionary. A rational line in spacetime imposes an integer affine relation on the characteristic endpoints. Its non-exceptional nodes are therefore simultaneous prime values of two affine-linear forms.

Theorem 4.15 (Affine-line dictionary for the Goodspeed nodal set)**.** *Let*

$$\ell = \{(x,t) \in \mathbb{R}^2 : \alpha x + \beta t = \delta\}, \qquad \alpha, \beta, \delta \in \mathbb{Q}, \quad (\alpha, \beta) \neq (0,0).$$

In characteristic coordinates its equation is

$$(\alpha - \beta)p + (\alpha + \beta)q = 2\delta.$$

After clearing denominators, write this as

$$Ap + Bq = C, \qquad A, B, C \in \mathbb{Z}, \quad (A, B) \neq (0,0).$$

Then

$$\ell \cap \mathscr{N}_G = \left\{ \left(\frac{p+q}{2}, \frac{q-p}{2} \right) : p, q \in \mathcal{P}_1, \ Ap + Bq = C \right\}.$$

The non-exceptional nodes are obtained by requiring $p, q \in \mathbb{P}$. If an integer endpoint pair exists, then $\gcd(A, B) \mid C$; after division by this common divisor, assume $\gcd(A, B) = 1$. For any particular integer solution (p_0, q_0), all integer solutions are uniquely parametrized by

$$P(n) := p_0 + Bn, \qquad Q(n) := q_0 - An, \qquad n \in \mathbb{Z}.$$

Here P and Q denote the two affine-linear endpoint forms; throughout this subsection, $\mathbb{P}$ continues to denote the rational primes and Q_G the Goodspeed wave. Consequently, the non-exceptional nodes on ℓ correspond bijectively to the integers n for which $P(n), Q(n) \in \mathbb{P}$. These endpoints are positive, and restriction to $t \geq 0$ additionally requires $P(n) \leq Q(n)$.

Proof. Substituting $x = (p+q)/2$ and $t = (q-p)/2$ into the line equation gives

$$\alpha x + \beta t = \frac{(\alpha - \beta)p + (\alpha + \beta)q}{2}.$$

The nodal identity follows from Theorem 4.2. The divisibility condition is necessary for an integer solution. After normalization, the displayed parametrization preserves the relation because

$$AP(n) + BQ(n) = Ap_0 + Bq_0 = C.$$

For completeness, choose integers a, b with $aA + bB = 1$. If $A\Delta p + B\Delta q = 0$, then $n = b\Delta p - a\Delta q$ satisfies $(\Delta p, \Delta q) = n(B, -A)$. Thus every solution has the stated form, uniquely since $(A, B) \neq (0,0)$. This argument also covers $A = 0$ or $B = 0$. Finally, $t = (Q(n) - P(n))/2$, giving the half-plane restriction. □

Theorem 4.15 is unconditional. It includes the vertical direction through $(A, B, C) = (1, 1, N)$ and the horizontal direction through $(A, B, C) = (-1, 1, h)$. A genuinely oblique example is supplied by Sophie Germain pairs: primes p and $q = 2p+1$ satisfy $-2p+q = 1$. Substitution gives $-x+3t = 1$, or $x = 3t - 1$. The three representative directions are therefore

$$\begin{aligned} p + q = N \quad &\Longleftrightarrow \quad x = N/2, \\ q - p = h \quad &\Longleftrightarrow \quad t = h/2, \\ q = 2p + 1 \quad &\Longleftrightarrow \quad x = 3t - 1. \end{aligned}$$

For the oblique line, explicit prime-endpoint nodes include

$$(2,5) \longmapsto \left(\frac{7}{2}, \frac{3}{2} \right), \qquad (3,7) \longmapsto (5,2),$$
$$(5,11) \longmapsto (8,3), \qquad (11,23) \longmapsto (17,6).$$

The same line also contains the exceptional arithmetic node $(1,3) \mapsto (2,1)$, which is excluded from the Sophie Germain interpretation.

We next separate the exact local obstruction from the conjectural counting law. Assume $\gcd(A, B) = 1$ and $AB \neq 0$, and use the forms P, Q above. For each rational prime ℓ, define

$$\nu_\ell(A, B, C) := \#\{n \bmod \ell : P(n)Q(n) \equiv 0 \pmod{\ell}\}.$$

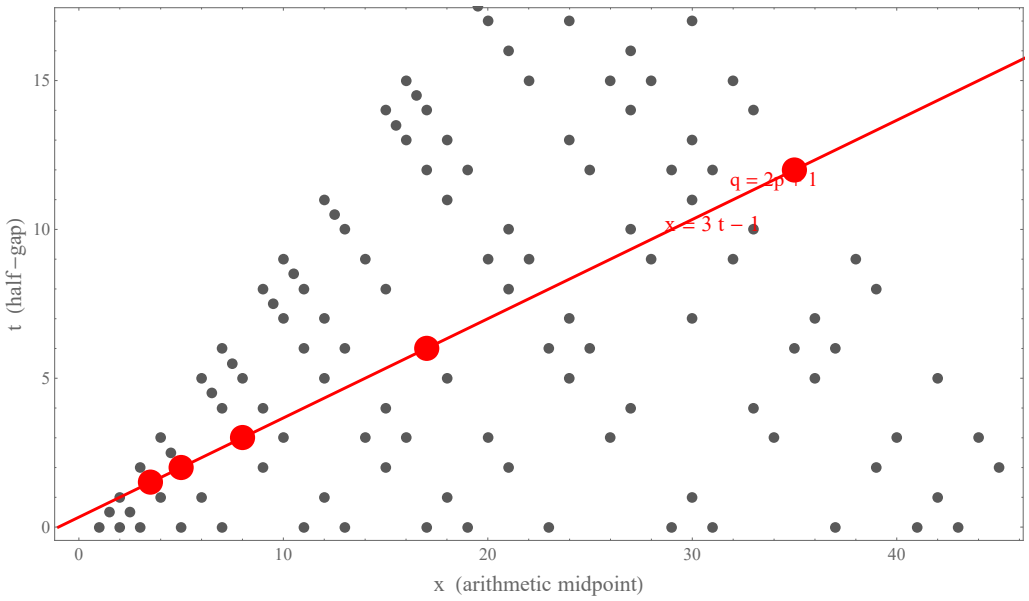


FIGURE 10. An oblique arithmetic slice of the Goodspeed nodal set. The background points are arithmetic nodes in the displayed range. The highlighted line $x = 3t - 1$ is equivalent, in characteristic coordinates, to $q = 2p + 1$. Its highlighted non-exceptional nodes therefore correspond to Sophie Germain prime pairs. This oblique slice complements the vertical and horizontal directions of Figure 9.

Call the relation *admissible* if $\nu_\ell(A, B, C) < \ell$ for every prime ℓ. For the two-prime singular series and counting principle, we impose the nondegeneracy condition $C \neq 0$. Indeed, the coefficient determinant $Bq_0 + Ap_0 = C$ shows that this is exactly the condition that P and Q are not proportional. In particular, the diagonal $p = q$, already excluded from the two-prime heuristic in Section 4, is a one-prime problem.

Under this nondegeneracy assumption, define the normalized product of local densities by

$$\mathfrak{S}(A, B, C) := \prod_{\ell} \frac{1 - \nu_\ell(A, B, C)/\ell}{(1 - 1/\ell)^2}.$$

Proposition 4.16 (Local admissibility and singular series)**.** *Suppose* $\gcd(A, B) = 1$ *and* $ABC \neq 0$. *The numbers* $\nu_\ell(A, B, C)$ *are independent of the chosen particular solution, and*

$$\nu_\ell(A, B, C) = \begin{cases} \ell, & \ell \mid AB,\ \ell \mid C, \\ 1, & \ell \mid AB,\ \ell \nmid C, \\ 1, & \ell \nmid AB,\ \ell \mid C, \\ 2, & \ell \nmid ABC. \end{cases}$$

Thus the relation is admissible exactly when

$$\gcd(AB, C) = 1, \qquad 2 \mid ABC.$$

For an admissible relation, $\mathfrak{S}(A, B, C)$ *converges to a finite positive value. For an inadmissible relation it vanishes.*

Proof. By Theorem 4.15, another particular solution has the form $(p_0 + Bk, q_0 - Ak)$ for some integer k. Its forms are $P(n + k)$ and $Q(n + k)$, so translation modulo ℓ preserves the number of excluded classes.

If $\ell \nmid AB$, both forms have one root modulo ℓ. These roots coincide exactly when $Ap_0 + Bq_0 = C \equiv 0 \pmod{\ell}$. If $\ell \mid AB$, coprimality ensures that precisely one form is constant modulo ℓ. That constant vanishes exactly when $\ell \mid C$; otherwise only the nonconstant form contributes a root. This proves the four cases. The only obstructions are therefore a prime dividing both AB and C, or the prime 2 when it divides none of A, B, C.

The factor $1 - \nu_\ell/\ell$ is the exact fraction of residue classes on which neither form is divisible by ℓ. For squarefree M, the Chinese remainder theorem gives

$$\frac{1}{M}\#\{n \bmod M : \gcd(P(n)Q(n), M) = 1\} = \prod_{\ell \mid M} \left(1 - \frac{\nu_\ell}{\ell}\right).$$

Dividing each local density by the naive independent factor $(1 - 1/\ell)^2$ gives the stated singular series. Outside the finitely many primes dividing ABC, its local factor is

$$\frac{1 - 2/\ell}{(1 - 1/\ell)^2} = 1 - \frac{1}{(\ell - 1)^2}.$$

The nonzero tail therefore converges to a positive value. Admissibility makes the remaining factors positive; inadmissibility supplies a zero factor. □

An inadmissible relation has a prime ℓ dividing $P(n)Q(n)$ for every integer n. Simultaneous primality can then occur only when $P(n) = \ell$ or $Q(n) = \ell$, allowing at most two parameter values. Thus local obstruction need not exclude every prime pair, but it precludes a positive-density two-prime law. Conversely, admissibility alone supplies no asymptotic count.

Conjecture 4.17 (Affine-line nodal counting principle)**.** *Let $Ap + Bq = C$ be a primitive admissible relation with $AB \neq 0$ and $C \neq 0$. The non-exceptional nodal counts obey the following two asymptotic laws.*

Unbounded-line regime. Suppose $AB < 0$, and multiply the relation by -1 if necessary so that $A < 0 < B$. Then $P(n), Q(n) \to +\infty$ as $n \to +\infty$. Choose an integer n_0 such that $P(n), Q(n) > 1$ for all $n \geq n_0$. As $X \to \infty$,

$$\#\{n \in \mathbb{Z} : n_0 \leq n \leq X,\ P(n), Q(n) \in \mathbb{P}\} \sim \mathfrak{S}(A, B, C) \sum_{n=n_0}^{\lfloor X \rfloor} \frac{1}{\log P(n) \log Q(n)}.$$

Bounded-line-family regime. Fix coprime $A, B > 0$ and let $C \to +\infty$ through admissible values. For each C, choose a particular integer solution and write

$$P_C(n) = p_0(C) + Bn, \qquad Q_C(n) = q_0(C) - An,$$

and

$$I_C := \{n \in \mathbb{Z} : P_C(n) > 1,\ Q_C(n) > 1\}.$$

Then

$$\#\{n \in I_C : P_C(n), Q_C(n) \in \mathbb{P}\} \sim \mathfrak{S}(A, B, C) \sum_{n \in I_C} \frac{1}{\log P_C(n) \log Q_C(n)}$$

as $C \to +\infty$ through admissible values.

The geometric distinction between the regimes is essential. When $AB < 0$, one fixed line has an unbounded positive ray, along which both endpoint forms grow. Fixed differences and Sophie Germain pairs belong to this regime. When $A, B > 0$, positivity bounds both endpoints on each line: $p < C/A$ and $q < C/B$ when $p, q > 1$. Each positive segment therefore contains only finitely many integer pairs. The asymptotic question must concern an expanding family of segments as C grows; Goldbach belongs to this second regime.

Both conjectural formulas count ordered endpoint pairs in the full cone. In the Goldbach specialization $A = B = 1$, the bounded-family formula counts ordered prime representations of C.

Restricting to $t \geq 0$ imposes $P_C(n) \leq Q_C(n)$ and selects the unordered representations. Changing the particular solution merely translates the integer parameter; in the bounded regime it leaves both the count and the logarithmic sum exactly unchanged.

Remark 4.18 (Relation with the Hardy–Littlewood programme). Conjecture 4.17 is a Goodspeed-spacetime formulation of classical Hardy–Littlewood–Dickson prime-pair heuristics, not independent arithmetic evidence for them. The unbounded-line regime is the simultaneous-primality prediction for two nonproportional affine-linear forms, including fixed prime gaps and Sophie Germain pairs. It may also be viewed as the degree-one, two-polynomial specialization of the Bateman–Horn heuristic [1]. The bounded-line-family regime includes the Hardy–Littlewood prediction for binary Goldbach representations. The contribution of the wave construction is geometric unification: these problems become directional intersection laws for one arithmetic nodal set. The exact affine dictionary and local admissibility factors are unconditional; the asserted asymptotic counts remain conjectural.

These conjectures concern one-dimensional directional counts. Section 4.5 returns to unconditional quantitative results, including the positive fixed-gap detector and the two-dimensional macroscopic nodal density law.

4.5. **Counting laws and macroscopic nodal geometry.** We now return to unconditional quantitative statements. Positivity gives a finite detector whose floor recovers an exact prime-pair count. At the two-dimensional level, the prime number theorem gives a macroscopic density law for the full prime-node measure. Neither result supplies the lower bounds needed for infinitude on a prescribed horizontal slice.

Lemma 4.19 (Exact Goodspeed values at composite integers)**.** *If $n \geq 2$ is composite, then*

$$G(n) = \frac{\sin^2(\pi/n)}{\pi^2},$$

and consequently

$$G(n) \geq \frac{4}{\pi^2 n^2}.$$

Proof. At an integer n,

$$G(n) = \frac{\sin^2(\pi W(n))}{\pi^2}, \qquad W(n) = \frac{(n-1)! + 1}{n}.$$

Suppose first that $n > 4$ is composite. Then

$$n \mid (n-1)!.$$

Indeed, write $n = ab$ with $2 \leq a \leq b < n$. If $a < b$, the distinct factors a and b both occur in $(n-1)!$, so their product n divides the factorial. If $a = b$, then $a \geq 3$, and both a and $2a$ occur among $1, \ldots, n-1$; their product $2a^2$ is divisible by $n = a^2$.

Hence

$$W(n) = m + \frac{1}{n}$$

for some integer m, and therefore

$$\sin^2(\pi W(n)) = \sin^2\left(\frac{\pi}{n}\right).$$

The remaining composite case is $n = 4$, for which

$$W(4) = \frac{7}{4}$$

and

$$\sin^2\left(\frac{7\pi}{4}\right) = \sin^2\left(\frac{\pi}{4}\right).$$

Thus

$$G(n) = \frac{\sin^2(\pi/n)}{\pi^2}$$

for every composite $n \geq 2$.

Finally, the chord bound

$$\sin u \geq \frac{2u}{\pi}, \qquad 0 \leq u \leq \frac{\pi}{2},$$

applied to $u = \pi/n$, gives

$$G(n) = \frac{\sin^2(\pi/n)}{\pi^2} \geq \frac{4}{\pi^2 n^2}.$$

□

Theorem 4.20 (Positive fixed-gap detector)**.** *Fix a positive even integer h. For every integer $Y > h + 1$, put*

$$T_3^*(Y) := \frac{4\pi^2 \log Y}{\sin^2(\pi/Y)}$$

and define

$$E_h(Y) := \sum_{n=2}^{Y-h} \exp\left(-T_3^*(Y)\big(G(n) + G(n+h)\big)\right).$$

Then

$$0 \leq E_h(Y) - C_h(Y) < Y^{-3}, \qquad C_h(Y) = \lfloor E_h(Y) \rfloor.$$

Every summand is nonnegative, and no cancellation is used. Moreover,

$$T_3^*(Y) \sim 4Y^2 \log Y \qquad (Y \to \infty).$$

This choice of temperature is strictly smaller than $\pi^2 Y^2 \log Y$.

Proof. For real $u \geq 2$, the function

$$g(u) := \frac{\sin^2(\pi/u)}{\pi^2}$$

is decreasing.

If both n and $n+h$ are prime, then $G(n) = G(n+h) = 0$, so the corresponding summand equals 1. These terms contribute exactly $C_h(Y)$.

Otherwise at least one endpoint m is composite, with $2 \leq m \leq Y$. By Lemma 4.19,

$$G(n) + G(n+h) \geq g(m) \geq g(Y).$$

Consequently every remaining summand is at most

$$\exp\left(-T_3^*(Y) g(Y)\right) = \exp(-4 \log Y) = Y^{-4}.$$

There are fewer than Y such terms. Hence

$$0 \leq E_h(Y) - C_h(Y) < Y^{-3} < 1.$$

Since $C_h(Y)$ is an integer, the floor identity follows.

Finally, $\sin(\pi/Y) \sim \pi/Y$ gives

$$T_3^*(Y) \sim 4Y^2 \log Y.$$

The strict inequality $\sin(\pi/Y) > 2/Y$ for $Y > 2$ gives

$$T_3^*(Y) < \pi^2 Y^2 \log Y.$$

□

The theorem gives a positive, cancellation-free expression from which the exact finite count can be recovered. It does not imply that $C_h(Y)$ is unbounded. To obtain prescribed-gap infinitude from this representation, one would still need a lower bound forcing $\mathcal{E}_h(Y)$ to grow without bound. The detector transfers the prime-pair counting problem into a particular analytic expression; its positivity alone does not resolve that problem.

For the macroscopic statement, define the prime-only endpoint and nodal measures

$$\mu_{\mathbb{P}} := \sum_{p\in\mathbb{P}} \delta_p, \qquad \mathcal{N}_{\mathbb{P}} := L_{\#}\big(\mu_{\mathbb{P}} \otimes \mu_{\mathbb{P}}\big),$$

where $L(p,q) = ((p+q)/2, (q-p)/2)$. Thus $\mathcal{N}_{\mathbb{P}}$ is obtained from $\mathcal{N}_G$ by deleting every atom with an endpoint equal to 1. It retains ordered prime pairs, diagonal pairs, and both signs of time.

Theorem 4.21 (Macroscopic nodal density law for Goodspeed nodes)**.** *For every $\Phi \in C_c(\mathcal{C}_+)$, extended by zero outside $\mathcal{C}_+$,*

$$\frac{\log^2 R}{R^2} \int_{\mathbb{R}^2} \Phi\left(\frac{x}{R}, \frac{t}{R}\right) d\mathcal{N}_{\mathbb{P}}(x,t) \longrightarrow 2 \int_{\mathcal{C}_+} \Phi(x,t)\, dx\, dt$$

as $R \to \infty$. Equivalently, with $D_R(x,t) = (x/R, t/R)$,

$$\frac{\log^2 R}{R^2} (D_R)_{\#} \mathcal{N}_{\mathbb{P}} \Longrightarrow 2\, dx\, dt \qquad \textit{vaguely on } \mathcal{C}_+.$$

Proof. Put

$$\eta_R := \frac{\log R}{R} \sum_{p\in\mathbb{P}} \delta_{p/R}.$$

For $0 < a < b$, the prime number theorem gives $\eta_R((a,b]) \to b - a$. It follows that $\eta_R \Longrightarrow du$ vaguely on $(0,\infty)$. The masses on compact intervals are uniformly bounded, so approximation by finite sums of product test functions gives

$$\eta_R \otimes \eta_R \Longrightarrow du\, dv \qquad \text{on } (0,\infty)^2.$$

Since L is a homeomorphism from the positive quadrant onto $\mathcal{C}_+$, the function $\Phi \circ L$ has compact support in that quadrant. Homogeneity of L gives

$$\begin{aligned} \frac{\log^2 R}{R^2} \int_{\mathbb{R}^2} \Phi(D_R(x,t))\, d\mathcal{N}_{\mathbb{P}}(x,t) &= \int_{(0,\infty)^2} \Phi(L(u,v))\, d(\eta_R \otimes \eta_R)(u,v) \\ &\longrightarrow \int_{(0,\infty)^2} \Phi(L(u,v))\, du\, dv. \end{aligned}$$

The inverse change of variables is $u = x - t$, $v = x + t$, with

$$\left|\det \frac{\partial(u,v)}{\partial(x,t)}\right| = \left|\det \begin{pmatrix} 1 & -1 \\ 1 & 1 \end{pmatrix}\right| = 2.$$

Thus the last integral equals $2\int_{\mathcal{C}_+} \Phi(x,t)\, dx\, dt$, as required. □

The limiting density 2 is precisely the characteristic Jacobian factor. The arithmetic input is the classical prime number theorem applied separately to the two endpoint variables. This controls the full two-dimensional cloud without estimating a correlation on any prescribed one-dimensional slice.

Let $\pi(Y) := \#\{p \in \mathbb{P} : p \le Y\}$ denote the prime-counting function. An exact average over positive even differences gives another unconditional consequence.

Corollary 4.22 (Average fixed-gap count)**.** *For every integer $Y \geq 3$,*

$$\sum_{\substack{2\leq h\leq Y\\ h \text{ even}}} C_h(Y) = \binom{\pi(Y)-1}{2}.$$

Consequently, as $Y \to \infty$,

$$\sum_{\substack{2\leq h\leq Y\\ h \text{ even}}} C_h(Y) \sim \frac{Y^2}{2\log^2 Y},$$

and

$$\max_{\substack{2\leq h\leq Y\\ h \text{ even}}} C_h(Y) \geq (1+o(1))\frac{Y}{\log^2 Y}.$$

Proof. Every unordered pair of distinct odd primes $p < q \leq Y$ has exactly one positive even difference $h = q - p$, necessarily at most Y, and contributes once to $C_h(Y)$. Conversely, a prime pair of positive even difference cannot involve 2, so every contribution arises from such an unordered pair. There are $\pi(Y) - 1$ odd primes at most Y, proving the exact identity. The prime number theorem gives the asymptotic formula. There are $\lfloor Y/2 \rfloor = Y/2 + O(1)$ positive even values of $h \leq Y$; the largest summand is at least their average, giving the final bound. □

This is a *moving-gap* consequence: at every sufficiently large scale Y, some even gap $h = h(Y)$ has at least the stated number of prime-pair occurrences. The maximizing gap may vary with Y. The average does not establish that a single fixed gap has arbitrarily many occurrences.

The remaining fixed-gap question can be stated entirely in the notation of this article. Write $\mathbf{1}_{\mathbb{P}}$ for the prime indicator.

Proposition 4.23 (Sharp fixed-gap obstruction)**.** *For a prescribed positive even integer h, the following are equivalent, with limits taken through integer Y:*

(i) The line $t = h/2$ contains infinitely many non-exceptional arithmetic nodes.
(ii) $C_h(Y) \to \infty$.
(iii) $\mathcal{E}_h(Y) \to \infty$.
(iv) The sums

$$\sum_{2\leq n\leq Y} \mathbf{1}_{\mathbb{P}}(n)\mathbf{1}_{\mathbb{P}}(n+h)$$

are unbounded as $Y \to \infty$.

Proof. The fixed-slice dictionary of Section 4.3 identifies the nodes in (i) with the prime pairs counted by C_h. Each finite endpoint range contains only finitely many such pairs, and $C_h(Y)$ is nondecreasing. Thus (i) and (ii) are equivalent. Exactly,

$$C_h(Y) = \sum_{2\leq n\leq Y-h} \mathbf{1}_{\mathbb{P}}(n)\mathbf{1}_{\mathbb{P}}(n+h),$$

while the sum in (iv) is $C_h(Y + h)$. A fixed shift of the cutoff does not change unboundedness, proving equivalence with (iv). Finally, Theorem 4.20 gives

$$0 \leq \mathcal{E}_h(Y) - C_h(Y) \leq Y^{-3} \longrightarrow 0,$$

which proves equivalence with (iii). □

Although $\mathcal{E}_h(Y)$ need not be monotone, the same estimate shows that its unboundedness is equivalent to all the conditions of Proposition 4.23: unboundedness forces the nondecreasing count $C_h(Y)$ to tend to infinity, and then so does the detector. The present Goodspeed theory proves none

of these unboundedness assertions for an arbitrary prescribed positive even h. The missing ingredient is a quantitative lower bound forcing unbounded growth of the intersection of the positive-real prime divisor with its translate by h. This is the classical prime-pair correlation problem.

Section 4.4 makes the local side of this distinction exact. For every positive even h, the relation $q-p=h$ is admissible and $\mathfrak{S}(-1,1,h)>0$. These local congruence densities describe survival of the pair modulo each prime; their positivity supplies no global lower bound for $C_h(Y)$. In particular, exact local admissibility does not estimate the simultaneous-primality sum in Proposition 4.23. The unresolved step is global prime correlation.

The macroscopic nodal density law concerns a different scale of information. A line has zero area in its limiting measure, and the fixed microscopic slice $t = h/2$ becomes $t = h/(2R)$ after rescaling. Vague convergence of the two-dimensional measure does not yield the one-dimensional lower bounds needed on that prescribed slice. Thus the positive detector, the exact all-gap average, and the macroscopic nodal density law coexist with the unresolved fixed-gap problem:

A prescribed slice requires prime-correlation estimates;

the full two-dimensional nodal cloud has an unconditional scaling law.

This distinction will be placed in the broader context of the classification and left-tail results in the final synthesis of Section 5. Goodspeed spacetime provides exact arithmetic structure and unconditional global counting laws, while prescribed directional infinitude remains governed by classical arithmetic correlation problems.

5. Synthesis and outlook

The three constructions developed above arise from the same Wilson–Gamma function but probe different aspects of its geometry. Taken together, they separate three levels of structure:

formal discrete organization, proved local complex geometry, real arithmetic nodal geometry.

This separation is useful because the logical status of the three levels is different.

Section 2 gives a global discrete model for the zero set. The normalized Gaussian coordinate

$$\widehat{\xi}_G \in \mathbb{Z}[i]$$

contains the large-scale lattice geometry, while the residue

$$\lambda_5 \in \mathbb{Z}/5\mathbb{Z}$$

uniformly records the remaining half-plane and sheet information. Together they recover every formally admissible TUCKE state. The formal combinatorics and reconstruction are proved; what remains open is the global analytic realization problem. In particular, the Fundamental Classification Conjecture asks whether every zero of G realizes exactly one admissible state and whether every admissible state is realized by exactly one zero.

Section 3 supplies a substantial analytic realization without assuming that conjecture. Near the puncture 0, the canonical Family $(-i)$ tail is proved to exist, to be simple and asymptotically isolated, and to be governed by the single holomorphic germ

$$z_c^+ = c^{-1/2} Z(c^{-1/2}).$$

The same germ also produces the mirror tail on the negative-real side. In the discrete language of Section 2, these two branches occupy the eventual $k = 0$ and $k = -1$ Family $(-i)$ columns. Thus the left-tail theory gives an explicit region in which the formal classification and the analytic zero geometry meet.

The local tail also exhibits a second phenomenon that is independent of the global classification problem. Its asymptotic coefficients retain the Gamma coefficients in triangular form. Once the canonical integer labels are fixed, the real-part jet recovers

$$\gamma, \zeta(2), \zeta(3), \ldots.$$

More strongly, the exact unlabelled zero cloud near 0 determines the Wilson germ up to its integer gauge within the normalized real-symmetric candidate class, and in the Gamma specialization that gauge is fixed by the Gamma normalization. The subsequent Newton–Laplace–Mellin–Möbius reconstruction then recovers the prime-zeta function on $\Re s > 1$. The arithmetic functions appearing in this chain are classical; the inverse-geometric content is that they can be reconstructed from a non-real zero configuration without using the positive-real prime zeros as input.

Section 4 begins from the opposite end of the theory. It requires neither the Fundamental Classification Conjecture nor the left-tail inverse problem. Its input is only the already known real divisor

$$\mathcal{P}_1 = \{1\} \cup \mathbb{P}.$$

The Goodspeed wave

$$Q_G(x,t) = \frac{1}{2}\big(G(x-t) + G(x+t)\big)$$

places every ordered pair

$$(p,q) \in \mathcal{P}_1^2$$

at the node

$$\left(\frac{p+q}{2}, \frac{q-p}{2}\right).$$

The characteristic coordinates therefore recover the two endpoints exactly, and the complete characteristic jet separates into the two real-axis jets of G.

This endpoint geometry organizes several classical arithmetic relations in a common plane:

$$p+q = N \quad \Longleftrightarrow \quad x = \frac{N}{2},$$

$$q-p = h \quad \Longleftrightarrow \quad t = \frac{h}{2},$$

and, more generally,

$$Ap + Bq = C \quad \Longleftrightarrow \quad \text{a rational affine line in Goodspeed spacetime.}$$

Accordingly, Goldbach representations, twin primes, prescribed prime differences, Sophie Germain pairs, and general two-prime affine relations appear as directional questions for a single nodal set.

The geometric reformulation does not alter the arithmetic difficulty of those problems. The nodal parametrization, measure projections, characteristic-jet splitting, Hessian identities, affine-line dictionary, and local admissibility factors are unconditional. The positive fixed-gap detector gives an exact finite count, and the macroscopic nodal density law gives an unconditional two-dimensional scaling limit derived from the prime number theorem. By contrast, infinitude on a prescribed one-dimensional slice still requires prime-correlation estimates. In particular, Goldbach existence, twin-prime infinitude, Polignac-type assertions, and the asymptotics described in Conjecture 4.17 retain their classical conjectural status.

The contrast between Sections 3 and 4 is therefore especially useful. Section 3 asks how much arithmetic can be reconstructed from the *non-real* zero geometry of G; Section 4 asks how the already known *real* arithmetic divisor is reorganized by characteristic evolution. The first is an inverse problem, while the second is a geometric encoding problem. Neither should be interpreted as replacing the classical arithmetic input underlying the Gamma function or the prime-distribution problems that arise on prescribed slices.

Several natural problems remain open. The most immediate is the global analytic realization of the formal lattice of Section 2. The local left-tail theory shows that a nontrivial portion of this geometry can be controlled directly, but a complete effective exhaustion of the remaining Family $(-i)$ and Type 2 configurations is still missing. The invariant-coincidence problem similarly remains global, despite its validity on the positive generated branches and several negative subclasses.

A second direction concerns stability of the inverse theory. The reconstruction results of Section 3 are exact-data statements. It would be natural to ask which parts of the Gamma germ, the zeta values, or the prime-zeta function can be recovered stably from finitely many or perturbed non-real zero locations, and how the quartic separation of the canonical tail affects such estimates.

A third direction is to extend the nodal viewpoint beyond the affine relations treated in Section 4. Rational affine slices are especially natural because they are exactly equivalent to two-variable affine Diophantine relations. Other geometric subsets of the characteristic plane may encode different arithmetic constraints, but their usefulness would depend on arithmetic information not supplied by the wave equation alone. Likewise, passing to logarithmic characteristic coordinates suggests a complementary multiplicative geometry in which products and ratios of prime endpoints replace sums and differences.

The common theme is that the Goodspeed function supports several distinct but compatible geometries. Its non-real zeros admit a formal Gaussian organization; one canonical part of that organization is governed analytically by a single holomorphic germ and carries an inverse arithmetic structure; and its real arithmetic divisor generates an exact nodal geometry for the wave equation. These results do not close the global classification or the classical prime-correlation problems. They instead identify a common analytic object in which discrete classification, local complex asymptotics, and arithmetic endpoint geometry can be studied within one framework.

References

[1] P. T. Bateman and R. A. Horn, *A heuristic asymptotic formula concerning the distribution of prime numbers*, Math. Comp. **16** (1962), 363–367.

[2] H.-T. Chen, *On locating the zeros and poles of a meromorphic function*, J. Comput. Appl. Math. **402** (2022), 113796.

[3] A. Connes, *Around Wilson's theorem*, J. Number Theory **194** (2019), 1–7.

[4] L. E. Dickson, *A new extension of Dirichlet's theorem on prime numbers*, Messenger of Mathematics **33** (1904), 155–161.

[5] C.-E. Fröberg, *On the prime zeta function*, BIT 8 (1968), 187-202.

[6] A. A. Goldberg and I. V. Ostrovskii, *Value Distribution of Meromorphic Functions*, Translations of Mathematical Monographs, vol. 236, American Mathematical Society, Providence, RI, 2008.

[7] S. A. Hambleton, H. C. Williams, Cubic fields with geometry, CMS Books in Mathematics, Springer, 2018.

[8] G. H. Hardy and J. E. Littlewood, *Some problems of 'Partitio numerorum'; III: On the expression of a number as a sum of primes*, Acta Math. **44** (1923), 1–70. DOI: 10.1007/BF02403921.

[9] G. H. Hardy and E. M. Wright, *An Introduction to the Theory of Numbers*, 6th ed., revised by D. R. Heath-Brown and J. H. Silverman, Oxford University Press, Oxford, 2008.

[10] M. Krishnapur, P. Kurlberg, and I. Wigman, *Nodal length fluctuations for arithmetic random waves*, Ann. of Math. (2) **177** (2013), no. 2, 699–737. DOI: 10.4007/annals.2013.177.2.8.

[11] R. Nevanlinna, *Analytic Functions*, translated from the second German edition by P. Emig, Grundlehren der Mathematischen Wissenschaften, vol. 162, Springer-Verlag, New York–Berlin, 1970.

[12] NIST Digital Library of Mathematical Functions, F. W. J. Olver, A. B. Olde Daalhuis, D. W. Lozier, B. I. Schneider, R. F. Boisvert, C. W. Clark, B. R. Miller, B. V. Saunders, H. S. Cohl, and M. A. McClain, eds., Release 1.2.8, 15 September 2026, `https://dlmf.nist.gov/`.

[13] J. Maynard, *Small gaps between primes*, Ann. of Math. (2) **181** (2015), no. 1, 383–413. DOI: 10.4007/annals.2015.181.1.7.

[14] D. H. J. Polymath, *Variants of the Selberg sieve, and bounded intervals containing many primes*, Res. Math. Sci. **1** (2014), Art. 12.

[15] W. A. Strauss, *Partial Differential Equations: An Introduction*, 2nd ed., John Wiley & Sons, Hoboken, NJ, 2007.

[16] Y. Zhang, *Bounded gaps between primes*, Ann. of Math. (2) **179** (2014), no. 3, 1121–1174.